AD-A098 937 TEXAS A AND M RESEARCH FOUNDATION COLLEGE STATION F/G 1/3
MECHANICAL BEHAVIOR OF BALLOON FILMS.(U)
NOV 78 L D WEBB F19628-76-C-0082
UNCLASSIFIED TAMRF-3332-2 AFGL-TR-79-0026 NL

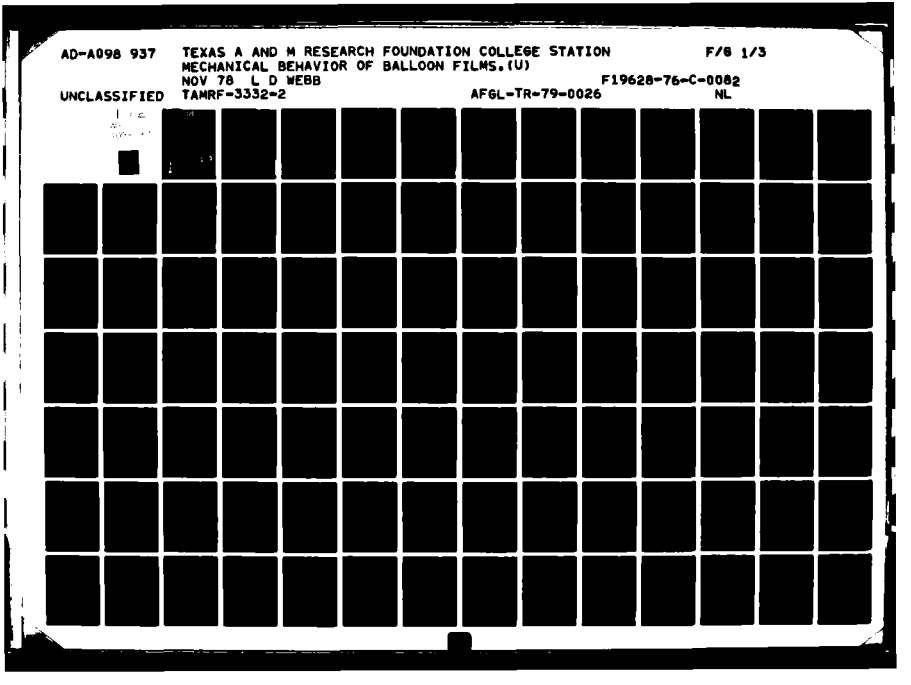

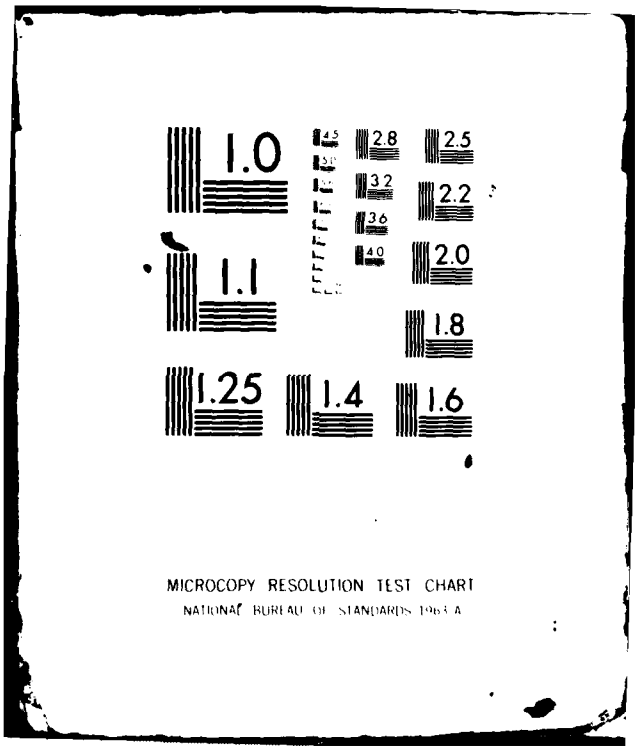
1.0
1.1
1.25
1.4
1.6
1.8
2.0
2.2
2.5
2.8
3.2
3.6
4.0
MICROCOPY RESOLUTION TEST CHART
NATIONAL BUREAU OF STANDARDS 1963 A

[redacted]

[redacted]

L. Dale Webb

Texas A&M University
Department of Civil Engineering
College Station, Texas 77843

Scientific Report No. 1

November 1978

Approved for public release; distribution unlimited

AIR FORCE GEOPHYSICS LABORATORY
AIR FORCE SYSTEMS COMMAND
UNITED STATES AIR FORCE
HANSCOM AFB, MASSACHUSETTS 01731

UNCLASSIFIED

SECURITY CLASSIFICATION OF THIS PAGE (When Data Entered)

REPORT DOCUMENTATION PAGE

READ INSTRUCTIONS BEFORE COMPLETING FORM

1. REPORT NUMBER: AFGL-TR-79-0026	2. GOVT ACCESSION NO.: AD-A079837
3. RECIPIENT'S CATALOG NUMBER:	
4. TITLE (and Subtitle): MECHANICAL BEHAVIOR OF BALLOON FILMS	5. TYPE OF REPORT & PERIOD COVERED: Scientific Report No. 2 Scientific Interim
6. PERFORMING ORG. REPORT NUMBER: TAMRF-3332-2	
7. AUTHOR(s): L. Dale Webb	8. CONTRACT OR GRANT NUMBER(s): F19628-76-C-0082
9. PERFORMING ORGANIZATION NAME AND ADDRESS: Texas A&M University, Department of Civil Engineering, College Station, Texas 77843	10. PROGRAM ELEMENT, PROJECT, TASK AREA & WORK UNIT NUMBERS: 62101F 6665O8AH
11. CONTROLLING OFFICE NAME AND ADDRESS: Air Force Geophysics Laboratory, Hanscom AFB, Mass. 01731, Contract Monitor: James F. Dwyer/LCB	12. REPORT DATE: November 1978
	13. NUMBER OF PAGES: 93
14. MONITORING AGENCY NAME & ADDRESS (if different from Controlling Office)	15. SECURITY CLASS. (of this report): Unclassified
	15a. DECLASSIFICATION/DOWNGRADING SCHEDULE

16. DISTRIBUTION STATEMENT (of this Report)

Approved for public release, distribution unlimited.

17. DISTRIBUTION STATEMENT (of the abstract entered in Block 20, if different from Report)

18. SUPPLEMENTARY NOTES

19. KEY WORDS (Continue on reverse side if necessary and identify by block number)

Balloon Materials	Polyethelene Film
Material Testing	Thin Film Behavior
Material Properties	Thin Film Characterization

20. ABSTRACT (Continue on reverse side if necessary and identify by block number)

This report summarizes the activities of the Mechanical Behavior Laboratory at Texas A&M University in a study of the problems faced in the design and flight of free balloons. Existing facilities at Texas A&M University were augmented by equipment provided by the Air Force Geophysics Laboratory. Material testing systems have been made operational over temperatures ranging from +100 to -100°C. Most of the testers are equipped with inert atmosphere environmental chambers and with full instrumentation necessary to monitor loading rates, stresses, strains and temperatures. Materials can be subjected to stress states which

DD FORM 1 JAN 73 1473

UNCLASSIFIED

SECURITY CLASSIFICATION OF THIS PAGE (When Data Entered)

include uniaxial, one-to-one biaxial by means of an inflated round diaphragm and two-to-one biaxial by means of an inflated "race track" diaphragm.

In addition, an apparatus has been devised to subject materials to a one-to-one biaxial or two-to-one biaxial strain field. This strain tester is especially useful for evaluating non-uniform samples such as those containing heat seals. Most of the test systems are now microprocessor controlled and data reduction is automatic.

The rate of loading and temperature dependence of polyethylene Stratofilm has been measured both by creep tests and by uniaxial testing. All the data are presented along with an analytical solution to the problem of presenting in a simple manner both the rate and temperature influence by means of "master curves."

A polyethylene balloon stored for twenty-two years was uncrated, dissected and tested to determine if there were detrimental aging effects during storage. The data show no such effect and the balloon appeared suitable for flight.

In response to the question of the validity of the quality control type uniaxial heat seal test for design purposes, a study was made of the influence of lateral constraint on the region of a heat seal in a uniaxial test. The seal "fin" was bonded to a metal tab to prevent "Poisson" lateral contraction from occurring. This induced a biaxial stress state at the heat seal known to be more realistic than uniaxial. The tests showed no reduction of seal strength at room temperature although testing at low temperature may show discrimination.

Strips of the heat sealed (melted) film originally consisting of back-up film, gore material and load tape fin fused together during heat sealing were tested and compared to the gore material alone. No discernible differences were observed in the mechanical behavior at room temperature.

Polyethylene's mechanical behavior is rate and temperature dependent as are most polymers. In addition, perhaps due to its crystallinity, it appears to have a strong dependency on stress history. The stress history is influenced by stress state, stress magnitude, temperature and the ordering and interaction of all. Until the mathematical description of polyethylene behavior is complete, it is imperative that flight parameters of temperature, stress or strain state and their histories be used to guide laboratory evaluations.

TABLE OF CONTENTS

LIST OF ILLUSTRATIONS

List of Illustrations (continued)

List of Illustrations (continued)

List of Illustrations (continued)

List of Illustrations (continued)

INTRODUCTION AND SUMMARY OF RESULTS

Following equipment transfer from the Air Force Geophysics Laboratory to Texas A&M University, research was initiated into the study and definition of free balloon design problems. The first major effort and a continuing effort throughout the period of the study was the establishment of the mechanical behavior of balloon films as influenced by rate of loading and temperature to provide material characteristics suitable for inclusion in computer codes for design and stress analysis of balloon structures. Master curves showing the combined influences of rate and temperature were developed and it is clear that "exposure" history, perhaps through its influence upon material crystallinity, is critically important. The temperature at which the film will react in a brittle fashion to imposed loads is seen to be influenced by strain rate, stress state, prior loadings and evidently, temperature history. Analysis of data generated at TAMU as well as those provided by the industry strongly suggest that scatter in strength, toughness and cold brittle behavior may result from changes in the degree of crystallinity of the polyethylene film. Future studies of this influence are anticipated.

Uniaxial data generation is hampered by the sample edge discontinuities, the need to hand load each sample into the grips within the environmental chamber and the continuing problem of grip slip or grip induced failure. All of the above factors influence tests results. Therefore, material testing systems were considered which would minimize the above factors. Diaphragm testing devices such as the "racetrack" system were improved in terms of uniformity of clamping, thermal stability and ease of sample loading. The thermal mass of the sample holder was cut by more

than 90% and experiments with gaskets and rubbers resulted in air tight non-hostile seals to the films under test. The desire to measure the influence of stress state, stress history, temperature and strain rate required the development of automated controls for the operation of the diaphragm testers. To control the strain rate in a diaphragm test the pressurization gas flow rate must be modulated by feedback of the height of the inflated diaphragm "blister". Inflation rates and operations speed necessitated the application of computer control techniques.

The system requirements were defined, the system prototyped, and checkout, including design modifications, all were accomplished during the contract duration. Examination of the tests to date (during system checkout) show that what appeared to be excessive scatter in the computer controlled data indeed reflect the importance of parameter interrelationships. Temperature, strain rate, stress state and prior stress and temperature history all influence the mode of failure. Although the discrimination between the parameter effects is not well defined, careful tracing of sample history including storage temperature and method of sample mounting prior to testing showed that virtually all widely deviating results could be correlated with some unusual "history".

Although not confirmed by a statistically significant test program the following observations are offered. Securing a sample in its holder prior to cooldown produces restrained thermal shrinkage upon which are superimposed the pressurization stresses. This causes the sample to fail in a brittle fashion at warmer temperatures than if the sample had been unstressed prior to cooldown.

This superposition is realistic for balloon systems where the skin is stressed prior, during and after cooldown. Samples which had been stretched (stressed) tightly and taped to the sample holder to produce a wrinkle free sample prior to clamping and cooldown showed as much as a 12°C shift toward the warmer temperatures. Thermal histories with or without stressing may be found to cause significant alterations in low temperature strength and toughness. Several diaphragm samples left inside an environmental chamber and thought to have been soaked at 40°C were seen to have a toughness (energy expended to fail the sample) value only half as large as expected as well as behaving in a brittle fashion when subjected to strain rates ordinarily too low to cause such brittle behavior.

In a balloon system the influence of rates, histories, temperature, and the like can be even more important than indicated by laboratory testing. The balloon skin must work as a system to uniformly distribute loads. When a few gores (or even segments within one gore) see a history at variance with the rest, then uniformity of behavior is destroyed. Unusual and unexpected stresses will result and ordinarily adequate designs can fail.

CHARACTERIZATION OF VISCOELASTIC MATERIALS

All engineering materials exhibit creep and relaxation behavior. The magnitude normally depends strongly on temperature, stress level, and loading duration. Many polymers are influenced appreciably by moisture content as well.[1,2]

The need for structural engineers to have a good understanding of time-dependent behavior has accelerated in recent years due to the increasing use of elastomers and polymers as structural components. These polymeric materials may be either monolithic or reinforced with particles or fibers, depending on the structural requirements. For example, the demand by the balloon industry for high strength-to-weight materials has, in the last few years, led to the development and application of composites consisting of plastic matrices reinforced with fibers of nylon, dacron or aramid (kevlar). These fibers, some of which currently can be produced with tensile strengths as high as 400,000 psi, when combined with lightweight plastic matrices form the so-called "high-performance" composites with strength-to-weight ratios superior to those of titanium and ultra-high strength (maraging) steel.[3] In contrast to structural metals, high temperatures are not required for appreciable creep or relaxation to occur in polymers; indeed, even high performance composites may exhibit this behavior at ambient temperatures.

---

1) Richards, C. W., Engineering Materials Science, Wadsworth Publishing Co, (1961).

2) Hayden, H. W., Moffatt, W. G., and Wulff, J., The Structure and Properties of Materials - Vol III, Mech. Behavior; John Wily & Sons, Inc. N.Y. (1965).

3) Sinclair, T. N., "Composites: Designers Wait and Contemplate Industrial Research," (Oct. 1969).

Many textbooks describe in some detail the creep of materials under constant load and temperature. Balloon structures may be subjected to large changes in these parameters during their service life. Therefore, in this section, an introduction to the problems of characterizing the time-dependent stress-strain behavior of materials under changing stress and temperature will be provided.

The starting point is the theory of linear viscoelasticity, which is widely used today in characterizing polymeric materials. This theory is applicable, in principle, to all materials if the applied loads are sufficiently small. While this "sufficiently small" range is not overly restrictive for some polymers, time-dependent behavior of many is so nonlinear that the linear theory is not valid except for stresses far below ultimate values.(4)

First, the isothermal stress-strain equation for a linear viscoelastic material under uniaxial loading will be derived. The theory will then be extended to include non-isothermal behavior.

The stress-strain equation for a linear viscoelastic material can be derived using mechanical models consisting of springs and dashpots, or by appealing to the mathematical properties governing all linear systems. Both approaches will be discussed and compared here.

I. Model Theory

The two elements that form the building blocks of the mechanical models are shown in Figure 1. By convention, they are each assumed to have unit cross-sectional area and initial length; thus, stress and strain can be used instead of force and displacement, respectively. Also, we assume $\varepsilon = \sigma = 0$ when $t = 0$.

Maxwell Model: One way of combining the two elements in

(4) Hult, J.A.H., "Creep in Engineering Structures," Blaisdell Publ. Co, (1966).

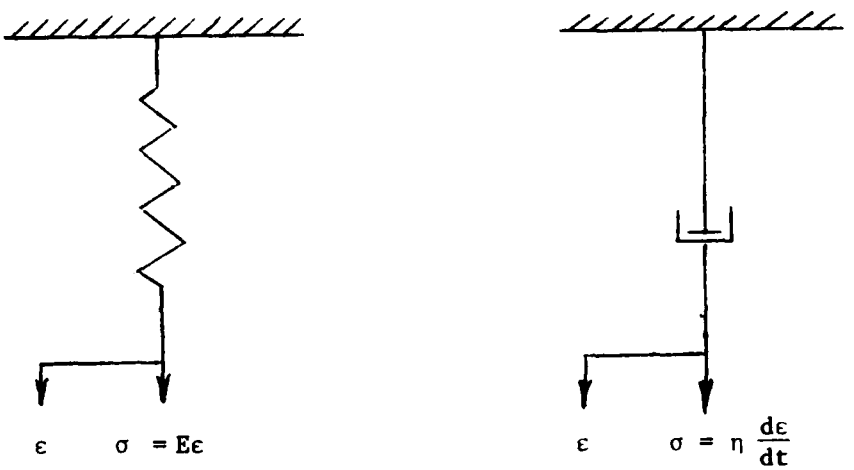

Hookean Spring

Newtonian Dashpot

Figure 1. Basic Rheological Model Elements

Figure 1 is to place them in series, which gives us the following equations (see Figure 2):

$$\varepsilon_d = \int_0^t \frac{\sigma_d}{\eta_m} \, d\tau \tag{1}$$

$$\varepsilon_s = \frac{\sigma_s}{E_m} \tag{2}$$

$$\varepsilon = \varepsilon_s + \varepsilon_d \tag{3}$$

$$\sigma = \sigma_d = \sigma_s \tag{4}$$

where the subscript (m) is used to designate constants in the Maxwell model. By combining these equations, we obtain the desired

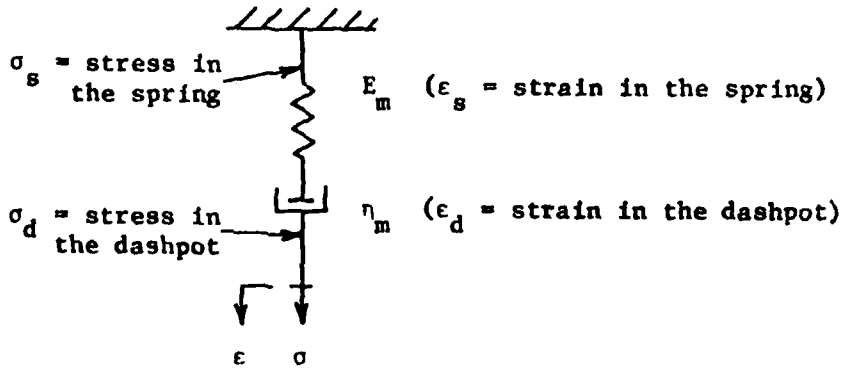

Figure 2. Maxwell Model

stress-strain equation:

$$\varepsilon = \frac{\sigma}{E_m} + \int_0^t \frac{\sigma}{\eta_m} \, d\tau \tag{5}$$

Equation 5 enables you to predict the strain in terms of a time-dependent stress. For the special case in which the stress is constant (creep test):

$$\varepsilon = \frac{\sigma}{E_m} + \frac{\sigma}{\eta_m} t \tag{6}$$

The ratio of strain-to-stress in the creep test is the "creep compliance", D, and for a Maxwell model we find

$$D = \frac{\epsilon}{\sigma} = \frac{1}{E_m} + \frac{t}{\eta_m} \qquad (7)$$

which is illustrated in Figure 3. We see that this model does not reproduce the curvature observed in actual creep data.

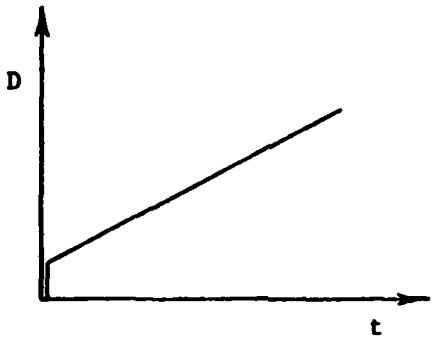

Figure 3. Creep Compliance of the Maxwell Model

Voigt Model: Another way of combining the elements in Figure 1 is to place them in parallel, as shown in Figure 4.

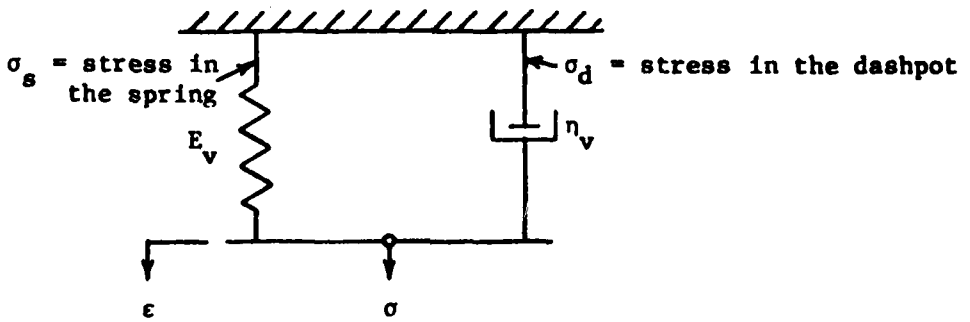

Figure 4. Voigt Model

The governing equations are:

$$\sigma_d = \eta_v \frac{d\varepsilon_d}{dt} \tag{8}$$

$$\sigma_s = E_v \varepsilon_s \tag{9}$$

$$\varepsilon = \varepsilon_d = \varepsilon_s \tag{10}$$

$$\sigma = \sigma_s + \sigma_d \tag{11}$$

which yield the stress-strain equation

$$\sigma = E_v \varepsilon + \eta_v \frac{d\varepsilon}{dt} \tag{12}$$

Equation 12 is a linear differential equation connecting stress and strain; it enables you to calculate stress, given the time-dependent strain, or vice versa.

For example, when the stress is constant the solution to this differential equation produces the creep compliance,

$$D = \frac{\varepsilon}{\sigma} = \frac{1}{E_v} (1-e^{-t/\tau_v}) \tag{13}$$

where $\tau_v \equiv \eta_v/E_v$ is called the retardation time. This compliance is illustrated in Figure 5.

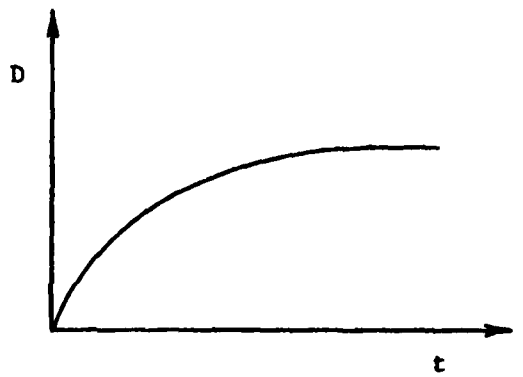

Figure 5. Creep Compliance of the Voigt Model

The creep compliances shown in Figures 3 and 5 are not general enough to represent most real materials. As a means of generalizing the model, one can combine the Maxwell and Voigt models in different ways. For example, if we add the Maxwell and Voigt models in series to obtain the model shown in Figure 6, the creep compliance illustrated in Figure 7 results; note that when the model in Figure 6 is under a

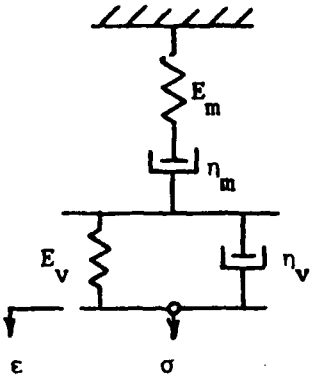

Figure 6. Series Arrangement of Maxwell and Voigt Models

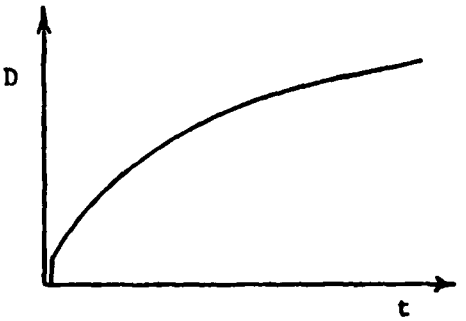

Figure 7. Creep Compliance of Model in Figure 6

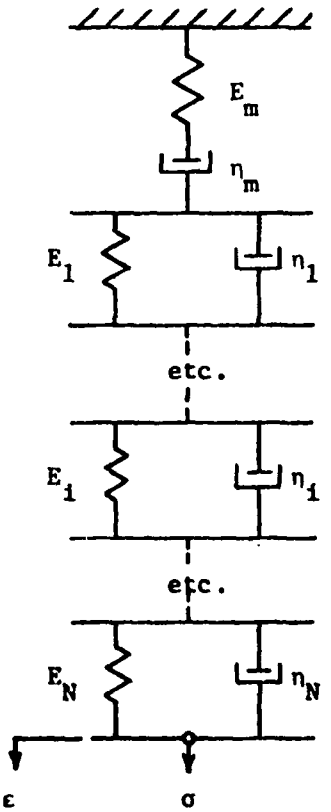

Figure 8. Kelvin Model

constant stress, the Voigt and Maxwell models are each under this same constant stress, which allows us to simply add the

creep compliances of each:

$$D = D_{max.} + D_{vo.} = \frac{1}{E_m} + \frac{t}{\eta_m} + \frac{1}{E_v}(1-e^{-t/\tau_v}) \qquad (14)$$

Kelvin Model: Obviously, when several Voigt models are added in series to one Maxwell element, the overall creep compliance is

$$D = \frac{1}{E_m} + \frac{t}{\eta_m} + \sum_{i=1}^{N} \frac{1}{E_i}(1-e^{-t/\tau_i}) \qquad (15)$$

where the subscript (i) refers to the modulus and viscosity of the i^{th} Voigt model. This general representation is called a "Kelvin model" and is illustrated in Figure 8; in order to characterize the creep of polymeric materials over their usually broad time range of variation, it is often necessary to use ten or more Voigt models arranged in series.

The Voigt and Maxwell models can be combined in other ways, but it can be shown that all other combinations are mathematically equivalent to the special arrangement in Figure 8 if the total number, N, is sufficiently large; the particular arrangement one chooses to use is based only upon convenience.

It is to be noted that the dashpot at the top of Figure 8 produces a continuously increasing strain under constant stress. Some materials, such as crosslinked polymers, do not have this unlimitted flow behavior and consequently this dashpot should be excluded in representing these materials.

Response of the general Kelvin model was derived above for only the special case of constant stress. A more general

relation between stress and strain can be obtained by returning to the underlying differential equations governing the behavior of this model. Alternatively, this generalization can be accomplished using the linear "black-box" theory given in the following section.

II. Linear Black-Box Theory

With this approach, the viscoelastic material is considered to be simply a "black-box", which means we do not know or attempt to specify a priori the contents of the box. We work directly with the input and response after specifying certain mathematical properties.

It is assumed that the black-box is linear, which means it satisfies the following two properties when stress and strain are taken as the input and response, respectively:

1) Superposition:

$$\varepsilon[\sigma + \sigma_1] = \varepsilon[\sigma] + \varepsilon[\sigma_1] \tag{16}$$

2) Proportionality:*

$$\varepsilon[\beta\sigma] = \beta\,\varepsilon[\sigma] \qquad (\beta = \text{constant}) \tag{17}$$

where $\sigma = \sigma(t)$ and $\sigma_1 = \sigma_1(t)$ are two different stress histories. Also, the strain, in general, depends on the entire stress histories, and not just instantaneous values of stress; the expression $\varepsilon[\sigma]$, for example, should be read "strain is a function of the stress history", or, equivalently, "strain is a functional of stress".

Any material that satisfies equations (16) and (17)

---

*Some authors call equation (17) the "homogeniety property,"

is said to be linearly viscoelastic.

Note, for example, that the stress-strain equation (5) for the Maxwell model satisfies these properties. Specifically, the strain due to the first stress history, $\sigma(t)$, is

$$\varepsilon[\sigma] = \frac{\sigma}{E_m} + \int_0^t \frac{\sigma d\tau}{\eta_m} \tag{18}$$

and the strain due to the second history is

$$\varepsilon[\sigma_1] = \frac{\sigma_1}{E_m} + \int_0^t \frac{\sigma_1}{\eta_m} d\tau \tag{19}$$

We now calculate the strain due to the stresses acting together to check the superposition property:

$$\varepsilon[\sigma + \sigma_1] = \frac{\sigma + \sigma_1}{E_m} + \int_0^t \frac{\sigma + \sigma_1}{\eta_m} d\tau$$

$$= \frac{\sigma}{E_m} + \int_0^t \frac{\sigma}{\eta_m} d\tau + \frac{\sigma_1}{E_m} + \int_0^t \frac{\sigma_1}{\eta_m} d\tau$$

Thus,

$$\varepsilon[\sigma + \sigma_1] = \varepsilon[\sigma] + \varepsilon[\sigma_1] \tag{20}$$

The last equation shows that the strain due to the combined loading is equal to the sum of the strains from each stress history. In order to check the homogeneity property set

$$\sigma_1 = \beta\sigma \qquad (\beta = \text{constant}) \tag{21}$$

in equation (19),

$$\varepsilon[\sigma_1] = \varepsilon[\beta\sigma] = \frac{\beta\sigma}{E_m} + \int_0^t \frac{\beta\sigma}{\eta_m} d\tau$$

$$= \beta\left[\frac{\sigma}{E_m} + \int_0^t \frac{\sigma}{\eta_m} d\tau\right]$$

Thus,

$$\varepsilon[\beta\sigma] = \beta\,\varepsilon[\sigma] \tag{22}$$

which shows that a proportional change in stress causes a proportional change in strain.

Without resorting to models now, let us derive a general stress-strain relationship based on linearity properties (16) and (17). We start by defining the creep compliance, $D = D(t)$, as the strain response due to a constant, unit stress applied at $t = 0$:

$$D(t) = \varepsilon[\sigma] \text{ for } \sigma = \begin{cases} 0, & t<0 \\ 1, & t>0 \end{cases} \tag{23}$$

According to the homogeneity property, when the stress is not unity but has some other constant value σ,

$$\varepsilon = \varepsilon\,[\sigma \cdot 1\,] = \sigma\ \varepsilon\ [1] = \sigma\ D(t)$$

or

$$\frac{\varepsilon}{\sigma} = D(t) \tag{24}$$

which shows that the ratio of strain to any constant area is independent of the stress magnitude and is equal to the creep compliance.

The creep compliance in (24) is shown to depend explicitly on the time, t, as measured from first application of the load, but not on the absolute value of time as measured say, from the time at which a material was made. Some materials change with age due to post-curing, drying, chemical degradation, etc. To characterize them, explicit dependence on absolute time should be taken into account along with the time during which the load is applied; inclusion of such effects creates no fundamental difficulty in deriving stress-strain equations, but is beyond the scope of these notes.

Now suppose the two-step stress history shown in Figure 9a, which can be represented as the sum of the two separate stress histories shown in Figures 9b and 9c, is applied to a specimen.

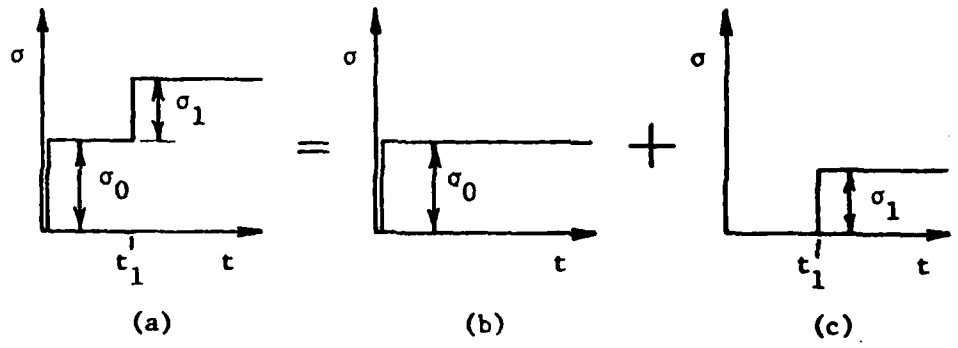

Figure 9. Two-step Stress History

If only the constant stress, σ_0, had been applied, the strain would be

$$\varepsilon_0 = D(t)\ \sigma_0 \tag{25}$$

Similarly the strain due to only σ_1 would be

$$\varepsilon_1 = D(t-t_1)\ \sigma_1 \tag{26}$$

where the time difference, $t-t_1$, enters in equation (26) because this is the time that has elapsed since application of σ_1. The superposition property (16) implies that the strain due to the originally given stress in Figure 9a can be calculated by adding equations (25) and (26); thus, when $t>t_1$:

$$\varepsilon[\sigma] = \varepsilon[\sigma_0 + \sigma_1] = D(t)\ \sigma_0 + D(t-t_1)\ \sigma_1 \tag{27}$$

Of course, (25) is to be used when $t<t_1$.

If the stress history consists of the series of steps

shown in Figure 10, the obvious generalization of (27) for $t_M < t < t_{M+1}$ is

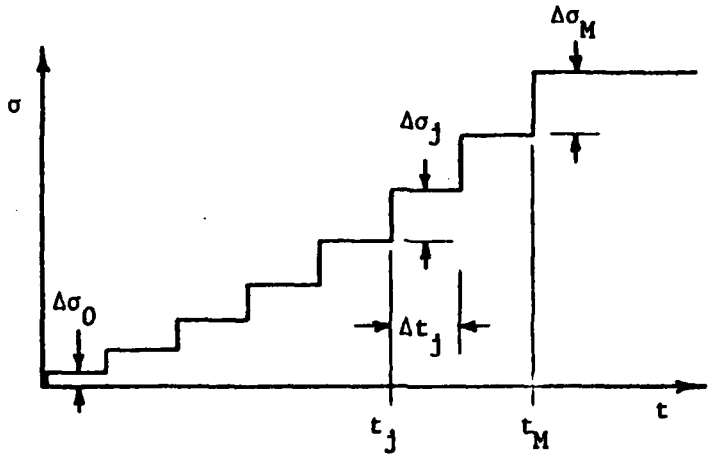

Figure 10. Multiple-step Stress History

$$\varepsilon = \sum_{j=0}^{M} D(t-t_j)\,\Delta\sigma_j \tag{28}$$

where $t_0 \equiv 0$; $\Delta\sigma_0$ corresponds to σ_0 in Figure 9.

Equation (28) enables you to calculate the strain history due to a staircase-type stress history in terms of the single material property, D(t), which was measured under a constant stress.

The generalization of this equation to a continuously varying stress follows immediately by writing

$$\Delta\sigma_j = \frac{\Delta\sigma_j}{\Delta t_j}\,\Delta t_j$$

and then taking the limit

$$\varepsilon = \underset{\substack{M\to\infty \\ \Delta t_j \to 0}}{\mathrm{LIM}} \sum_{j=0}^{M} D(t-t_j)\,\frac{\Delta\sigma_j}{\Delta t_j}\,\Delta t_j \tag{29}$$

which is simply the definition of the integral

$$\varepsilon = \int_0^t D(t-\tau) \frac{d\sigma}{d\tau} d\tau \qquad (30)$$

in which t_j has been replaced by the "dummy" variable of integration τ.

Equation (30)[5] relates continuous strain and stress histories through a single material property function, D(t). By proper interpretation, this integral can also be used with discontinuously applied stresses, as in Figure 10, and with stress history consisting of continuous and discontinuous regions. In order to extract equation (27) from (30), for example, one must be careful to interpret the dummy variable of integration, τ, as the time at which each (finite or infinitesimal) change in stress occurs. Thus, based on Figure 9a we write

$$\frac{d\sigma}{dt} = 0 \qquad (31)$$

except when $t = 0$ and $t = t_1$. The integral (30) becomes

$$\varepsilon = \int_0^{\delta} D(t-\tau) \frac{d\sigma}{d\tau} d\tau + \int_{t_1-\delta}^{t_1+\delta} D(t-\tau) \frac{d\sigma}{d\tau} d\tau \qquad (32)$$

where δ is a very small positive number.

Since $\delta \ll 1$, the compliance is essentially independent of the variable of integration and therefore can be placed outside the integrals,

$$\varepsilon = D(t-o) \int_0^{\delta} \frac{d\sigma}{d\tau} d\tau + D(t-t_1) \int_{t_1-\delta}^{t_1+\delta} \frac{d\sigma}{d\tau} d\tau$$

$$= D(t)\, \sigma_0 \Big|_0^{\delta} + D(t-t_1)\, \sigma \Big|_{t_1-\delta}^{t_1+\delta} \qquad (33)$$

---

[5] This integral is often called the "Boltzmann superposition integral" or a "hereditary law".

which reduces to (27) when the stresses are evaluated at the limits.

So far we have derived equations which express strain as a function of stress history. If the stress is known, strain can be predicted by numerical or analytical integration . On the other hand, it is desirable to have an inverse form of the stress-strain equation when strain history is given. The derivation of this latter equation is accomplished in a manner that is entirely analogous to the above procedure except that the roles of stress and strain are reversed. By analogy, therefore,

$$\sigma = \int_0^t E(t-\tau) \frac{d\varepsilon}{d\tau} \, d\tau \qquad (34)$$

Here, the material property is the relaxation modulus, $E(t)$; it is equal to σ/ε when σ is the stress due to a strain applied at $t=0$ and held constant thereafter (relaxation test).

The creep compliance and relaxation modulus in equations (30) and (34) , respectively, are not independent; only one is needed to completely define the stress-strain behavior of any given material. Their interrelationship can be deduced by specializing equation (34) to a creep test. For this case, the strain is given by equation (24), which, when substituted into (34), yields

$$1 = \int_0^t E(t-\tau) \frac{dD}{d\tau} \, d\tau \qquad (35)$$

This equation is called a "linear integral equation"; it enables one to calculate the creep compliance, given the relaxation modulus, and vice versa. Methods of solving such equations are beyond the scope of this report, but are described in the literature.[6]

Creep and Recovery Test: Although the stress-strain equations (30) and (34) are relatively general, they are restricted to behavior which is, at least, approximately linear. A common method of experimentally checking linearity is to obtain creep compliance data at several constant stresses; then, in view of equation (24), it is customary to assume the material is linearly viscoelastic as long as the compliance is (approximately) independent of stress. An analogous procedure is often followed using relaxation data.

Strictly speaking, however, stress-independence of the creep compliance (or strain-independence of the relaxation modulus) is a necessary, but not sufficient, condition for linearity. An additional check on linearity, and the superposition property (16) in particular, can be made using data from a creep and recovery test, which is illustrated in Figure 11. (In this test, a constant stress is applied up to the time t_1 and then removed; strain is measured during both

---

[6] See, for example: M.L. Williams, "The Structural Analysis of Viscoelastic Materials," AIAA J. (May 1964); J.D. Ferry, Viscoelastic Properties of Polymers, John Wiley & Sons, Inc. (1961).

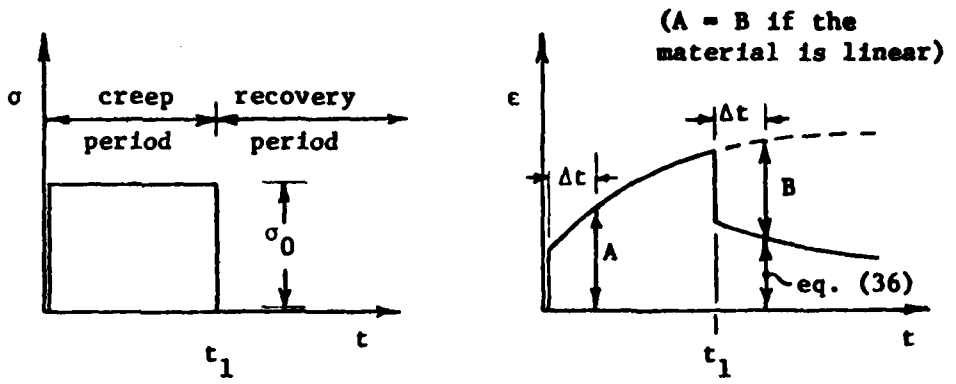

(a) Stress history (b) Strain history

Figure 11. Creep and Recovery Test

creep and recovery periods.) Strain in the recovery period is compared with that predicted by equation (30) or, equivalently, by equation (27) after setting $\sigma_1 = -\sigma_0$:

$$\varepsilon = \{D(t) - D(t-t_1)\}\sigma_0 \qquad (t > t_1) \tag{36}$$

We see that recovery strain (36) can be predicted from creep strain by the simple graphical procedure illustrated in Figure 11b; namely, the recovery strain at any time, $t > t_1$, is equal to the creep strain that would have existed if the stress had remained on the material, $D(t)\,\sigma_0$, minus the creep strain due to a stress applied at t_1, $D(t-t_1)\,\sigma_0$ (indicated by B in Figure 11b).

In view of equation (36), it is also seen that the ratio of recovery strain-to-stress, ε/σ_0, is independent of stress if the material is linear.

Constant Stress Rate Test: Another stress history that

permits an easy verification of the linear theory is shown in Figure 12. When the constant stress rate, $\frac{d\sigma}{d\tau} = R$ (R = constant)

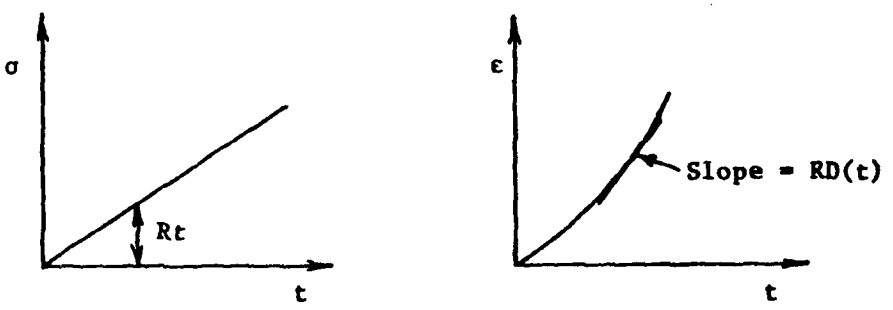

Figure 12. Constant Stress Rate Test

is substituted into equation (30) we find

$$\varepsilon = R \int_0^t D(t-\tau)d\tau \tag{37}$$

Change the variable of integration to u,

$$u \equiv t-\tau, \quad du = -d\tau$$

and obtain

$$\varepsilon = -R \int_t^0 D(u)\, du = R \int_0^t D(u)du \tag{38a}$$

which can be differentiated to find

$$\frac{d\varepsilon}{dt} = RD(t) \tag{38b}$$

The creep compliance of many plastics obeys the power law

$$D = D_0 + D_1 t^n \tag{39}$$

(which is a special case of the Kelvin model (15) when $N = \eta_m = \infty$)[6]

where D_0, D_1 and n are positive constants. For this case, equation (38a) can be integrated analytically,

$$\varepsilon = R \int_0^t (D_0 + D_1 u^n) du = R(D_0 t + \frac{D_1}{1+n} t^{1+n})$$

$$= \sigma(D_0 + \frac{D_1}{1+n} t^n) \qquad (40a)$$

The constant-strain-rate secant compliance

$$\frac{\varepsilon}{\sigma} = D_0 + \frac{D_1}{1+n} t^n \qquad (40b)$$

is, therefore, essentially equal to the creep compliance when $n << 1$.

Concluding Remarks: In concluding this section on isothermal behavior there are a few points we want to emphasize. Specifically:

1. All stress-strain equations derived from mechanical models consisting of Hookean springs and Newtonian dashpots can be shown to satisfy linearity properties (16) and (17). Therefore, all such equations are contained in equations (30) and/or (34). What the mechanical model does is provide an explicit form for the modulus and compliance. If, for example, we represent the material by a Maxwell model, the creep compliance is given by equation (7). The relaxation modulus for this same material can be obtained by solving integral equation (35) or by resorting to the differential equation governing the model behavior. The latter method is

not difficult to use with a Maxwell model; equation (5) is first differentiated with respect to time,

$$\frac{d\varepsilon}{dt} = \frac{1}{E_m}\frac{d\sigma}{dt} + \frac{\sigma}{\eta_m} \tag{41}$$

and then solved for a constant strain input:

$$\varepsilon = \begin{cases} 0, & t < 0 \\ \text{constant}, & t > 0 \end{cases}$$

It can be verified directly by substitution that the solution to (41) is an exponentially decaying stress,

$$\sigma = \varepsilon\, E_m e^{-t/\tau_m} \tag{42}$$

where $\tau_m \equiv \eta_m/E_m$ is the "relaxation time" of the Maxwell model; consequently, the relaxation modulus is

$$E(t) = E_m e^{-t/\tau_m} \tag{43}$$

Thus, for a Maxwell material, strain response to an arbitrary stress history is calculated using equation (30), or (5), along with D(t) given by (7), and stress response to an arbitrary strain history is calculated using equations (34) and (43).

2. The conditions (16) and (17) do not place any limitations on the time-dependent form of the creep compliance and relaxation modulus. However, it can be shown from principles of non-equilibrium thermodynamics[7] that all real materials can be represented by the Kelvin model in Figure 8. In

---

[7] M.A. Biot, "Linear Thermodynamics and the Mechanics of Solids," Proc. Third U.S. National Congress of Applied Mechanics (1958).

addition, all other combinations of springs and dashpots can always be reduced to this model.

3. We have discussed relations connecting only uniaxial stress and strain. Viscoelastic stress-strain equations for multiaxial loading, which are often needed in the analysis of engineering structures can be found throughout the literature on viscoelastic analysis[6,7,8].

III. Nonisothermal Behavior

An introduction to the temperature dependence of mechanical behavior is given in the two books.[1,2] Analytical representation of the effect of temperature on polymeric materials will be discussed here.

The nonisothermal behavior of polymeric materials can be characterized using the same mechanical models described above, except the spring moduli and dashpot viscosity coefficients may now depend on temperature. The primary effect of temperature on amorphous polymers is to change the latter properties. With crystalline polymers, in addition to this effect, the spring moduli may vary significantly as the temperature is changed due to softening or melting of the crystalline regions. Here we shall discuss only amorphous polymers.

---

[8] W. Flugge, Viscoelasticity, Blaisdell Publishing Co. (1967).

There is a good deal of experimental evidence that all of the viscosity coefficients of an amorphous material are affected equally by temperature[6]; namely, for the Kelvin model we write

$$\eta_m = a_T \eta_m' , \quad \eta_i = a_T \eta_i' \ (i = 1,2,\ldots N) \tag{44}$$

where the primed properties are, by definition, independent of temperature, and a_T represents the effect of temperature on the material. (Deviations from this behavior have been observed for an uncrosslinked polymer, in that the coefficient, a_T, in η_m is different from the one used to describe temperature dependence of η_i[9].

Upon substituting this special representation into equation (15), we find that the creep compliance can be expressed in terms of a single argument,

$$\xi \equiv t/a_T . \tag{45}$$

Thus,

$$D = \frac{1}{E_m} + \frac{\xi}{\eta_m'} + \sum_{i=1}^{N} \frac{1}{E_i}(1-e^{-\xi/\tau_i'}) \tag{46}$$

in which the retardation times, $\tau_i' \equiv \eta_i'/E_i$, are now constant; the variable ξ reflects both time and temperature dependence and is often called "reduced time" in the polymer literature[6] and "temperature compensated time" in the metals literature[10].

---

[9] D.J. Plazek, "Temperature Dependence of the Viscoelastic Behavior of Polystyrene," J. Physical Chemistry (October 1965).

[10] O.D. Sherby and J.E. Dorn, "Some Observations on Correlations Between Creep Behavior and the Resulting Structures in Alpha Solid Solutions," Journal of Metals (February 1953).

The initial value of compliance, $1/E_m$, may also depend on temperature, especially if the temperature is below the glass transition value, T_g; but we shall neglect this dependence in the subsequent discussion.

The significance of the simple temperature dependence in (46) is illustrated in Figure 13, in which creep compliances obtained at

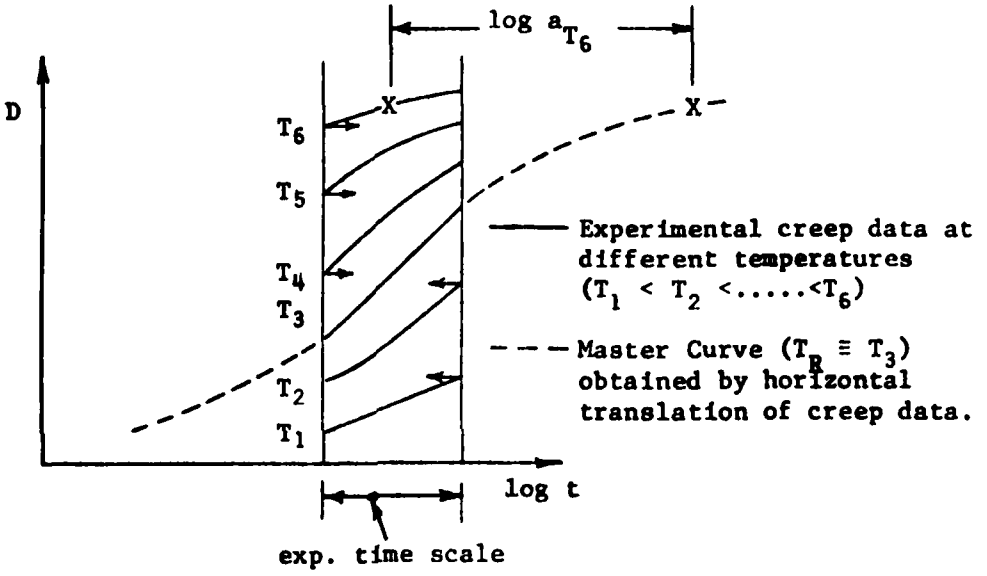

Figure 13. Creep Compliance Curves at Different Temperatures

several constant temperatures are plotted on semi-log paper. Equation (46) implies that these curves can be superposed by rigid horizontal translations; this follows from the fact that the only difference between the curves is in their time scale, and the time-scale factor a_T in (45) is additive on a logarithmic scale,

$$\log t/a_T = \log t - \log a_T$$

Any one of these curves can be chosen as the reference compliance for which $a_T = 1$. The horizontal distance required to

superpose another curve on this reference one is equal to log a_T.

The distance log a_T is positive when a shift to the left is required, and negative when the required shift is to the right. That this is the correct sign convention can be easily checked by recognizing that a material at a temperature lower than the reference value has a smaller compliance (i.e., it is stiffer) and therefore its compliance will lie to the right of the reference one; this behavior is predicted by (46) when log a_T is greater than zero or, equivelently, a_T is greater than one.

Dependence of the creep compliance on temperature through the reduced time parameter, ξ, implies that the relaxation modulus depends on temperature through the same parameter, as this is the only way equation (35) can be satisfied at all times.

The composite (dashed) curve in Figure 13 obtained by shifting data at different temperatures is generally called the "master curve". Typically, it may cover as many as ten or twenty decades of reduced time over its full range of variation. Although the master curve is nothing but the creep compliance at the reference temperature, this range makes it impossible to determine directly the entire compliance (or modulus) by conducting tests at the single temperature T_R.

Materials that can be characterized in terms of a common time and temperature parameter, ξ, are called "thermorheologically simple" (unfortunately!).

These materials allow one to make long-time predictions without actually having to test the material over an extended

time scale. For example, suppose that the design of a certain part requires the prediction of deflection over a period of 20 years. One could run short-time creep tests at several temperatures above and equal to the expected service temperature, T_R say, shift the data to derive a_T and the master curve, then predict the long-time compliance at the service temperature. Obviously, this accelerated testing method will not be valid when chemical degradation or other aging phenomena exist due to the long use period.

The so-called "shift factor", a_T, for amorphous polymers can be expressed analytically, with the particular form depending on whether or not the temperature is above or below the glass transition value, T_g. When $T < T_g$, the familiar Arrhenius relation usually can be used,

$$\log_{10} a_T = \frac{\Delta F}{2.303R} \left(\frac{1}{T} - \frac{1}{T_R}\right) \tag{47}$$

where ΔF is the activation energy per gram mole and $R = 1.987$ (cal/g-mole°K) is the universal gas constant; when $\log_{10} a_T$ is plotted against the reciprocal of absolute temperature, $1/T$, a straight line results, as shown in Figure 14A. On the other hand, when $T > T_g$ the so-called WLF equation normally applies;

$$\log_{10} a_T = -C_1(T-T_R)/(C_2 + T-T_R) \tag{48}$$

where C_1 and C_2 are constants; this factor is generally drawn as shown in Figure 14B. Equation (48) is different than the

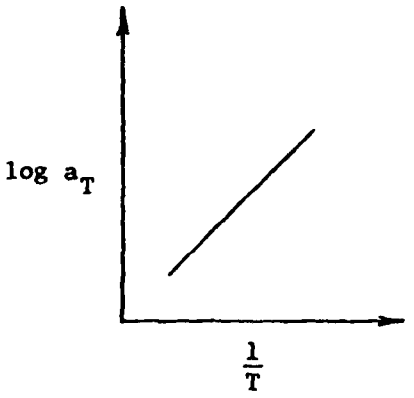

Figure 14A Arrhenius Shift Factor

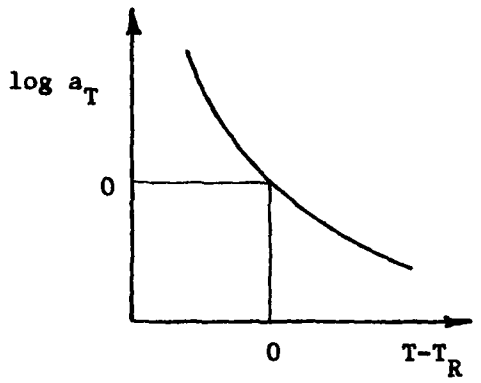

Figure 14B WLF Shift Factor

Arrhenius form (47) because the molecular mechanism for creep and relaxation above the glass transition temperature is different from that below. Equation (48) is based on the notion that molecular mobility above the glass transition temperature depends on the amount of "free volume" or "holes" available for molecular rearrangement ; as a material is heated the free volume expands, just as the overall volume of a specimen expands, thereby leading to a reduction in viscosity.

It can be easily shown that the form of equation (48) is independent of the choice of T_R; the values of C_1 and C_2 do, however, depend on T_R. Moreover, it has been found that C_1 and C_2 do not vary appreciably from material to material when T_R is approximately 50°C above the glass transition temperature, and for this case have the values

$$C_1 = 8.86 \qquad (°C^{-1})$$
$$C_2 = 101.6 \qquad (°C) \tag{49}$$

When a material is thermorheologically simple, data obtained at constant temperatures can be used to predict the response under transient temperatures. In order to see this, consider first the Maxwell model in Figure 2. Write the viscosity coefficient as

$$\eta_m = a_T \eta_m' \tag{50}$$

and then substitute this into equation (5),

$$\epsilon = \frac{\sigma}{E_m} + \int_0^t \frac{\sigma}{\eta_m'} \frac{d\tau}{a_T} \tag{51}$$

Introduction of a new variable of integration ξ', defined by

$$\xi' \equiv \int_0^\tau du/a_T \tag{52a}$$

or, equivalently,

$$d\xi' \equiv d\tau/a_T \tag{52b}$$

renders equation (51) in the form

$$\epsilon = \frac{\sigma}{E_m} + \int_0^\xi \frac{\sigma}{\eta_m'} d\xi' \tag{53}$$

where

$$\xi \equiv \xi'(t) = \int_0^t \frac{du}{a_T} \tag{54}$$

Notice that equation (53) is identical to (5) at $T = T_R$ except

the reduced time, ξ, is used in place of real time. Also, when the temperature is independent of time a_T is constant and (54) reduces to (45).

Under a constant stress and transient temperature equation (53) yields

$$\varepsilon = \frac{\sigma}{E_m} + \frac{\sigma}{\eta'_m}\,\xi \tag{55}$$

which, in turn, provides the creep compliance

$$D = \frac{1}{E_m} + \frac{\xi}{\eta'_m} \tag{56}$$

Notice that this compliance is simply the "master curve", which was defined above as the isothermal creep compliance at temperature T_R.

Thus, to predict creep under a transient temperature, one first calculates reduced time according to equation (54) and then evaluates the master curve at this value.

Similarly, it is not hard to show that creep of a material described by the general Kelvin model in equation (15) can be predicted in the same way; i.e., use the master curve,

$$D = \frac{1}{E_m} + \frac{\xi}{\eta'_m} + \sum_{i=1}^{N} \frac{1}{E_i}\,(1-e^{-\xi/\tau'_i}) \tag{57}$$

and calculate reduced time from equation (54).

Generalization of equations (30) and (34) to include transient temperatures can be accomplished in a similar way by using reduced times (52) and (54) in place of τ and t, respectively. For

example, it can be shown that the stress-strain equation (30) for a thermorheologically simple material under a transient temperature is given by

$$\varepsilon = \alpha(T-T_R) + \int_0^{\xi} D(\xi-\xi') \frac{d\sigma}{d\xi'} d\xi' \qquad (58)$$

With changing temperatures one normally must take into account the thermal expansion, $\alpha(T-T_R)$, shown in this equation; notice that in the absence of stress, equation (58) predicts simple linear expansion, $\varepsilon = \alpha(T-T_R)$.

A POWER LAW SUPERPOSITION METHOD

A simple method for using the measured elongations of uniaxial tensile specimens of polyethylene balloon film, subject to a constant stress (Creep Test), to predict the stresses resulting in the same material when it is subjected to a linearly increasing strain has been demonstrated.

The creep tests were performed at each of three temperatures ranging from -22°C to +43°C. The data were then used to predict the results of constant strain rate tests at intermediate temperatures and at a cold temperature as low as -80°C. This is an especially important result in light of the fact that a semi-crystalline material such as that tested was not expected to have a useful or predictable time-temperature interrelationship.

Several simplifying techniques were incorporated into the analyses including a linear time-temperature shift, a simple power law representation of the tensile modulus and the normal assumption that the modulus and compliance were reciprocals. These features are important because they permit the analyses to be based on the simplest possible laboratory tests and because the calculations can be quickly performed. In other words, these techniques provide an excellent tool for "back of the envelope" type calculations.

Polyethylene, a common balloon grade film, was used in these tests. The film, with a trade name Stratofilm, was extruded by Winzen Research Inc. Polyethylene is a crystalline polymer specially blown and annealed to produce a balanced mechanical behavior. Films designated by the manufacturer as 1/2, 3/4 and 1 mils in thickness (with probable errors in thickness of 5%) were used. The creep tests were performed over a wide range of temperatures by dead weight loading. Each sample was epoxied

between pairs of aluminum end tabs. The samples were temperature conditioned for several hours prior to loading. Once the loads were applied, readings were taken until equilibrium was established in the creep behavior. The loads were then removed and the extension was again charted until recovery equilibrium was established.

In the constant strain rate tests, samples were cut to have a ten inch gage length and a one inch width. They were gripped between rubber-cork faced one inch square plates and pulled until the force-extension trace showed equilibrium well into the plastic flow region. As ultimate strengths are drastically influenced by edge effects due to sample cutting, the majority of the tests were terminated after extensive plastic flow but before actual fracture. Tests were performed at $38^{o}C$, $23^{o}C$, $-23^{o}C$, and $-80^{o}C$ and at each temperature, rates of 2%, 20%, and 200% per minute were used.

Master Curves for the Creep Behavior of Polyethylene Film

Plots of strain versus time were obtained from constant stress creep tests at several temperatures. At selected points the compliance (ε/σ) was calculated. The log compliance was plotted versus log of the time. At this point there were three curves of log D vs. log t for each thickness and direction of material. This is because at lower temperatures the compliance will always be lower than at warmer temperatures.

The theory behind the master curve is that for a given temperature, the creep curve after a long period of time will have the same shape as a curve for a warmer temperature at a lower value of time. (Figure 15)

Figure 15

Therefore, doing several tests at different temperatures should yield data valid for a longer period of time than it took to run the tests.

A reference temperature (the temperature of the curve which is not shifted) of 50°F was used for the master curves. The curves for other temperatures were then shifted along the time axis until they lined up with the 50°F curve. The distance they were shifted was measured and recorded on each sheet. There is a separate curve for each combination of of material thickness and direction.

Time-Temperature Shift

If it is desired to predict the mechanical behavior of an amorphous polymer outside of the temperature range over which it has been characterized in the laboratory it is necessary initially to presuppose the validity of a time-temperature shift equation. Doolittle has suggested

$$\log_{10} a_T = \frac{(T - T_g)}{2.303^{\phi}_g \left[\left(\frac{\phi_g}{\alpha_e - \alpha_g} \right) + (T - T_g) \right]} \qquad (59)$$

where a_T is the well known time-temperature shifting factor; $^{\phi}g$ is the fractional free volume at T_g, the glassy transition temperature; and $(\alpha_e - \alpha_g)$ is the difference in the coefficients of thermal expansion above

and below T_g. All temperatures are in degrees K. Stratofilm however fails to exhibit a time-temperature interrelationship of this form. Neither the results of constant stress creep tests nor of the constant strain rate tests could be fit to this hyperbolic form. At least three factors are believed to account for this failure to shift; 1) The relatively high degree of oriented crystallinity 2) The nearness of the material melting point temperature to the hotter test temperatures and 3) The associated, uncorrected, large stresses and strains.

Consequently an artificial time-temperature shift was empirically devised. It was selected so as to give a reduced relaxation modulus curve that would at least approximately fit the results of both the creep tests and constant strain rate tests that were performed during the program. A straight line shift was selected and, if the reference temperature is selected as 0°C, its equation can be expressed for $T > T_g$ as

$$\log a_T = -0.160\ T + 1.20 \tag{60}$$

This equation is shown plotted in Fig. 16

Algebraic Representation of Laboratory Data

It was desired to formulate a representation of the viscoelastic stiffness properties that would be simple and yet reasonably relate the stresses and strains over a broad time-temperature span. To do this, a simple power law relaxation function was assumed which, when plotted on log-log paper, is straight line. Such a curve is of the algebraic form

$$D(t) = D_1 \left(t/a_T\right)^n \tag{61}$$

where D_1 is constant, n is the log-log slope, and a_T the time-temperature shift factor shown in Fig. 16. The sign of n is negative indicating a relaxing (when subjected to a constant strain) material. The usual way of determining D(t) in the laboratory is to impose a constant stress, σ_0, and monitor the increasing strain, $\varepsilon(t)$. This permits one to write

$$D_{crp}(t) = \varepsilon(t)/\sigma(t) \tag{62}$$

where the subscripted D_{crp} implies the compliance was evaluated by a creep test. In an analogous manner in the relaxation test a constant strain, ε_0, is imposed and the responding stress, $\sigma(t)$, are monitored to give a modulus.

$$E(t) = E_1 \left(t/a_T\right)^{-n} \tag{63}$$

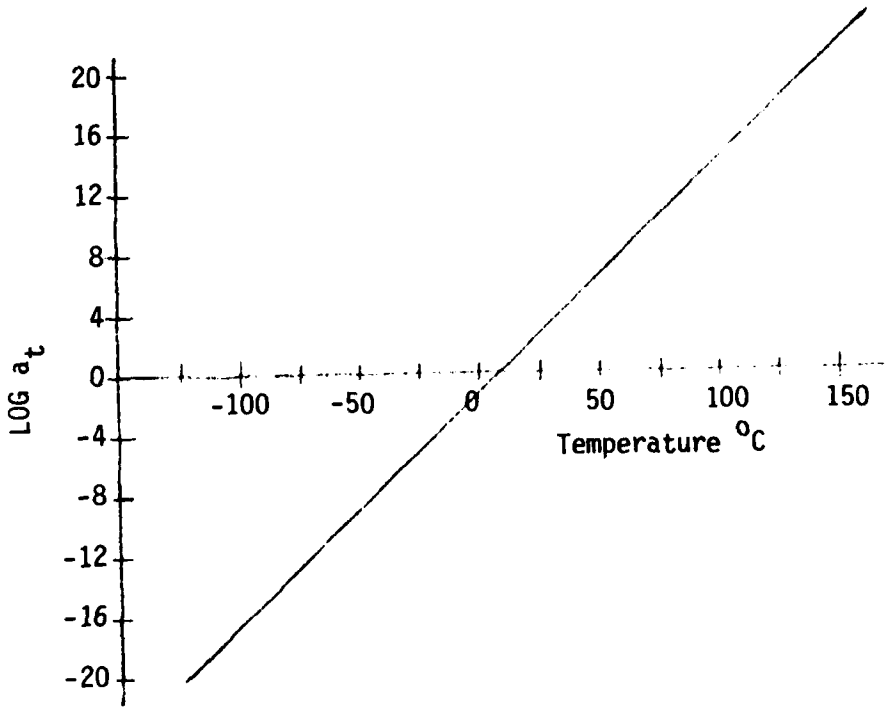

Figure 16. Proposed Temperature Shift Factor for Stratofilm

Figures 17 and 18 show the experimental data that resulted from the creep tests in the machine and transverse directions respectively. The points were shifted in accordance with Fig. 16. Remembering that both scales are logarithmic, the experimental scatter is readily apparent. Indeed, it is so great, that conclusions concerning the effects of film thickness and test direction cannot be drawn. However, one conclusion can be made. If the moduli resulting from the 500 psi tests is compared with those from the 1000 psi tests it is readily apparent that Stratofilm is more compliant when subjected to a higher stress level. This phenomenon is often referred to as stress (or strain) softening, and is especially pronounced in Stratofilm at the higher temperatures.

The fit of straight lines through the data of Figs. 17 and 18 resulted in the following equations which empirically represent the results of the laboratory creep tests.

$$D(t) = \frac{1}{25{,}000} \left(t/a_T\right)^{0.11} \quad \text{for 1000 psi in machine direction}$$

$$D(t) = \frac{1}{35{,}000} \left(t/a_T\right)^{0.08} \quad \text{for 500 psi in machine direction}$$

$$D(t) = \frac{1}{21{,}000} \left(t/a_T\right)^{0.13} \quad \text{for 1000 psi in transverse direction}$$

$$D(t) = \frac{1}{33{,}000} \left(t/a_T\right)^{0.94} \quad \text{for 500 psi in transverse direction}$$

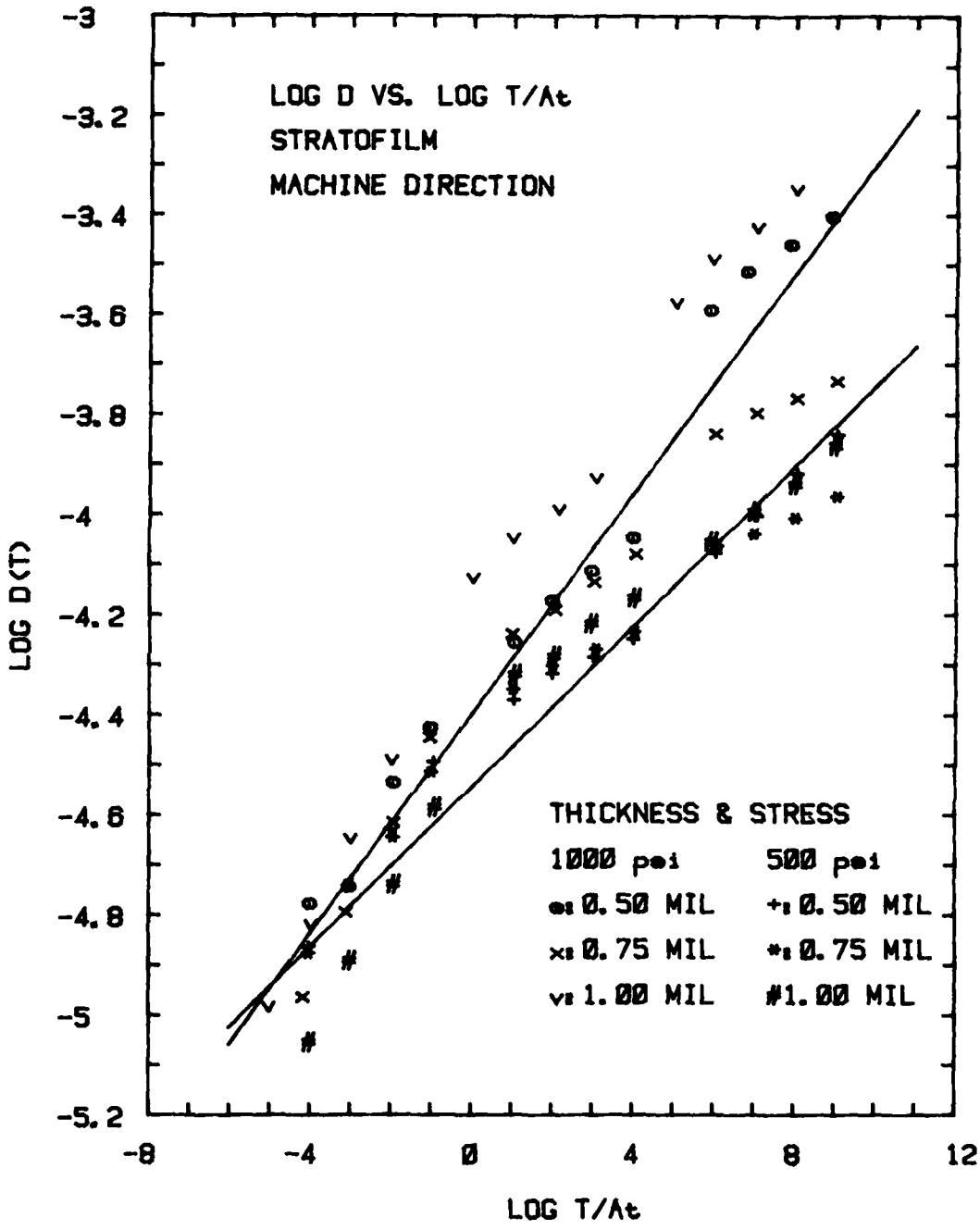

Figure 17. Creep Compliance Deduced from the Uniaxial Creep Tests in the Machine Direction of Stratofilm.

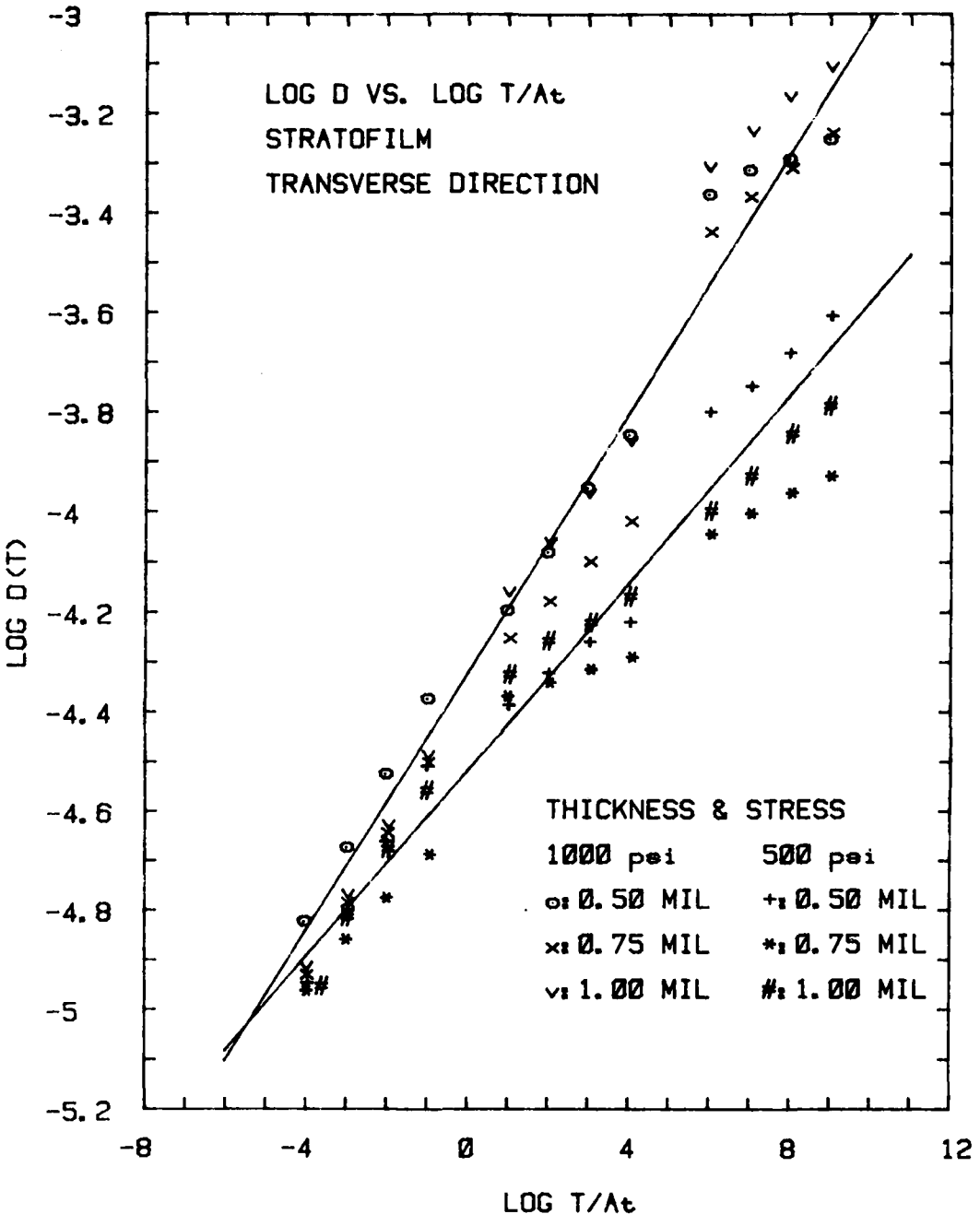

Figure 18. Creep Compliance Deduced from the Uniaxial Creep Tests in the Transverse Direction of Stratofilm.

Constant Strain Rate Tests

Using the master stress relaxation curve representative of laboratory creep test results it is possible to predict the response to other loading histories using the convolution integral. This integral is usually written with the dummy variable, τ, used in the integrand, thus

$$\sigma(t) = \int_0^t \frac{1}{D(t-\tau)} \frac{d\varepsilon}{d\tau} d\tau \qquad (65)$$

The effects of temperature, whether constant or changing as a function of time can be incorporated into the integral simply by inserting the time-temperature shift factor, a_T, and writing

$$\sigma(t) = \int_0^t \frac{1}{D(t/a_T - \tau/a_T)} \frac{d\varepsilon}{d\tau} d\tau \qquad (66)$$

A quasi-solid for which Eq. (66) is valid for reasonable variations of the temperature with time is said to be a thermorheologically simple, viscoelastic material.

Most experimenters will agree that there are very few, if any, materials for which the assumptions of thermorheological simplicity are valid, at least to the degree necessary for Eq. (66) to give predictions accurate enough for engineering use. A sensitive test that defines the extent to which a material is thermorheologically simple is to simultaneously apply a constant stress and a changing temperature. If the convolution equation predicts the observed response to within engineering accuracy, then the assumption of thermorheogical simplicity is valid for most purposes.

This is particularly important to the analyst of balloon film because the temperature changes somewhat predictably during both ascent and float.

A less conclusive test, but one that uses the laboratory data available for Stratofilm, is to see if Eq. (66) in conjunction with the reduced compliance curve will predict the results of constant strain rate tests at intermediate cold temperatures. To do this it is necessary to evaluate Eq. (66) for a constant strain rate, k (cm/cm/min)

$$\frac{\partial \varepsilon}{\partial t} = K \tag{67}$$

and for the reduced compliance

$$D(t) = D_1 \left(t/a_T\right)^n \tag{68}$$

Substituting these simple expressions site Eq. (66) gives for any temperature (constant with respect to time, t)

$$\sigma(t) = \frac{K}{D_1} \frac{1}{a_T{}^n} \int_0^t \frac{d\tau}{(t - \tau)^n} \tag{69}$$

which when integrated and evaluated at the prescribed limits becomes

$$\sigma(t) = \frac{K}{D_1} \frac{t^{1-n}}{a_T{}^{-n} (1 - n)} \tag{70}$$

which is a simple prediction of stress resulting from a specified constant strain rate and temperature. To express stress as a function of strain take equation (67) and substitute ε/K for time, t.

$$\sigma(t) = \frac{k^{n}\ \dot{\varepsilon}^{(1-n)}}{a_T^{-n} D_1^{(1-n)}} \tag{71}$$

The calculations of the predictions for constant strain rate tests at several temperatures actually run in the laboratory have been completed and are plotted in Figures 19a and 19b.

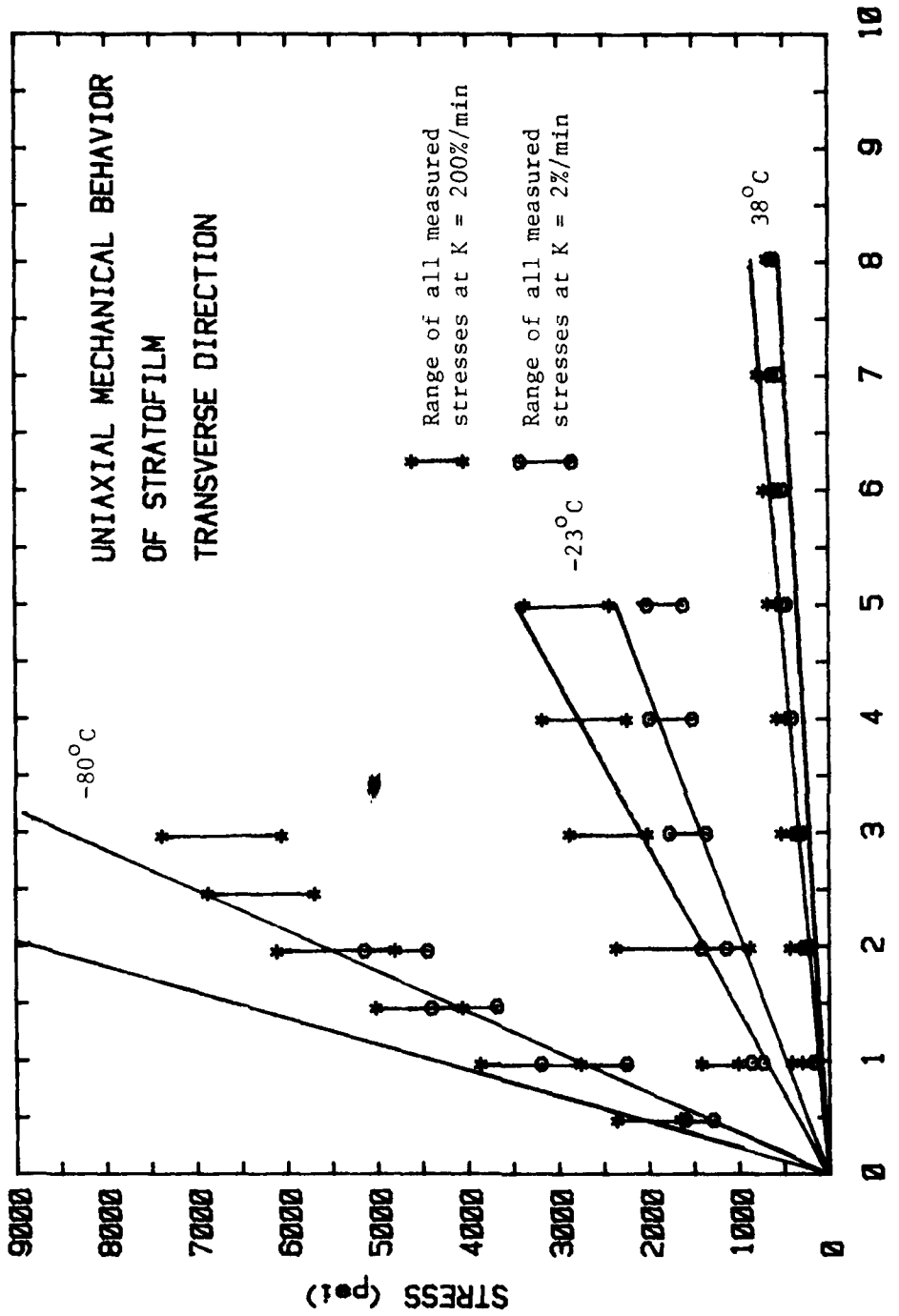

Figure 19A. Comparison of the predicted and measured stresses in stratofilm when subject to two constant strain rates at each of the three temperatures in the transverse direction.

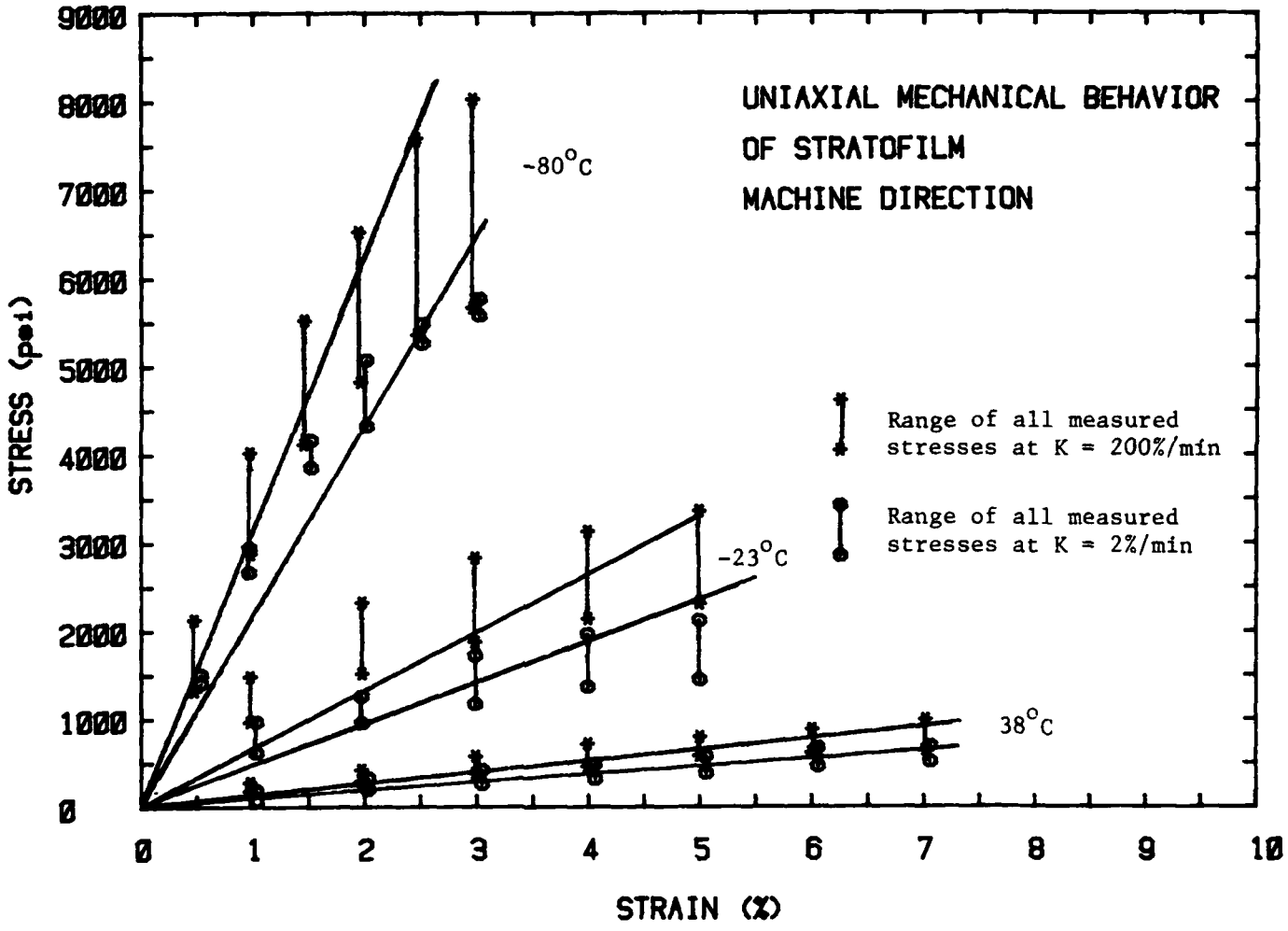

Figure 19B. Comparison of the predicted and measured stresses in the stratofilm when subject to two constant strain rates at each of the three temperatures in the machine direction.

UNIAXIAL CONSTANT STRAIN-RATE TESTS

Winzen Stratofilm, a crystalline polyethylene, was selected for strain rate and temperature characterization studies. Three common film thicknesses of 1/2, 3/4 and 1 mils were each tested at temperatures of +30°C, +23°C, -23°C and -80°C. For each thickness at each temperature a set of five samples was pulled at each of three rates, 2% min, 20%min and 200%min. Further, for each test condition both machine direction (the direction of the film extrusion) and transverse direction were independently tested. This totalled to more than four hundred tests when repeat runs and checks were computed.

The samples were prepared by razor cutting a folded stack of film held under a templet. The blade cutting edge was used for one twelve inch stroke and then discarded. In this manner the sample edge defects were held to a minimum. Each sample was measured for thickness at six locations and an average reading was computed for use in stress evaluation. Each group of five runs were averaged for stress at fixed strain levels and the average result was plotted for each test condition. The results of this study are presented in Figs. 20 through 25. These data formed the basis for the study of the viscoelastic superposition of strain rate and temperature dependence discussed in section Characterization of Viscoelastic Materials.

Included in Fig. 26 is a study of the mechanical behavior of a newly developed balloon film candidate prepared by the Bemis Corporation. For the test conditions used for the Bemis tests, the film is seen to hold possibilities for future use in high altitude balloons.

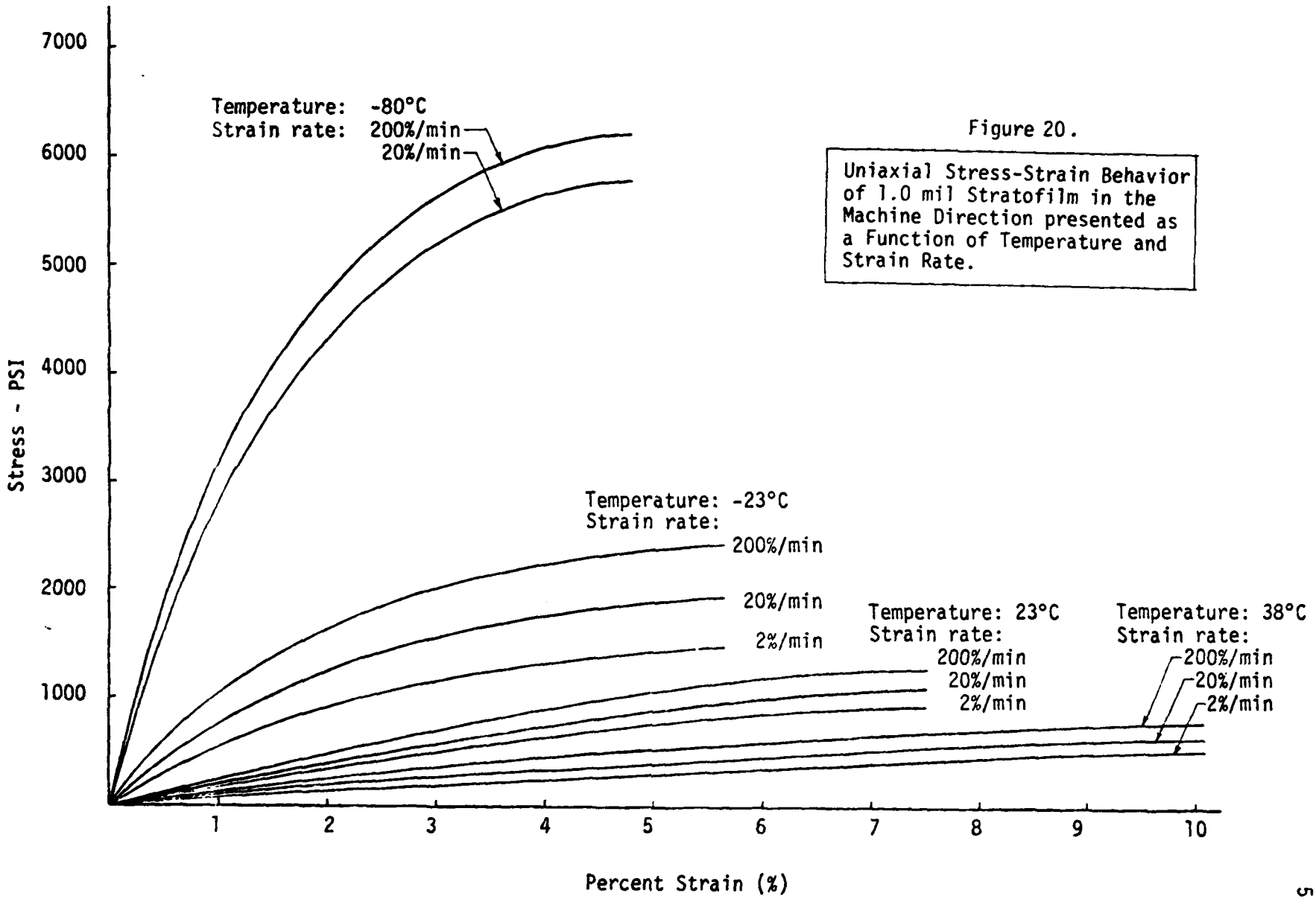

Figure 20.

Uniaxial Stress-Strain Behavior of 1.0 mil Stratofilm in the Machine Direction presented as a Function of Temperature and Strain Rate.

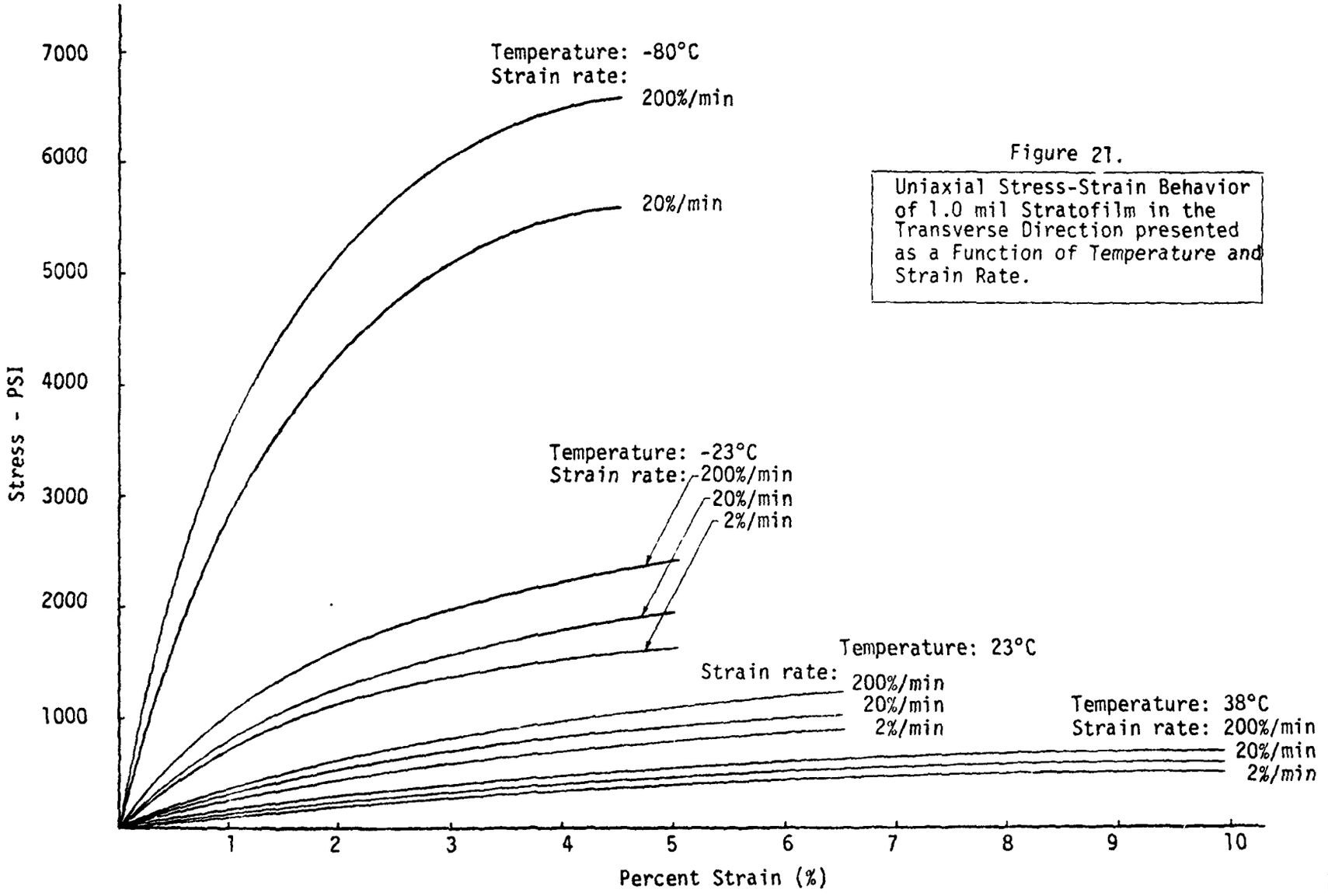

Figure 21.

Uniaxial Stress-Strain Behavior of 1.0 mil Stratofilm in the Transverse Direction presented as a Function of Temperature and Strain Rate.

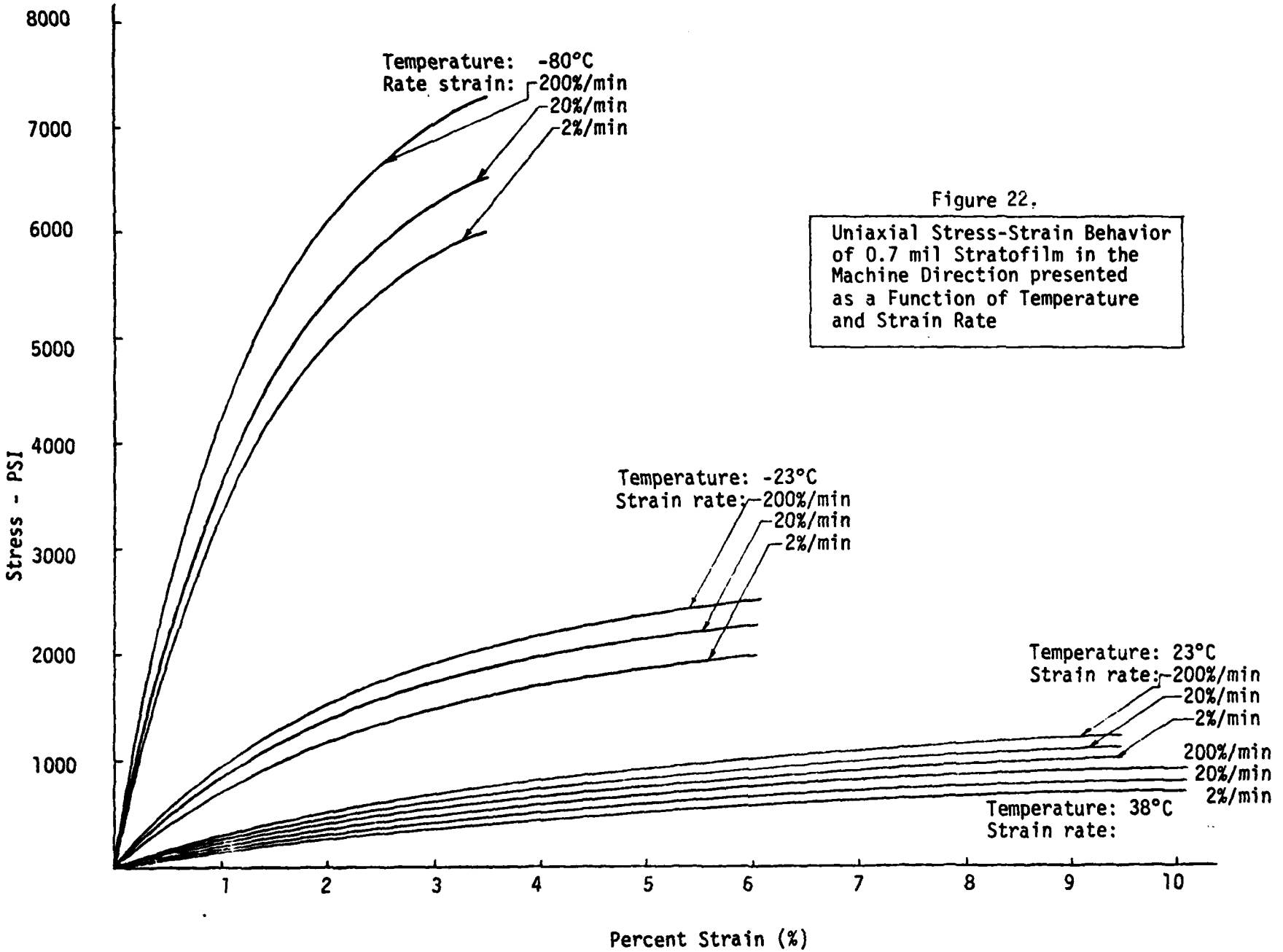

Figure 22.

Uniaxial Stress-Strain Behavior of 0.7 mil Stratofilm in the Machine Direction presented as a Function of Temperature and Strain Rate

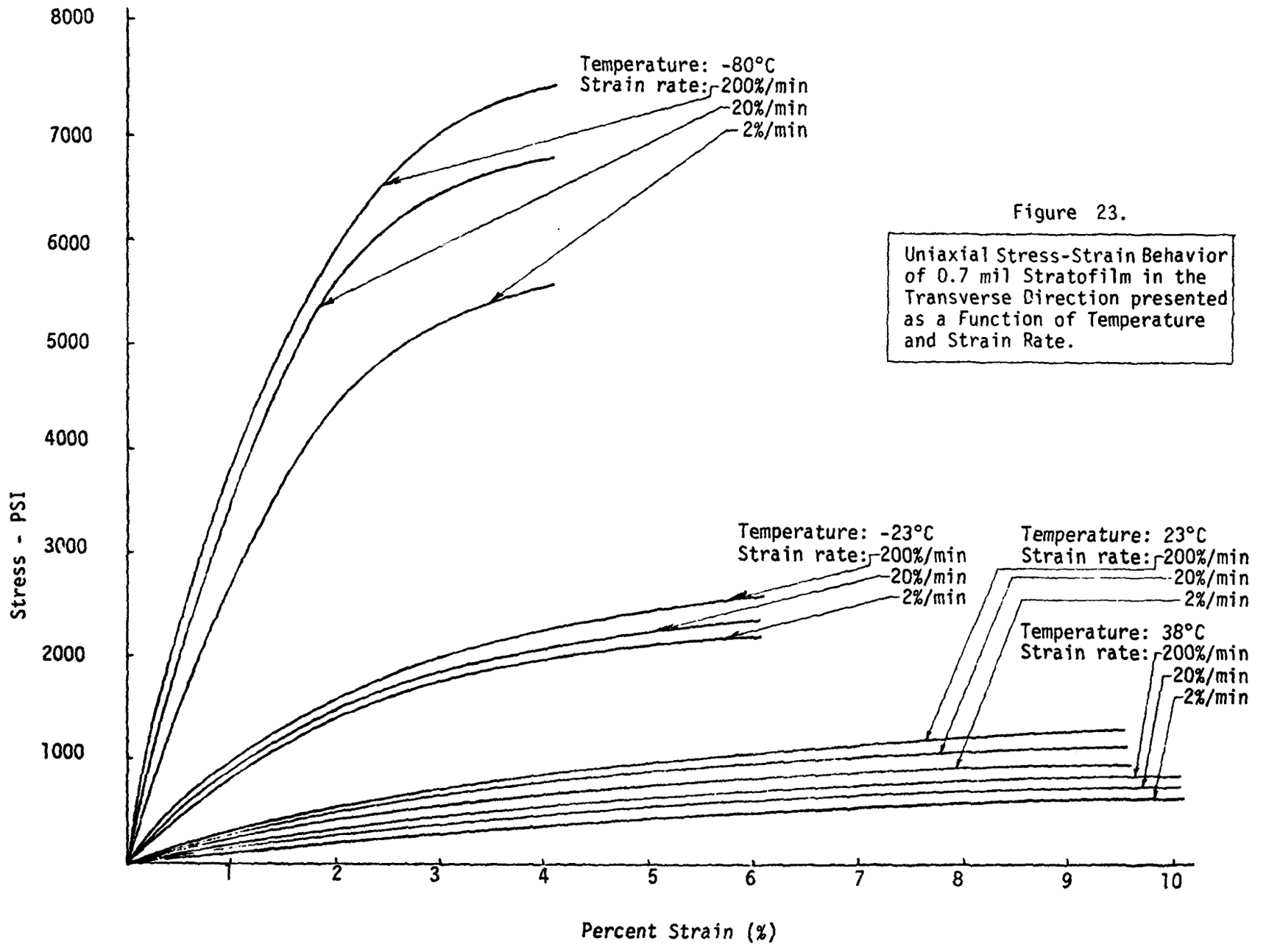

Figure 23.

Uniaxial Stress-Strain Behavior of 0.7 mil Stratofilm in the Transverse Direction presented as a Function of Temperature and Strain Rate.

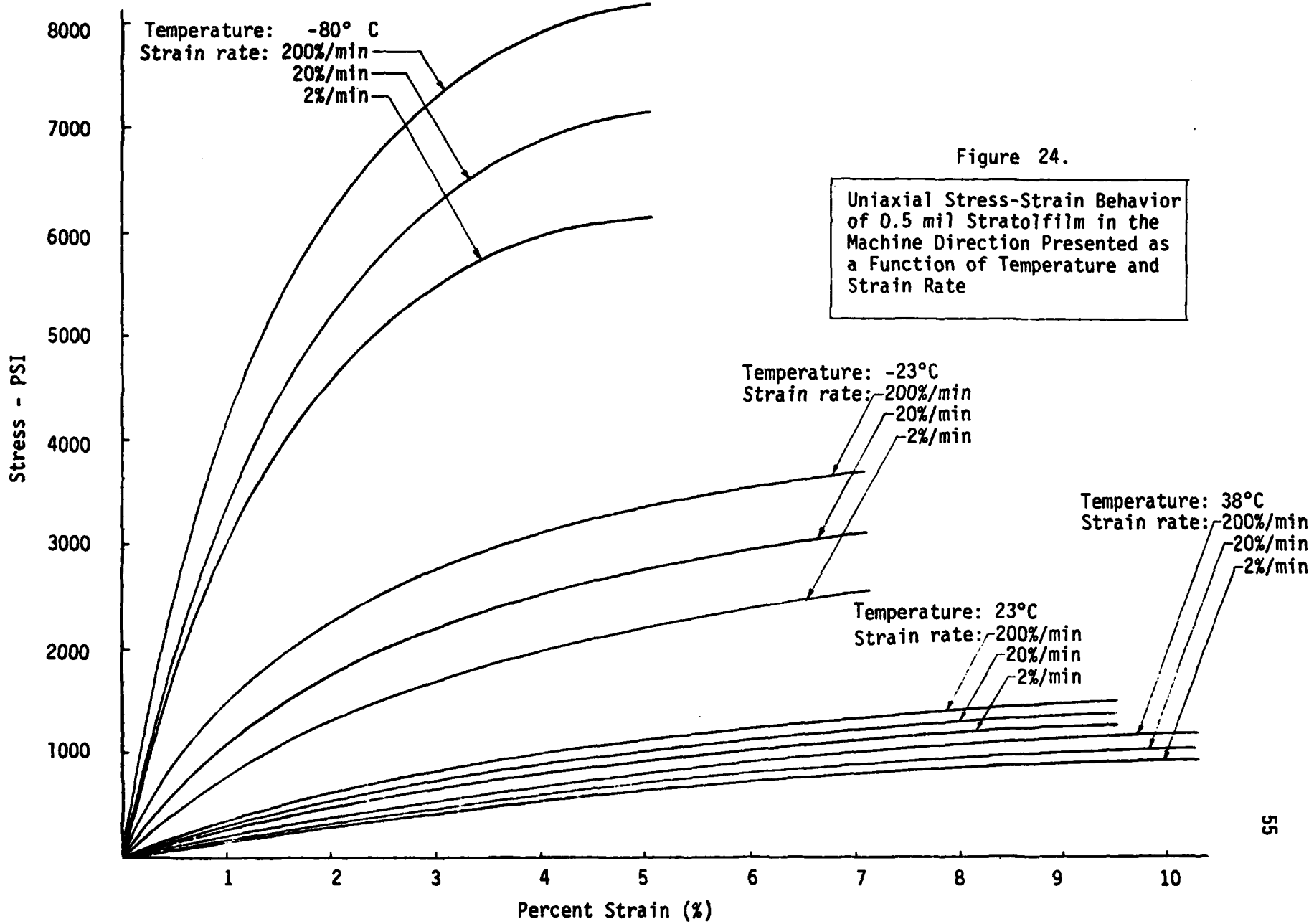

Figure 24.

Uniaxial Stress-Strain Behavior of 0.5 mil Stratolfilm in the Machine Direction Presented as a Function of Temperature and Strain Rate

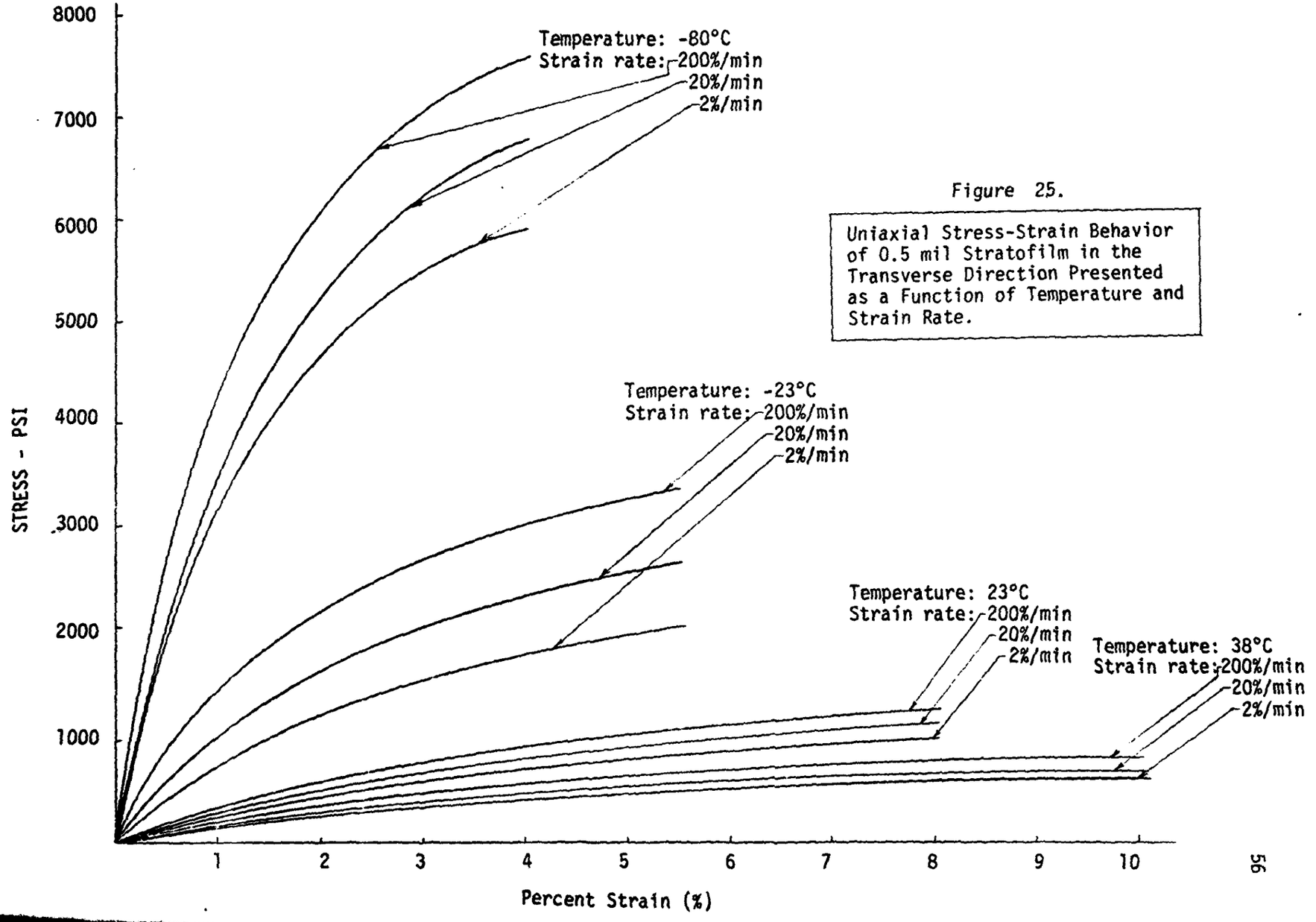

Figure 25.

Uniaxial Stress-Strain Behavior of 0.5 mil Stratofilm in the Transverse Direction Presented as a Function of Temperature and Strain Rate.

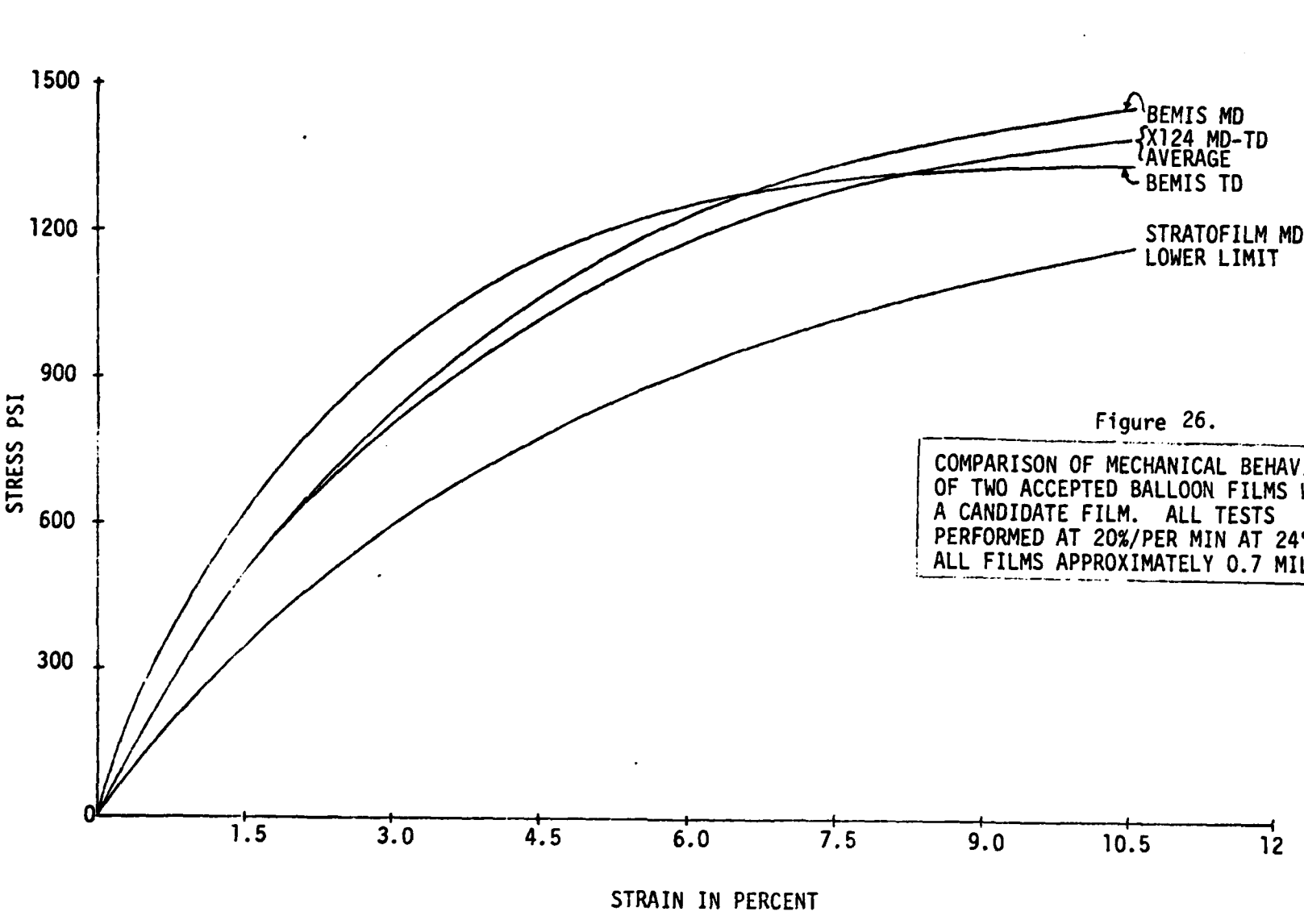

Figure 26.

COMPARISON OF MECHANICAL BEHAVIOR OF TWO ACCEPTED BALLOON FILMS WITH A CANDIDATE FILM. ALL TESTS PERFORMED AT 20%/PER MIN AT 24°C. ALL FILMS APPROXIMATELY 0.7 MIL.

UNIAXIAL CREEP STUDY

Polyethylene balloon grade films sold under Winzen, Inc.'s trade name, Stratofilm, were selected for evaluation. Typical film thicknesses of 0.5, 0.75, and 1.0 mils were cut into one inch wide strips and subsequently epoxy bonded to aluminum end tabs to form ten inch gage length test specimens. Each sample was measured for thickness at six locations and the average value was used for stress calculations. The samples were dead weight loaded in environmental chambers where their extension under constant load was continuously measured. Their creep behavior was observed for stress levels of 500 and 1000 psi under temperature conditions ranging from -17°C to +43°C. A typical run included both load and recovery responses. In Figure 27A is shown a typical data trace of the result of dead weighting a creep sample. At first loading, the sample instantaneously deforms in an elastic manner then begins to deform viscoelastically in an ever slowing fashion. The transition between the immediate deformation and the more slowly developing or time dependent deformation is very smooth.

Mechanically, to avoid an impact loading, each weight was applied smoothly over a period of about one second. The first reading of resulting deformation was five seconds later. The same procedure was followed in reading the recovery portion of the curve. In Figure 27B the creep curve is seen to rebound elastically then recover over a long time period.

To present the creep and recovery data the ordinate, strain, was initialized at the first "five second" reading taken. As shown in Figure 27C this enhances the creep and recovery presentation on a single plot. Examples of these data are presented in Figs. 27D and 27E and were used as the bases of the power law superposition method discussed in pages 36 through 49.

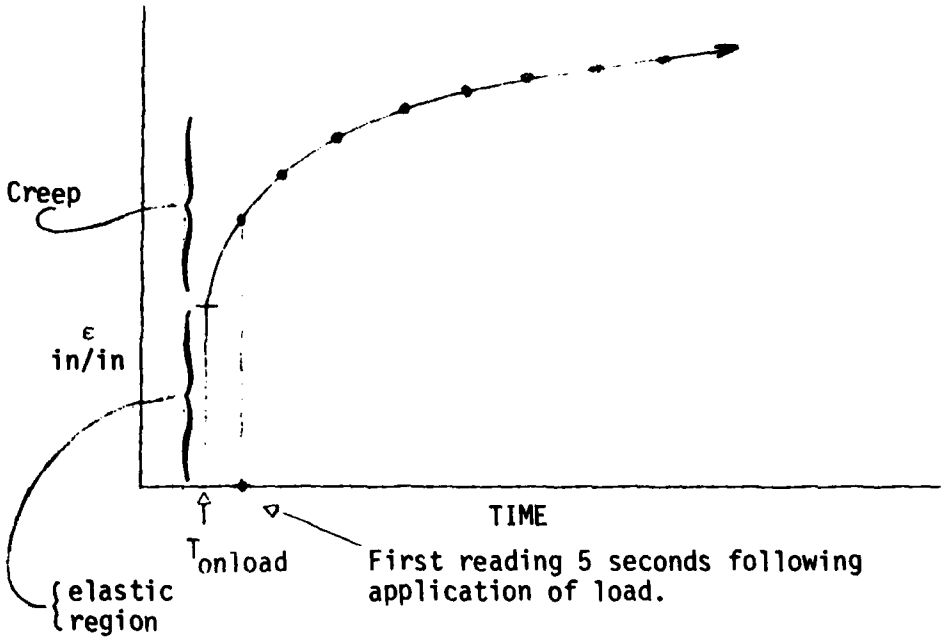

Figure 27A. A plot of strain versus time showing the initial elastic response followed by the time dependent part of strain called creep.

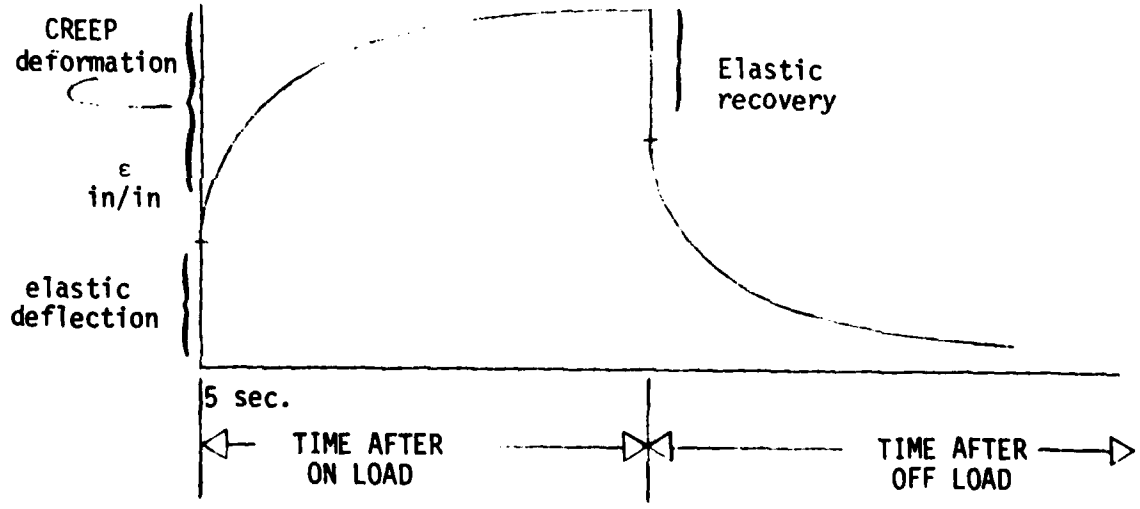

Figure 27B. A plot of strain versus time showing the fully developed "creep" curve followed by recovery strains.

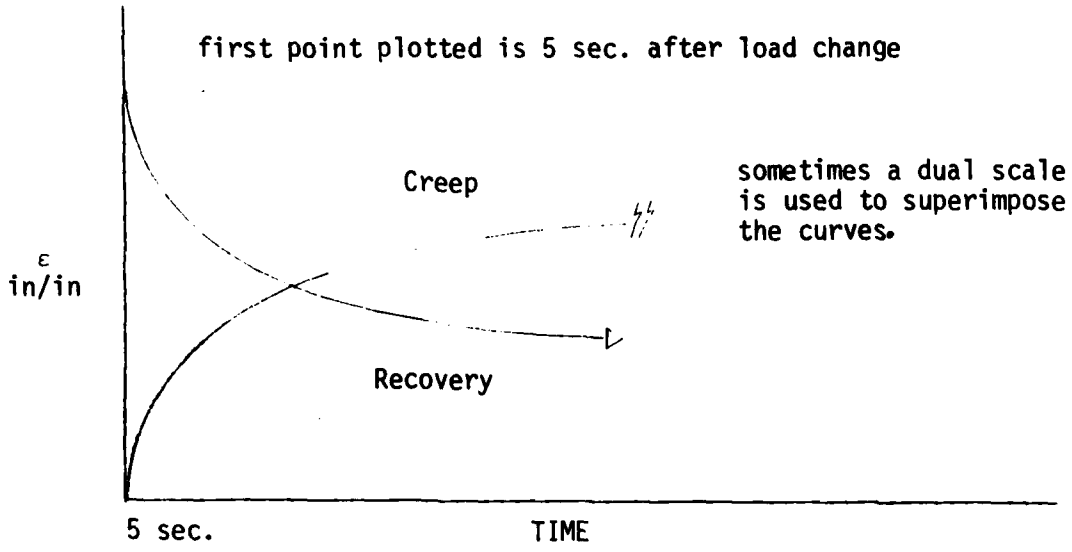

Figure 27C. A plot of creep strain and recovery strain superimposed without the initial linear "quick response" portions shown.

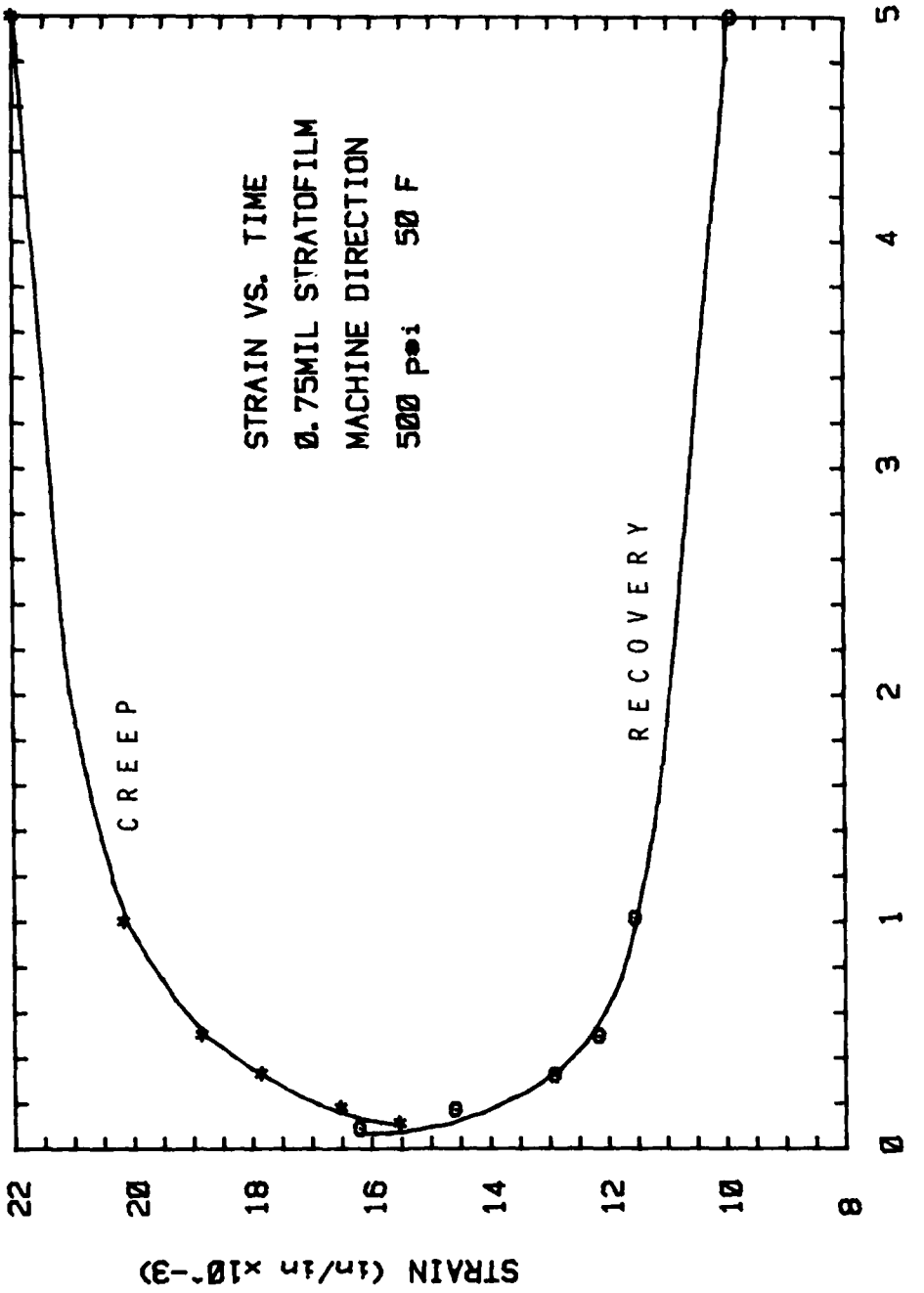

Figure 27D. Creep and Recovery Strain versus Time for 0.75 mil. Stratofilm Loaded in the Machine Direction at a Stress Level of 500 psi at $50^{o}F$.

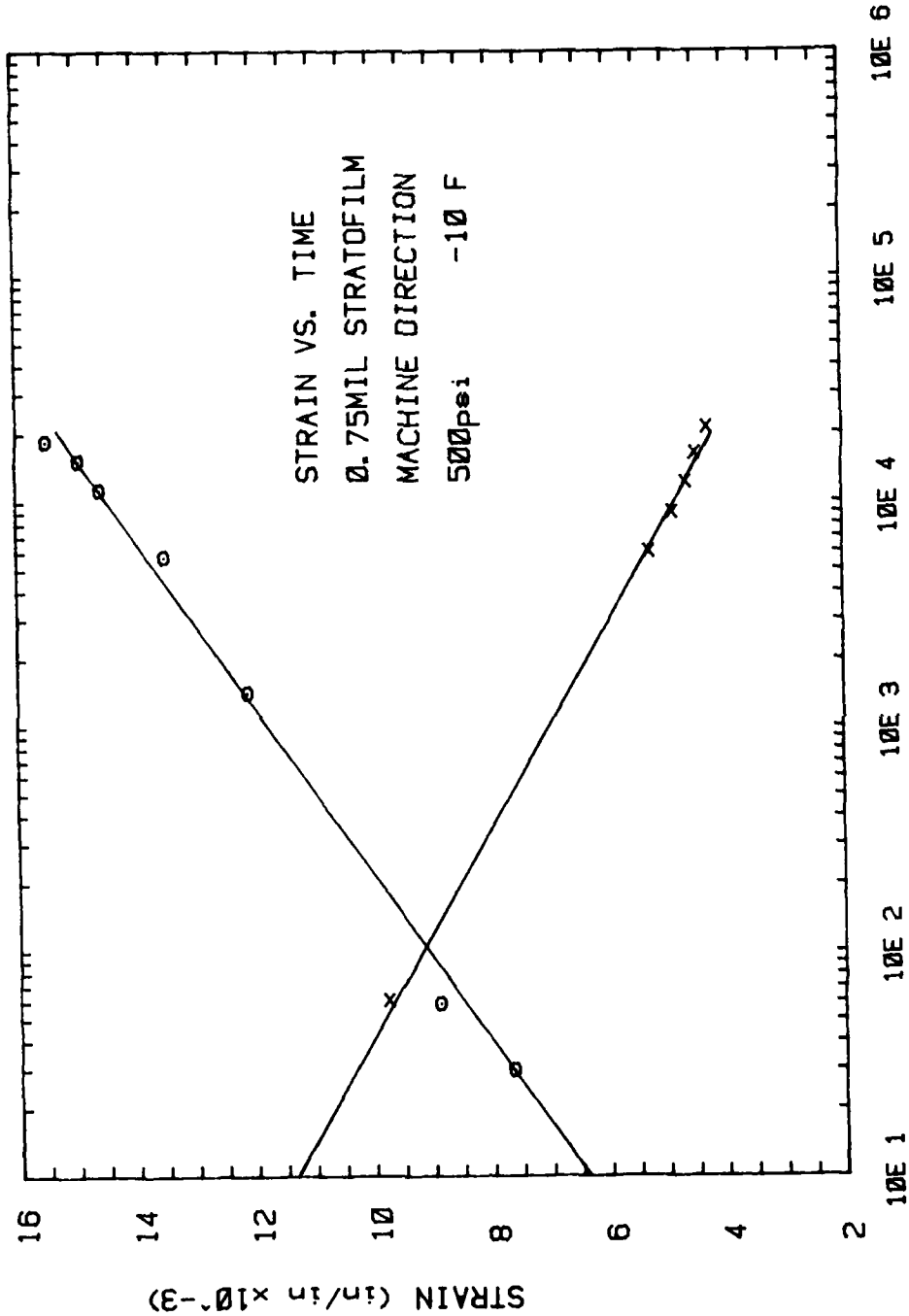

Figure 27E. Strain versus Time for 0.75 mil. Stratofilm Loaded in the Machine Direction at a stress level of 500 psi at -10°F.

AGING STUDY

A balloon built by General Mills and packed in its crate since 1955 was subjected to a variety of tests to determine if any aging effects could be discerned. The film was known to be a DFD 5500 type successfully flown for many years. Because little comparable data were available on the original behavior of this film, comparisons were made to modern Stratofilm.

When the balloon was uncrated, specimens were selected from locations where damage was expected to most probably occur. Flat sections at the bottom of the crate were expected to show the effects of long term creep. Sharp creases in this region were expected to display the effects of any significant stress concentrations. Similar specimens were taken from the top of the crate for comparison purposes. Some film at the top of the crate appeared to have flaws in the form of a small cracks. A group of specimens was removed from this section. In addition, an unusual packing phenomenon was noted. Several folds were laid vertically on the side of the crate and then crushed by the end fittings. Specimens were cut from this region as well. In addition, for each location, film in the region of the heat seal was tested.

All of these films were tested at 23°C and at a constant strain rate of 20%/min. Three specimens at each location were loaded in the "elastic" region and the average stress-strain curve obtained. Tests were conducted in both the machine and transverse directions. Finally, 12 specimens from the top flat locations were tested at -80°C and at 20%/min.--half in the machine direction and half in the transverse direction.

The results of the testing program are presented in the attached figures (28 through 45). It is concluded that there has been no significant degradation in this balloon due to long term creep, chemical changes, or stress concentration due to folding and creasing. The low temperature test failed at 2.5% strain whereas Stratofilm will fail at 4.6% and 3.75% in the machine and transverse directions respectively. However, it is felt that this effect is not a matter of degradation but more a reflection of the change in the formulation of the particular DFD polyethylene.

It is our considered opinion that based on these results, no significant mechanical degradation will occur due to long term storage of polyethylene balloon film in a controlled environment.

Table I

Identification of samples cut from a balloon stored since 1955 showing location of the sample, test direction, and test temperature.

No.	Location	Direction	Temperature
1	Top Flat	Machine	23°C
2	Bottom Flat	Machine	23°C
3	Bottom Crease	Heat Seal	23°C
4	Bottom Crease	Transverse	23°C
5	Packing Fold	Machine	23°C
6	Packing Fold	Transverse	23°C
7	Top Crease	Heat Seal	23°C
8	Bottom Crease	Machine	23°C
9	Top Crease	Transverse	23°C
10	Top Crease	Machine	23°C
11	Top Flat	Heat Seal	23°C
12	Bottom Flat	Heat Seal	23°C
13	Top Flat	Transverse	23°C
14	Bottom Flat	Transverse	23°C
15	Top Flat	Machine	-80°C
16	Top Flat	Transverse	-80°C
17	Top Flat Flawed	Machine	23°C
18	Top Flat Flawed	Transverse	23°C

The following figures, 28 through 45, are plots of stress in psi applied in uniaxial tension presented as a function of induced strain where a common code is used to identify test conditions and sample locations as defined by Table I on page 65. For example, in figure 28, page 67, the term top flat means at the top apex area of the balloon in a region without creases. Machine means the sample was tested along the gore in the film extrusion direction and $23^{o}C$ is the temperature of the test.

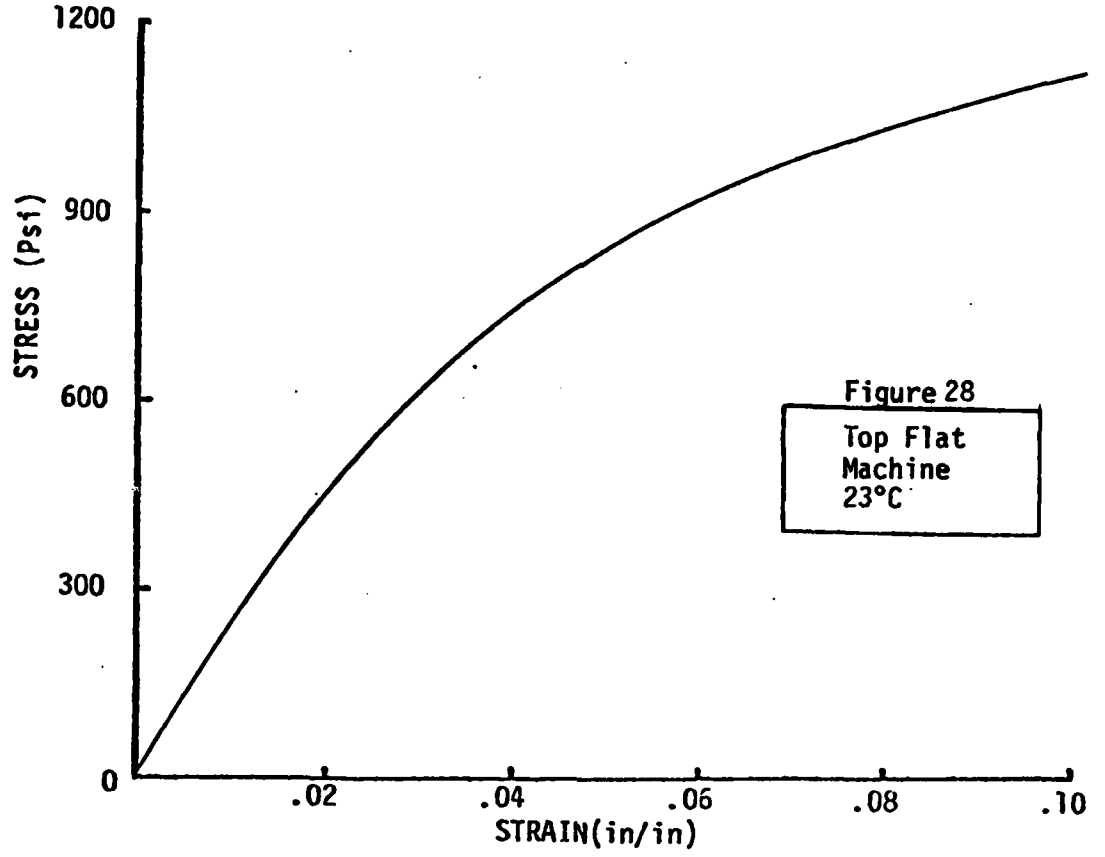

Figure 28

Top Flat
Machine
23°C

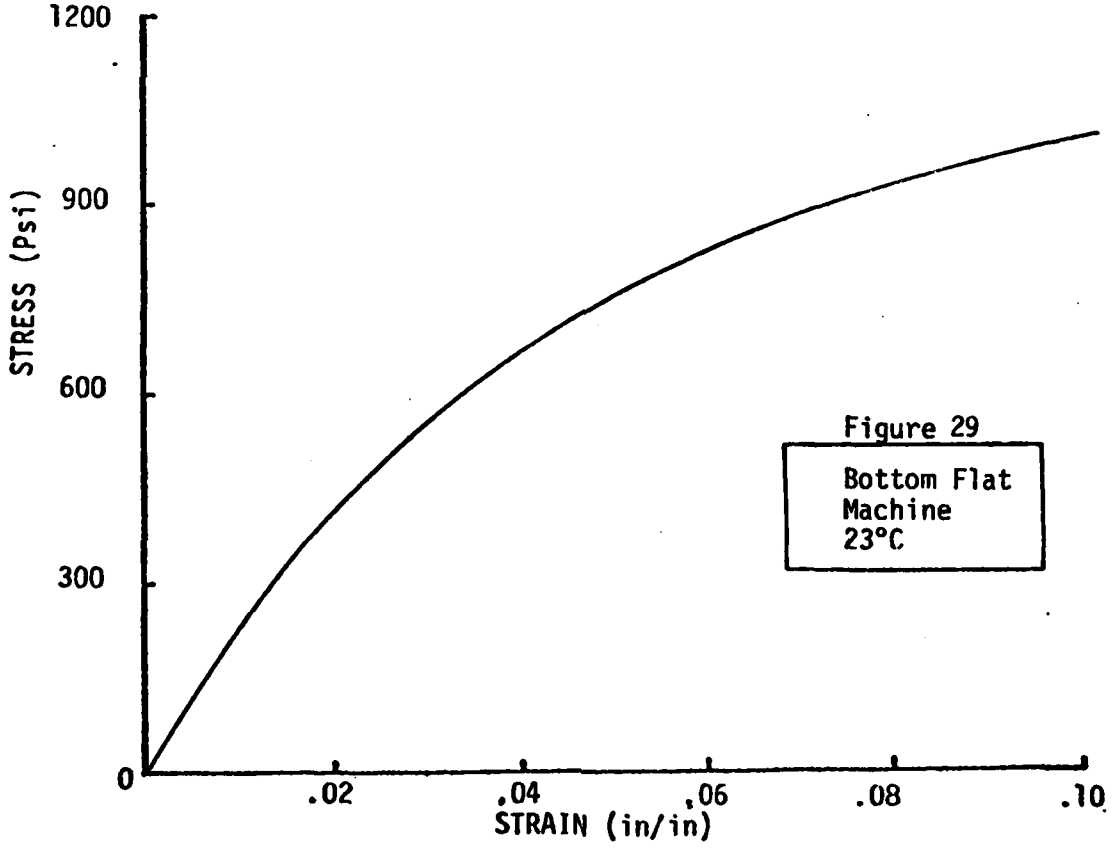

Figure 29

Bottom Flat
Machine
23°C

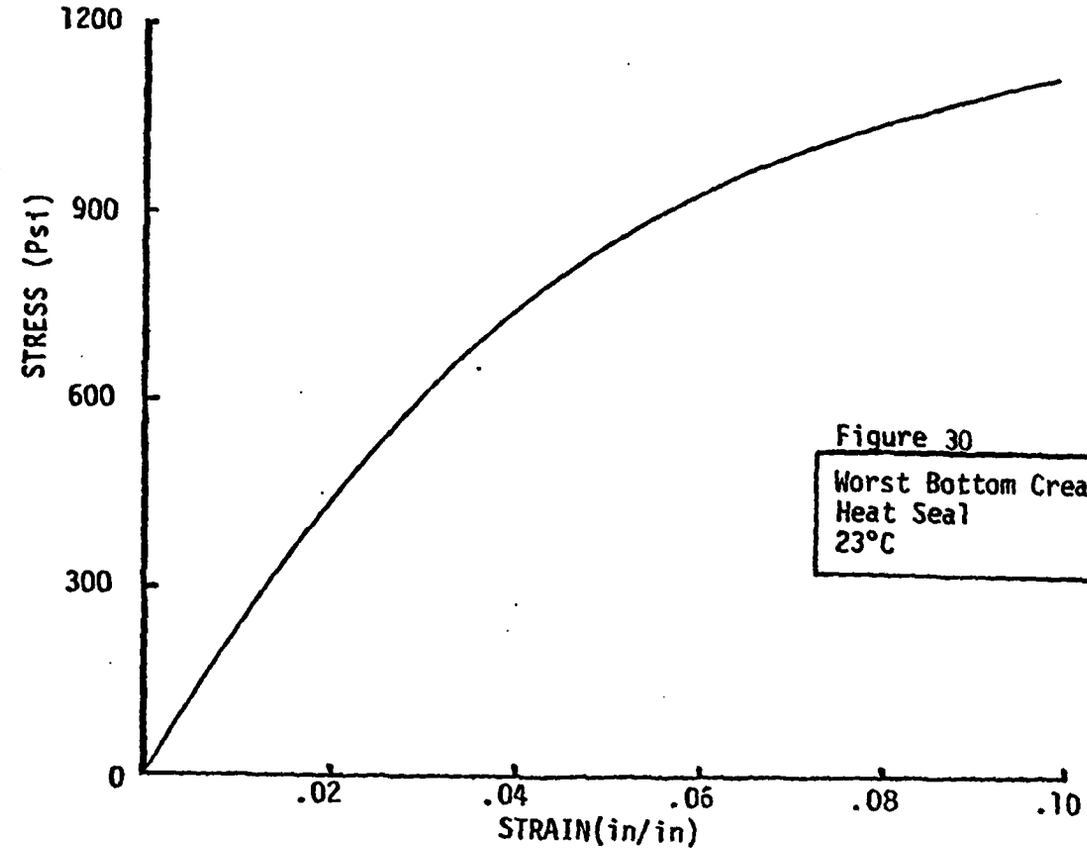

Figure 30

Worst Bottom Crease
Heat Seal
23°C

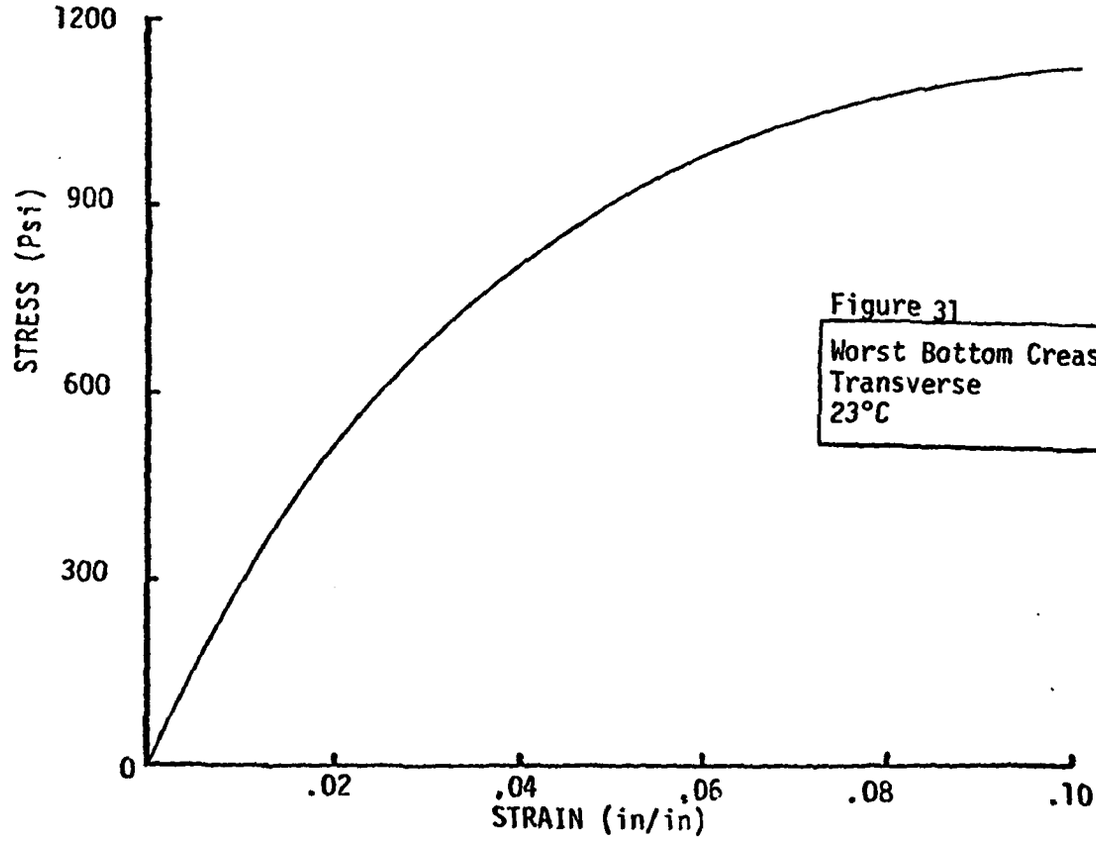

Figure 31

Worst Bottom Crease
Transverse
23°C

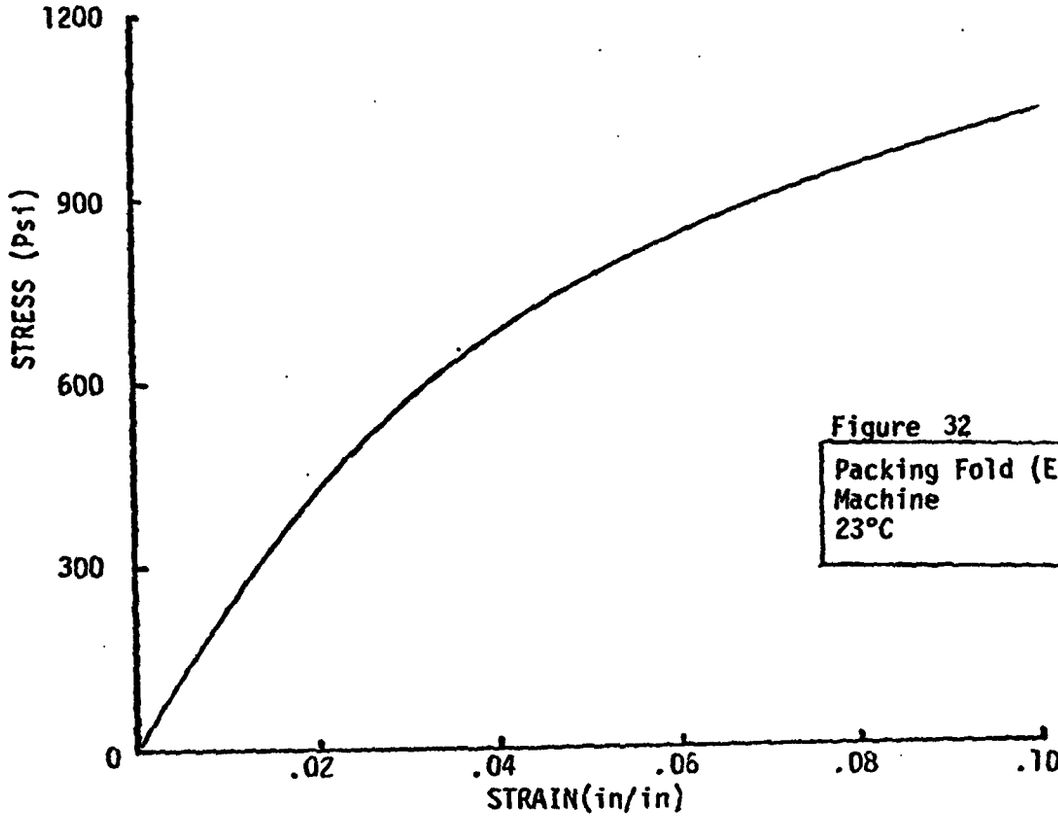

Figure 32

Packing Fold (Extremely Creased)
Machine
23°C

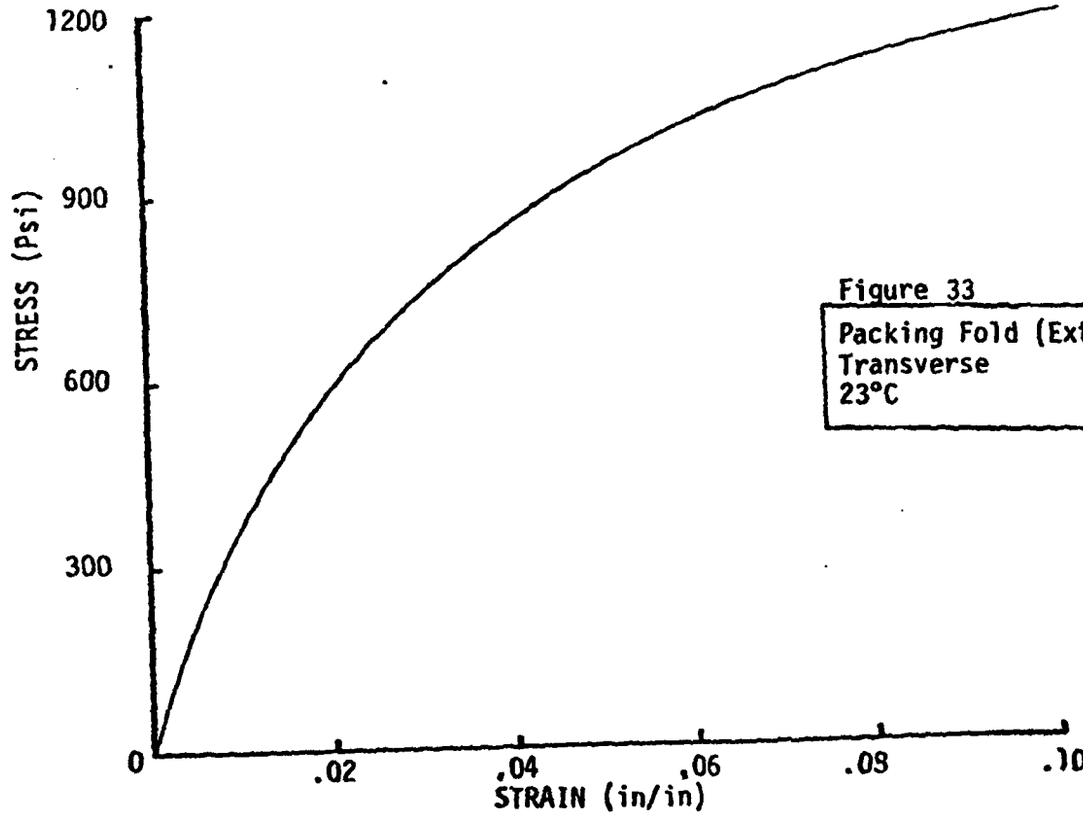

Figure 33

Packing Fold (Extremely Creased)
Transverse
23°C

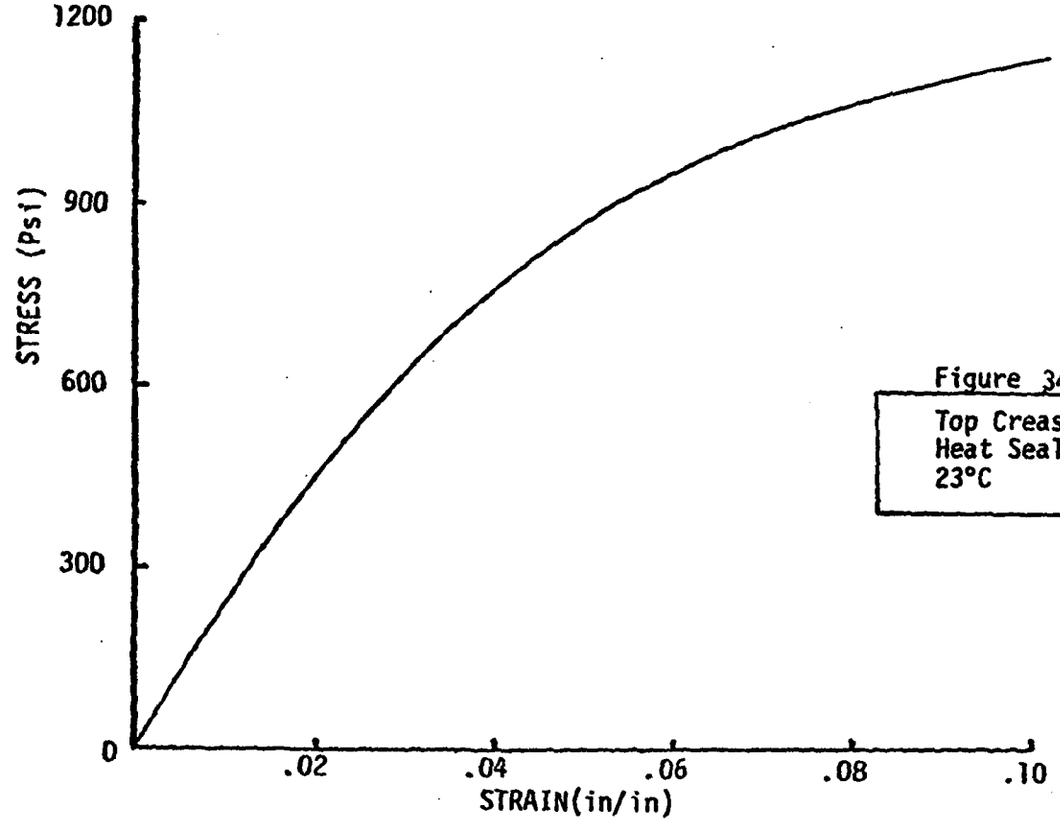

Figure 34

Top Crease
Heat Seal
23°C

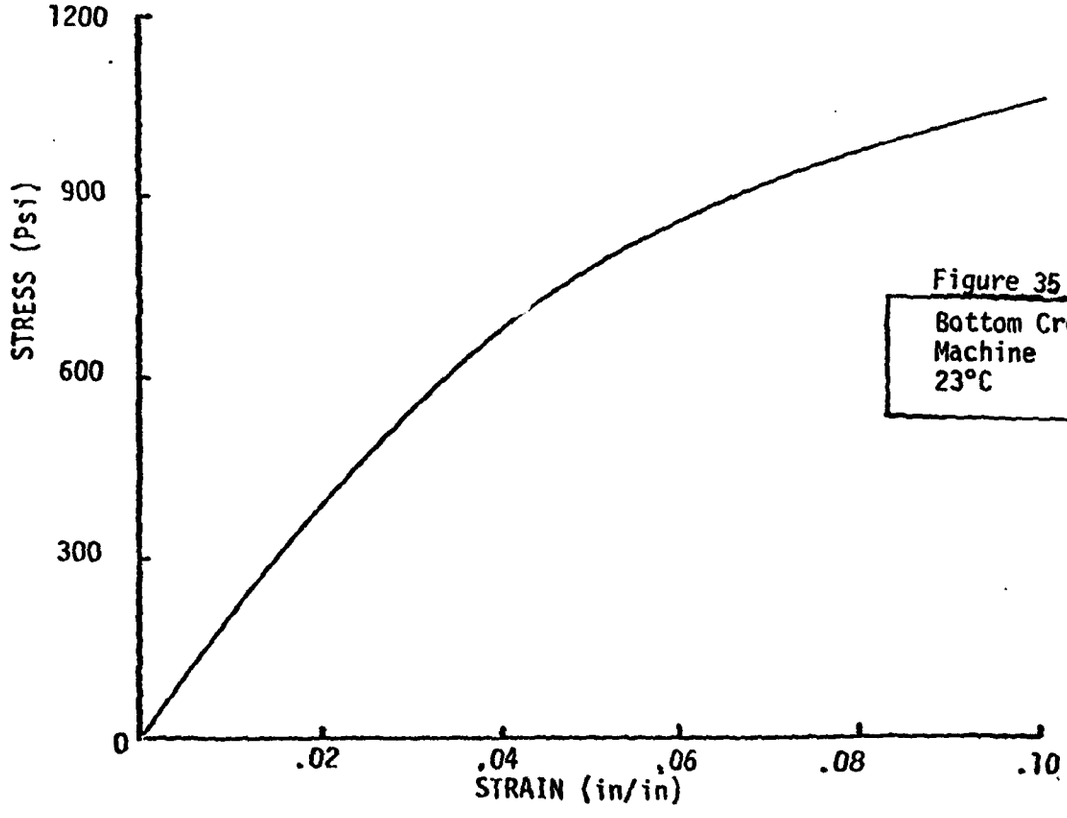

Figure 35

Bottom Crease
Machine
23°C

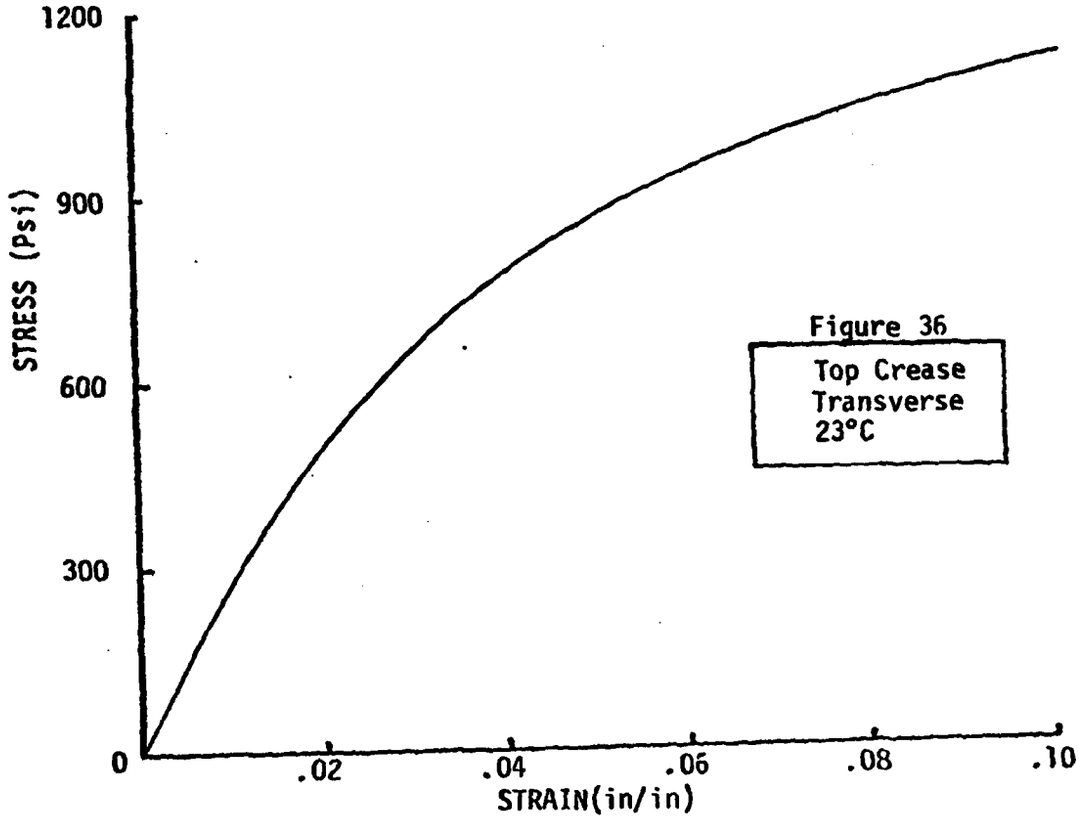

Figure 36

Top Crease
Transverse
23°C

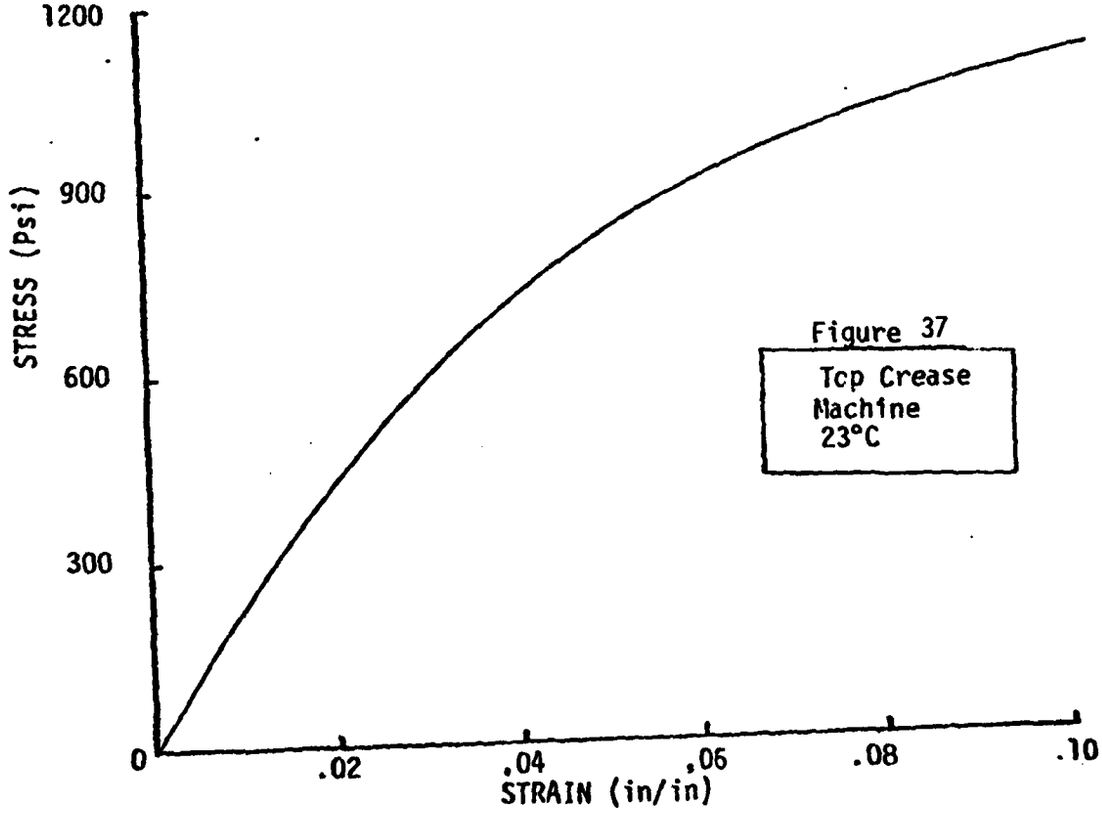

Figure 37

Top Crease
Machine
23°C

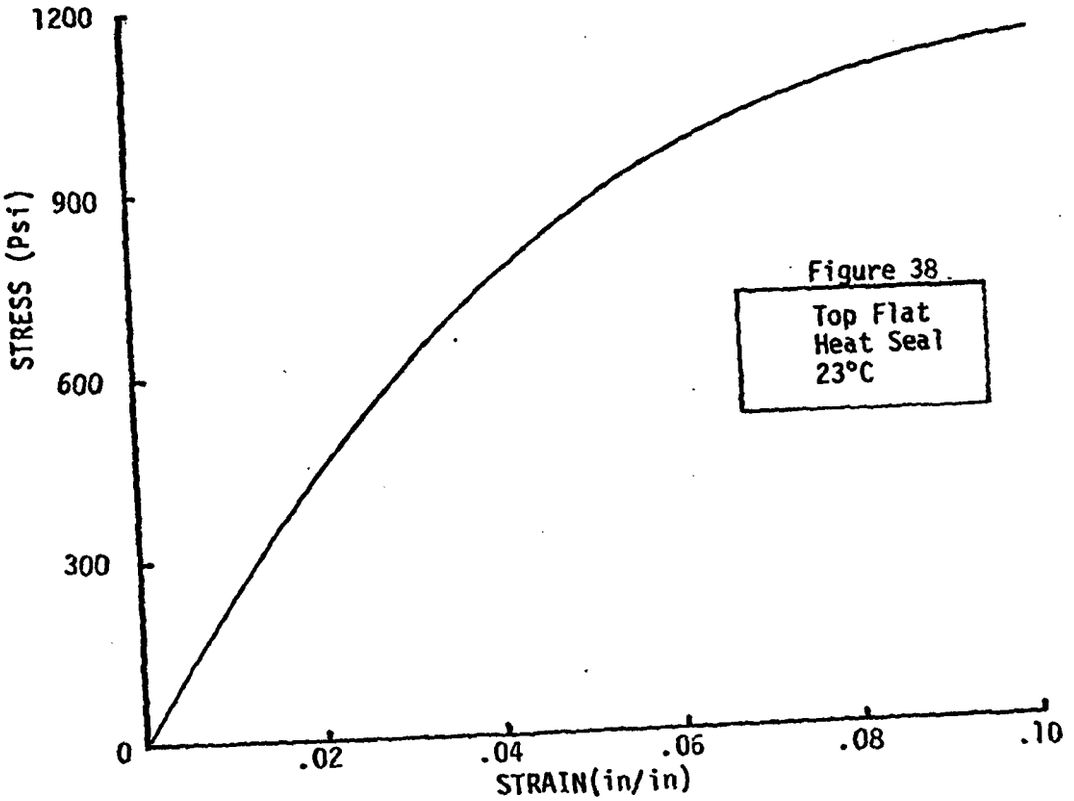

Figure 38
Top Flat
Heat Seal
23°C

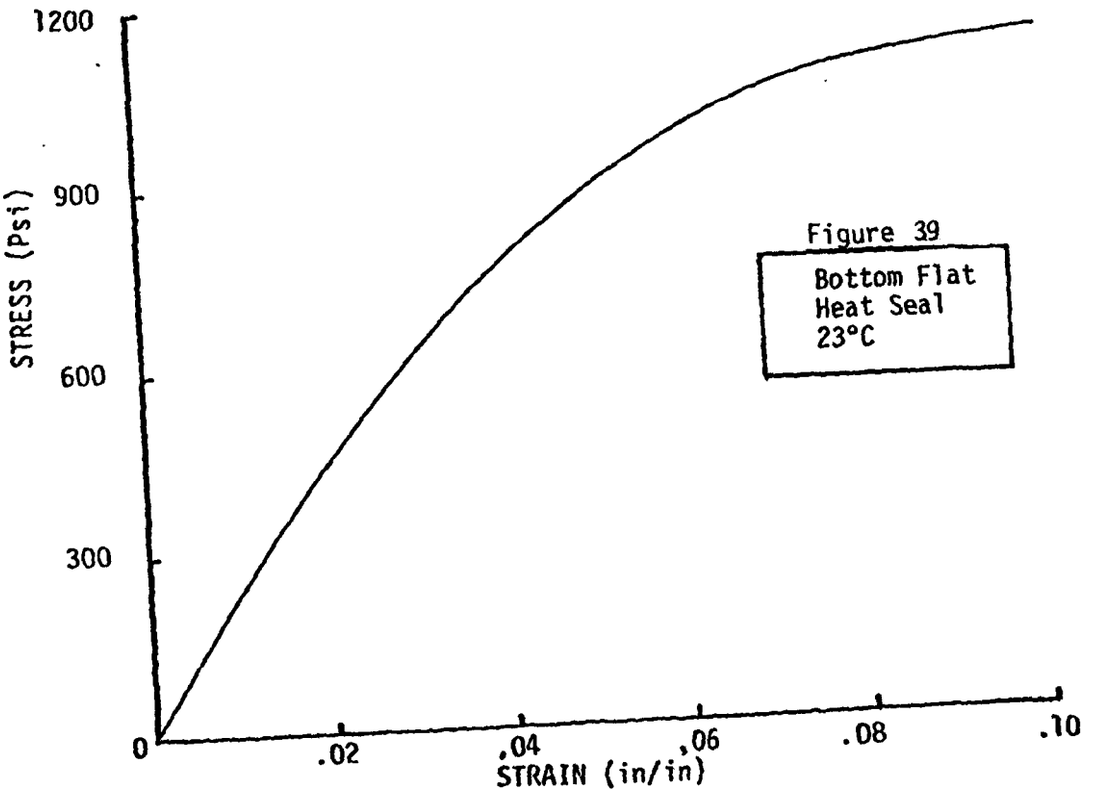

Figure 39
Bottom Flat
Heat Seal
23°C

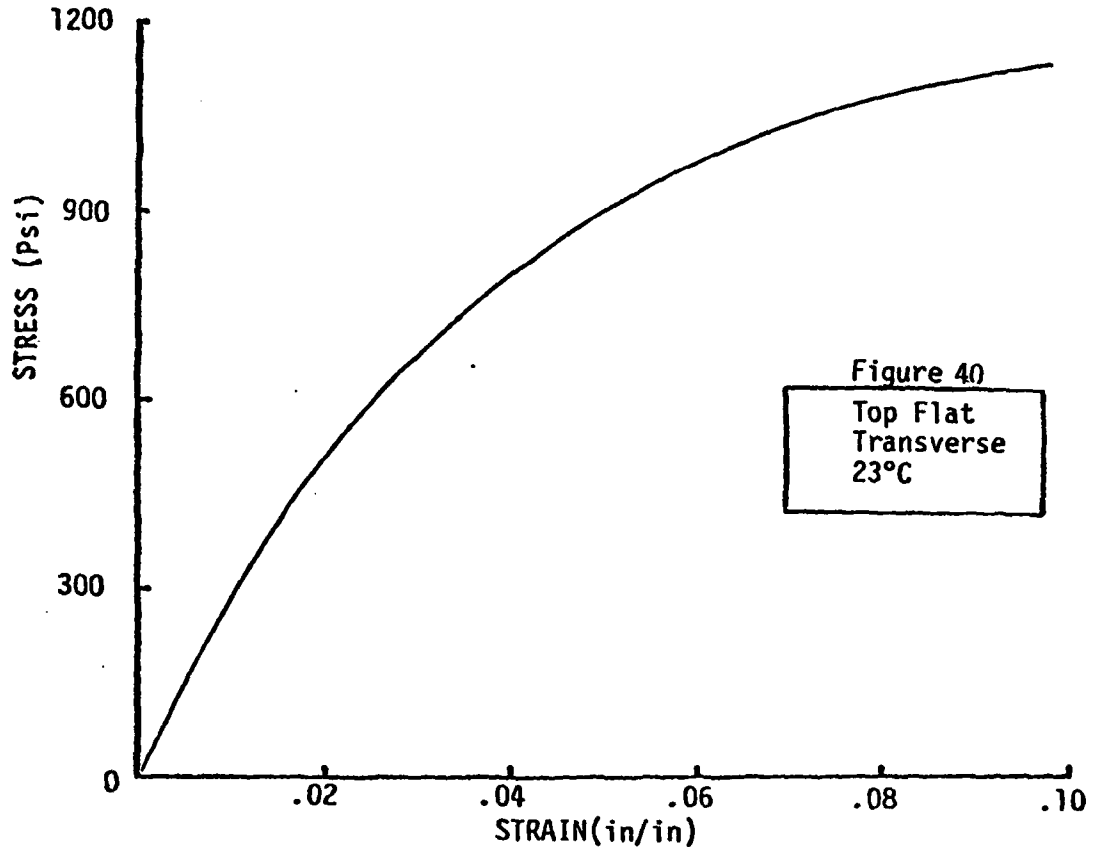

Figure 40
Top Flat
Transverse
23°C

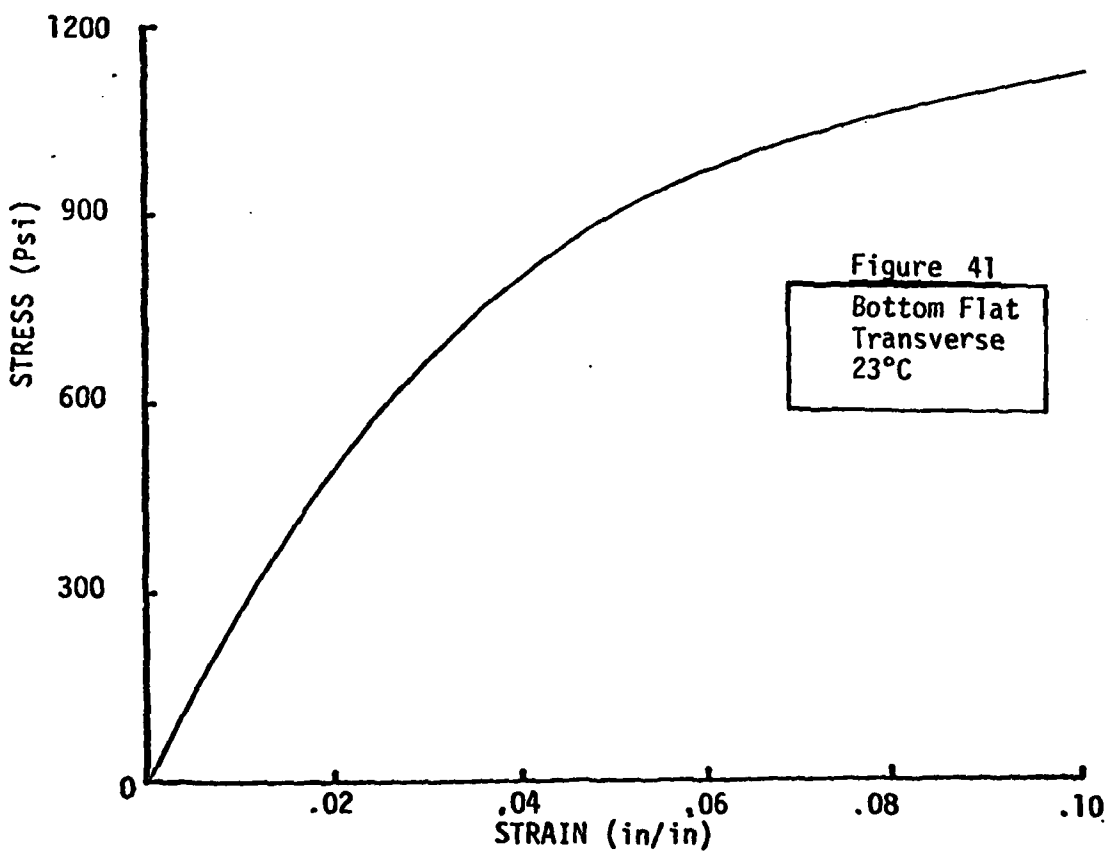

Figure 41
Bottom Flat
Transverse
23°C

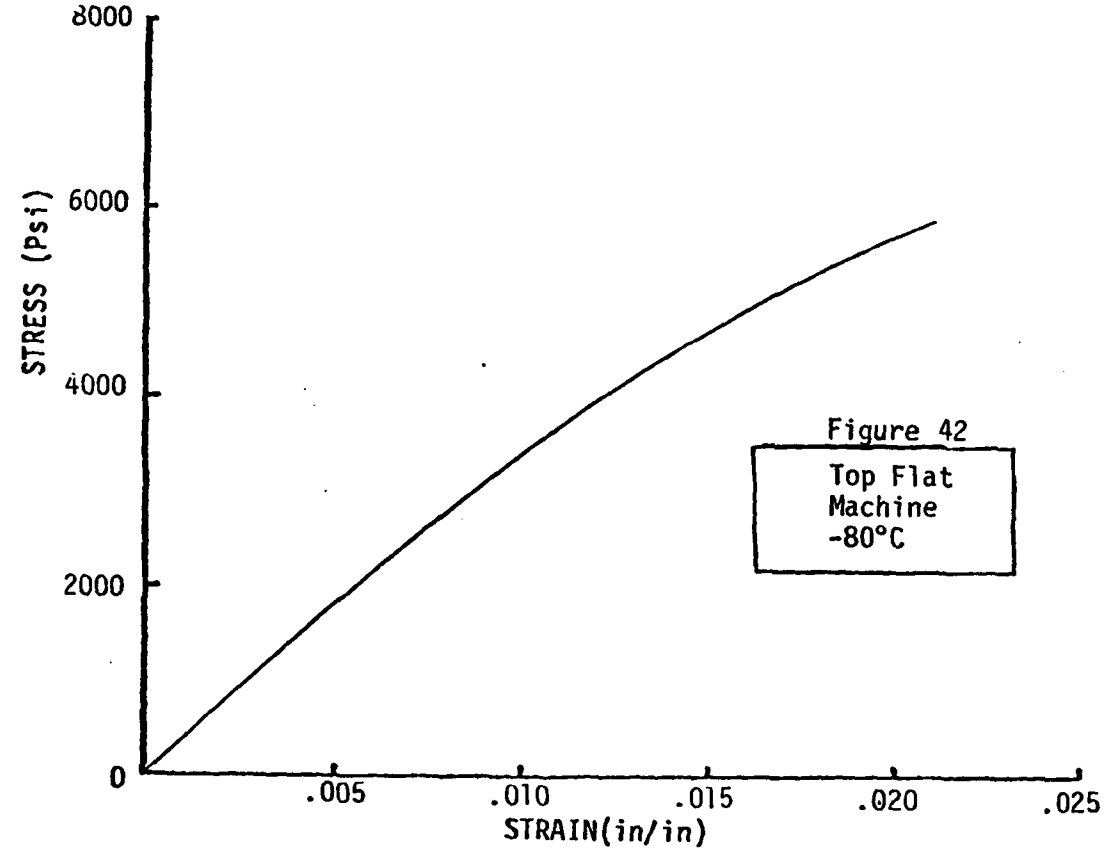

Figure 42

Top Flat
Machine
-80°C

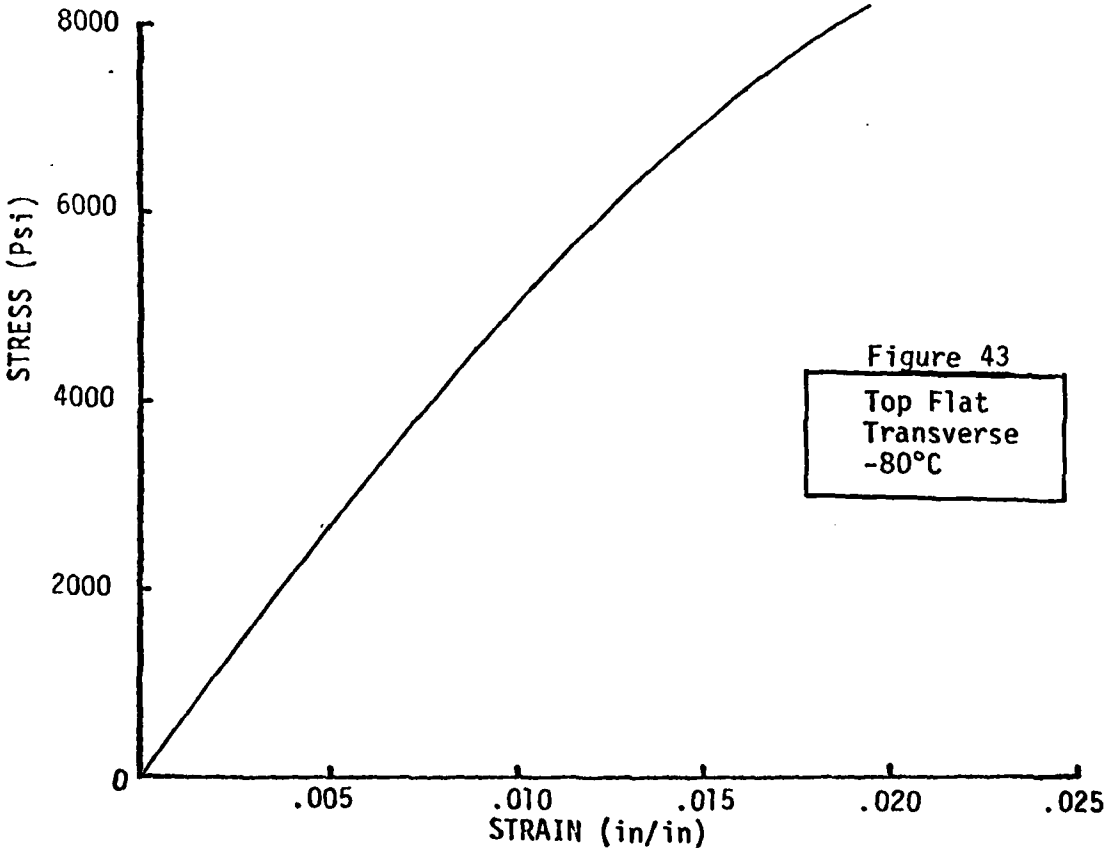

Figure 43

Top Flat
Transverse
-80°C

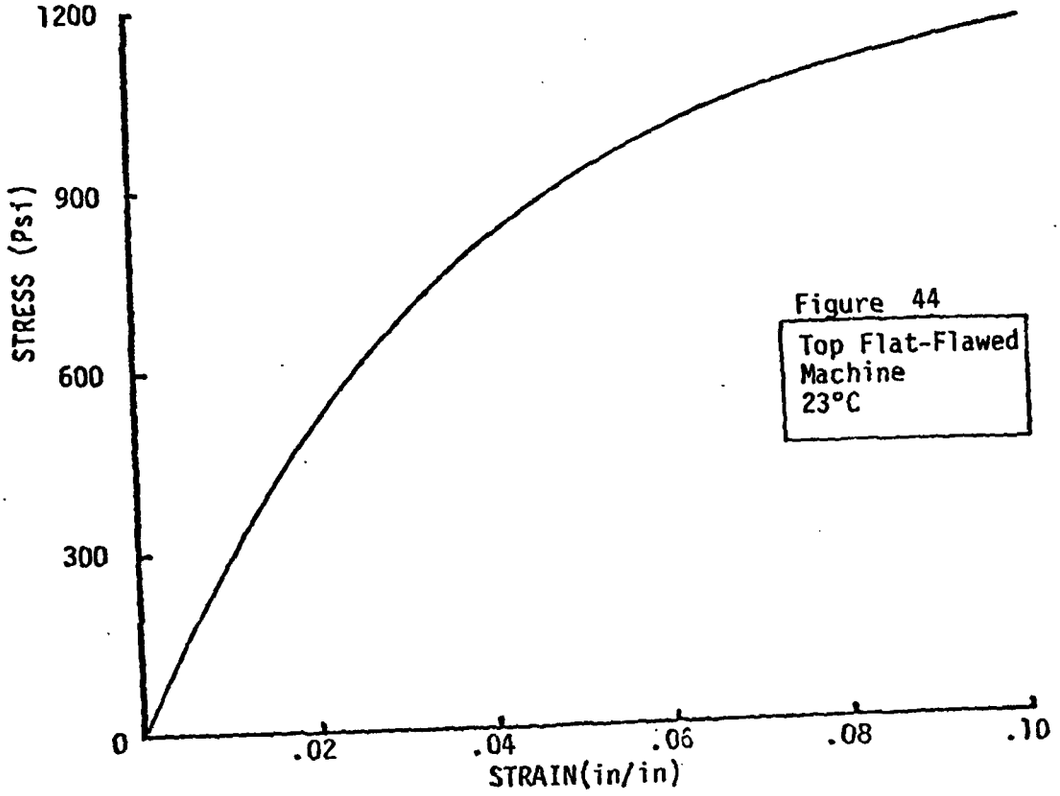

Figure 44

Top Flat-Flawed
Machine
23°C

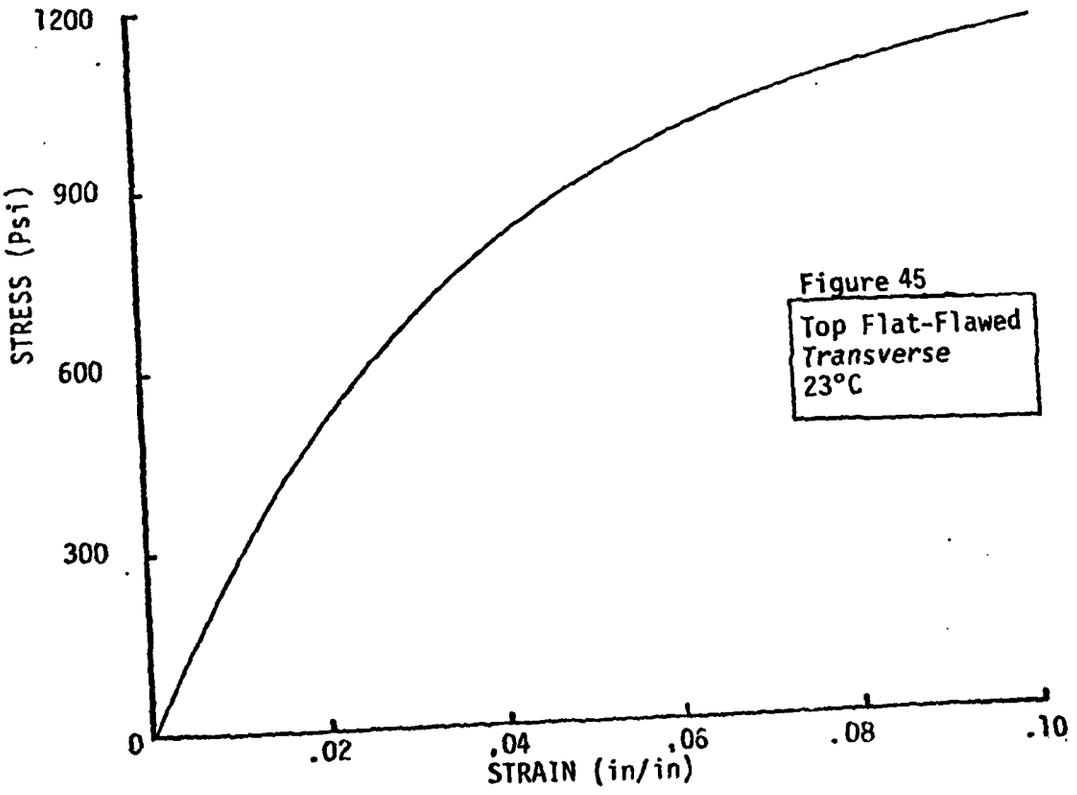

Figure 45

Top Flat-Flawed
Transverse
23°C

HEAT SEAL TESTS

Summary

An investigation has been conducted of the influence of lateral constraint on the strength of a uniaxial sample containing a heat seal. Since the possibility existed for conventional uniaxial tests to yield a high strength for the film-heat seal, higher than the system might show in response to in-flight loadings, a new method of testing was sought, one which would be more discriminating than ordinary uniaxial quality control tests.

Uniaxial samples were prepared and some were tested while restrained and others were tested conventionally. In addition, samples were tested without heat seals for strength comparisons and several tests were made of actual material within the heat seal itself. The restrained samples were prepared by clamping the "fin" of the heat seal to prevent any "Poisson" contraction effect in the vicinity of the seal. This method leaves a continuous load path from one end of the sample through the heat seal to the other end of the sample while preventing the heat seal region from contracting laterally. The results of the tests show no clear reduction of strength of the restrained seal compared to a conventional test. The next stage in the search for a more realistic quality control seal test is to investigate the use of a more controlled biaxial loading state. The laboratory quality devices in use today are rather complex and may not be suitable for in-plant or quality control service. A more simplified in-situ evaluation is contemplated.

To compare the relative mechanical behavior of laterally restrained heat seals with conventional unrestrained seals, a series of tests were performed at 23°C on an Instron with the crosshead rate set at a standard

2"/min. The samples were cut to have a ten inch gage length to insure a pure uniaxial field.

The initial series of tests utilized one inch wide samples. A second series used two inch wide samples to check for any influence of the width to length ratio. Samples were cut from the gore on either side of the heat seal near the location of the heat seal samples.

The stress versus strain behavior of the gore (transverse without heat seal) is shown in Figures 46 and 47. Figure 48 represent four sets of tests of unrestrained heat seal samples. Figure 49 represents the behavior of laterally restrained heat seal samples. Within the data scatter all these curves show the mechanical behavior of the samples to be essentially identical. There is no discernible influence of restraint on strength. A further experiment was conducted to answer the question of the extent to which heat sealing modifies the behavior of Stratofilm. Heat seal strips were trimmed free of load tape and balloon film to produce test samples measuring approximately 0.25 inches by 0.008 inches by 6 inches long samples. These were pulled uniaxially at 23°C and at a cross head rate of 2.0 inches per minute as were the previously discussed heat seal samples. The results of these tests are shown in Figure 50 where, by nature of superimposed curve of Stratofilm behavior, there is seen to be no difference in mechanical behavior. The heat seal strip was cut and pulled in what is referred to on the balloon as the meridional direction whereas the film samples were cut and pulled in the circumferential direction.

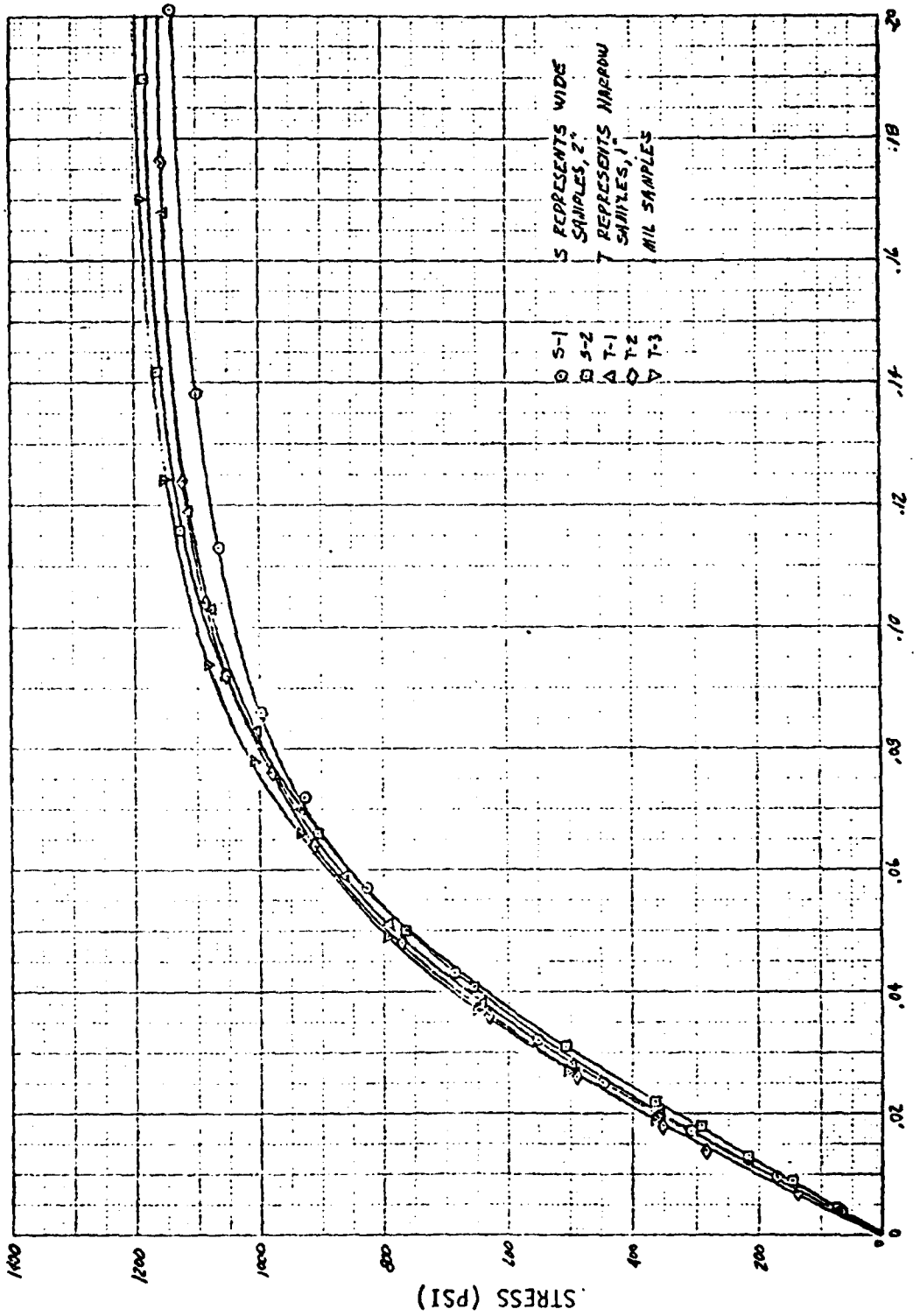

Figure 46. Stress versus strain behavior of the gore fabric tested uniaxially, in the transverse direction at 23°C, where one mil thick samples of two widths were tested.

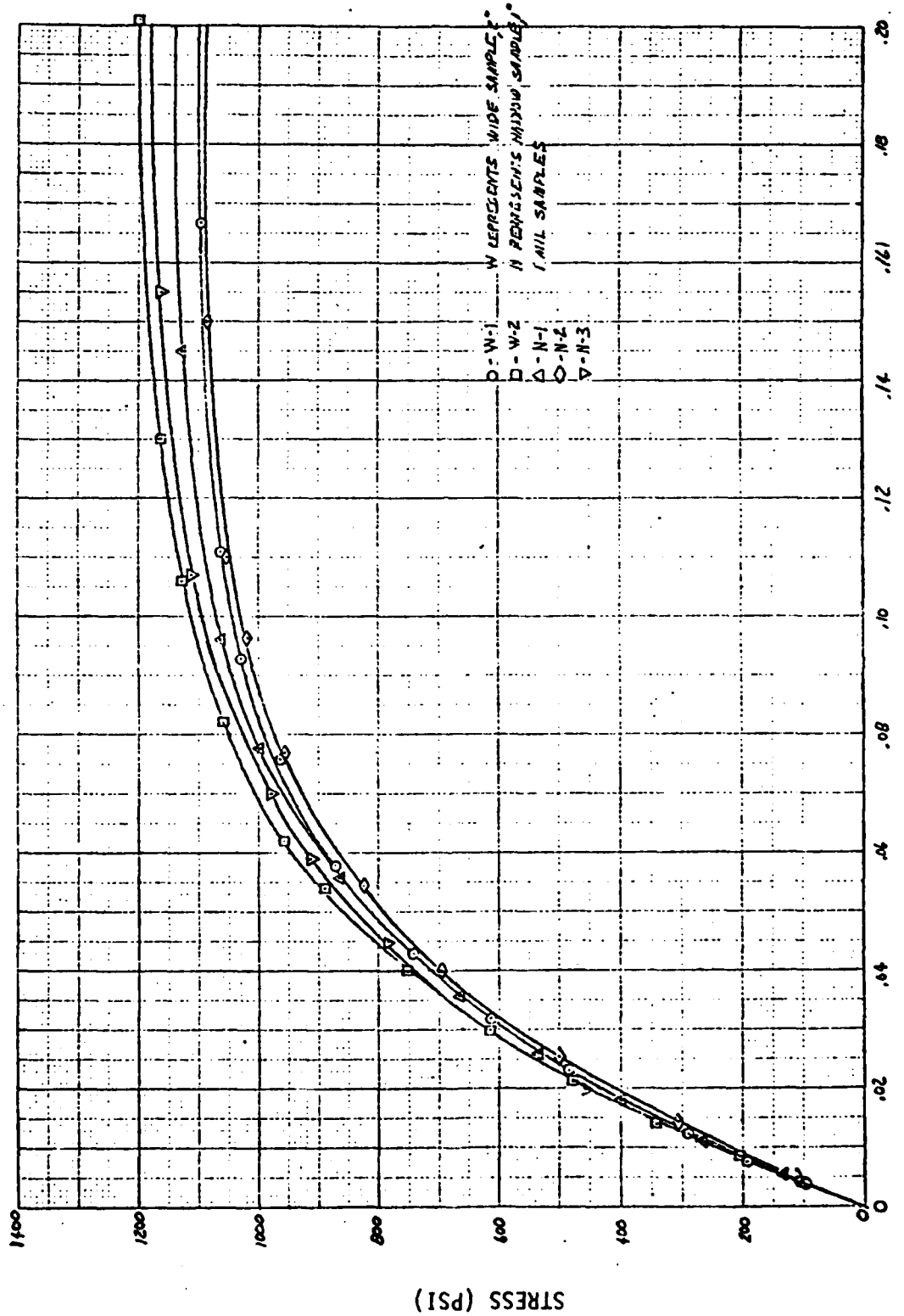

Figure 47. Stress versus strain behavior of the gore fabric tested uniaxially, in the transverse direction at 23°C, where one mil thick samples of two widths were tested.

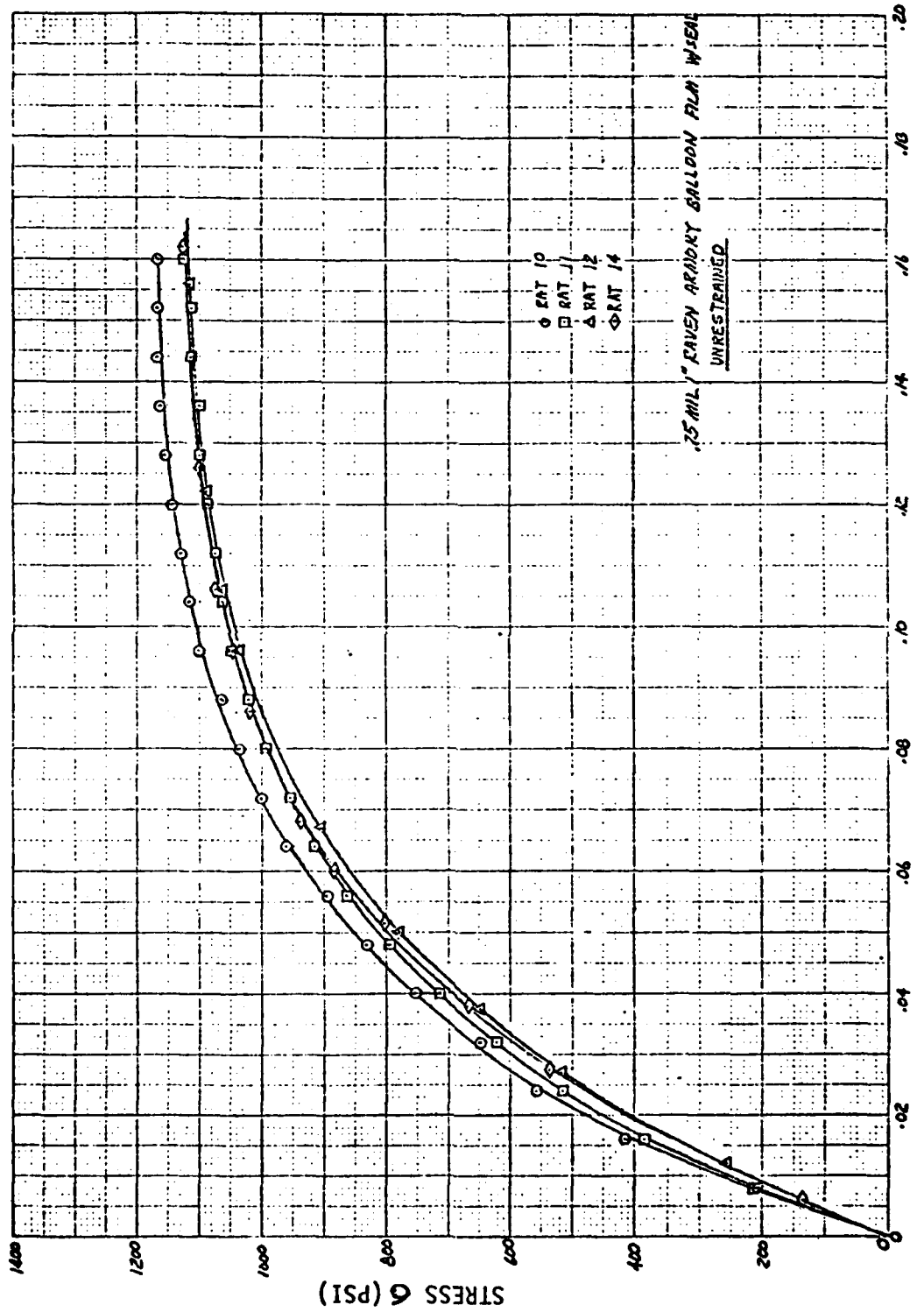

Figure 48. Stress versus strain for four sets of samples of unrestrained heat seal samples of 0.75 mil polyethylene.

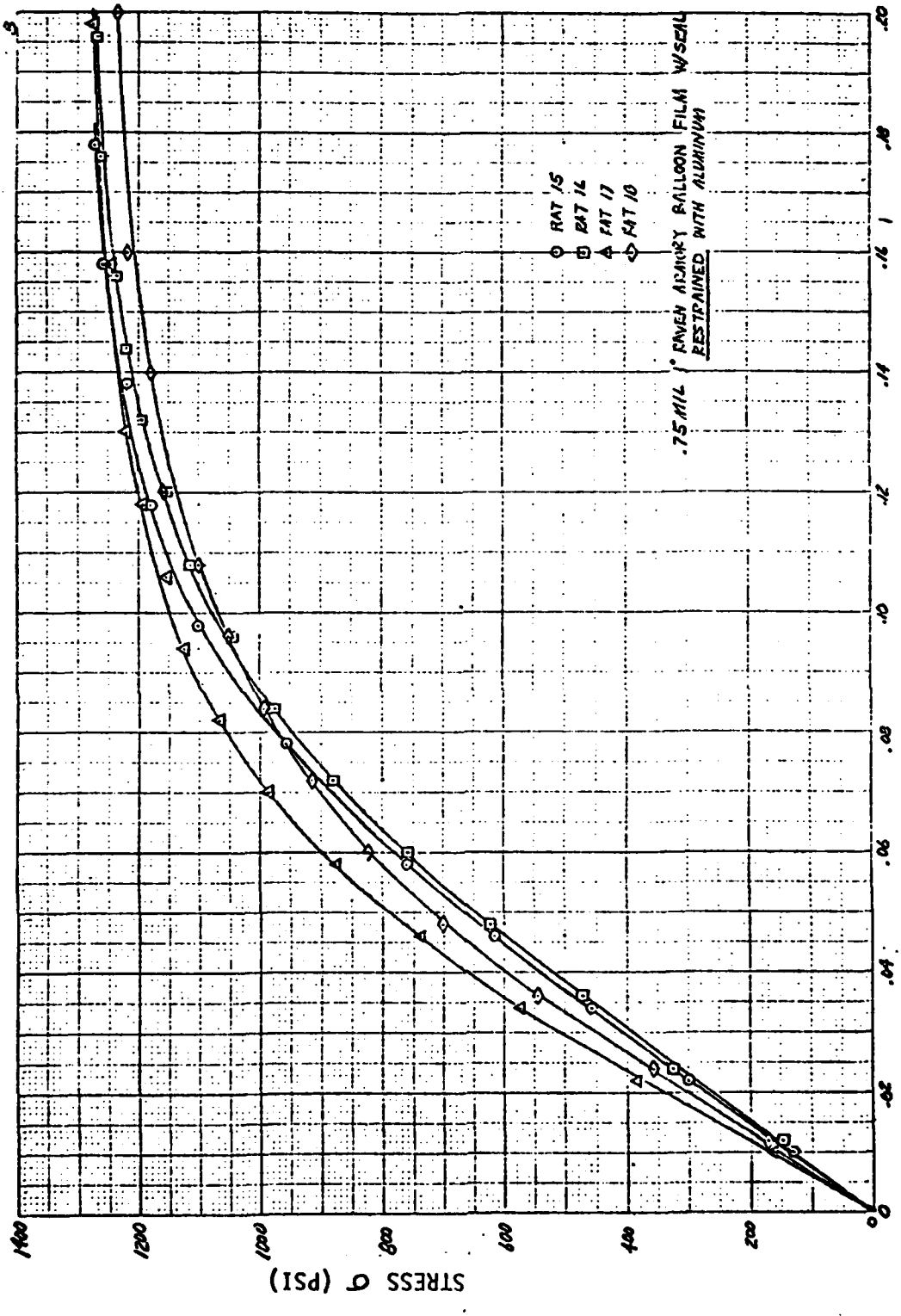

Figure 49. Stress versus strain for four sets of samples of restrained heat seal samples of 0.75 mil polyethylene.

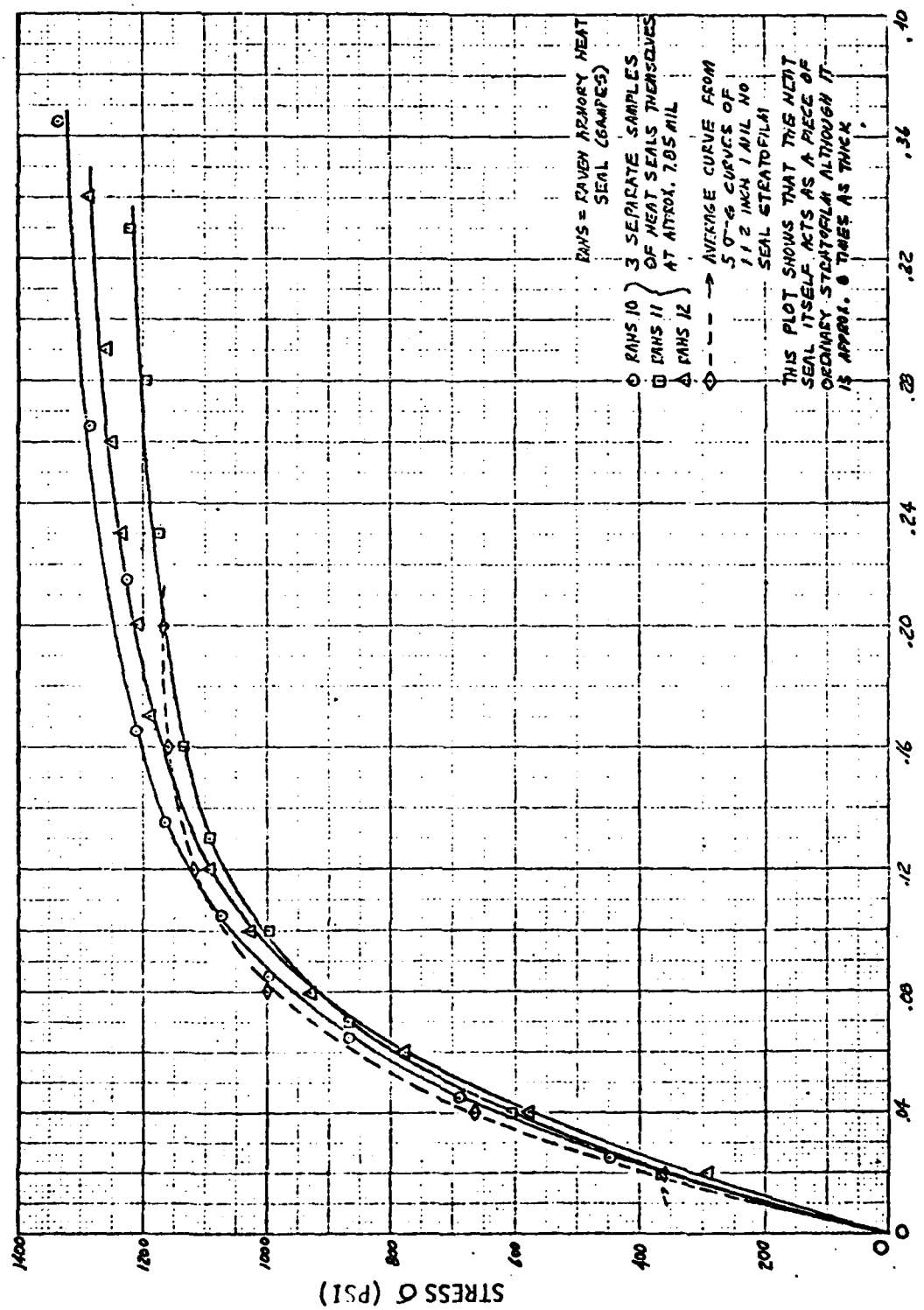

Figure 50. Stress versus strain test in uniaxial tension of fused film trimmed from the heat seal and pulled along the direction of the heat seal.

BIAXIAL STRAIN TESTER

Summary

The study of how to measure the strength of heat seals under biaxial loads has led to the design of a cruciform test apparatus capable of inducing various biaxial stress ratios. The cruciform apparatus consist of overlapping "V" members where the apex angle in each V can be set and locked. The apex of the V members is attached to the Instron - one to the movable cross head and one through the load cell to the rigid frame. The test arrangement has one V inverted and overlapping the other such that when the distance between their vertices increases the horizontal spacing between their points of overlap also increases. For a vertex angle of 90° the vertical and horizontal displacments of the cruciform sample are identical. For a homogeneous and isotropic sample this would induce a one-to-one biaxial stress state. Adjusting the vertex angles enables various other ratios to be induced such as two-to-one as induced by the race-track. Load cells are built into both arms so that accurate load ratios can be achieved. Through secondary adjustments of the horizontal grips, various load histories can be accomplished, e.g., the load in the meridional direction along a heat seal can be held constant while the circumferential stress (across the seal) is increased to failure.

A continuing problem has been faced in the testing of heat seals. Attempts at conducting inflated diaphragm tests have proven difficult to interpret analytically due to the complicated geometry assumed by the diaphragm. Normally, the diaphragm inflates essentially into a segment of a sphere due to the membrane action of thin films. A sample containing a heat seal, however, forms a doubled lobed bubble where the radius of curvature varies almost continuously with position. In a spherical segment the radius is constant. Since the stress in the diaphragm is dependent upon the radius of curvature, a heat seal diaphragm sample cannot as yet be analyzed.

Since uniaxial loading is not a realistic test mode and inflated biaxial tests, though more realistic, cannot be analyzed at this point, a new style of tester was conceived. The device was constructed to produce a constant strain in two orthogonal directions. The arms of the system can be set to produce a one-to-one strain field or a two-to-one strain field. A square sample approximately 8" x 8" is secured on each edge by four independent clamps to result in a test section measure 6" x 6". The clamps are mechanically interlocked such that they move apart equally in the one-to-one mode or one pair moves twice as much as the other in the two-two-one mode. Load cells are attached to one orthogonal pair of the grips and a trace of input strain versus induced stress can be generated. The general layout of the device is shown in Figure 51 and in Figure 54. There it is seen that the arms are locked together in pairs with each arm making an angle of 90° with each other. In Figure 128, the upper pair constitute one half of the tester, the lower pair

making up the other. The upper and lower halves are interlocked through roller bearings such that as the halves more apart the roller bearings track the moving intersection. This causes the horizontal clamps to move apart the same amount as the vertical clamps creating an equal component biaxial strain field. The clamps are detailed in Figure 52. The sample is sandwiched between layers of silicone foam which can retain some degree of flexibility to below -80°C. The use of large washers on each side of the clamping plates insures a uniform clamping pressure.

The loads in each are measured by means of "proving ring" load cells as shown in Figures 51 and 53. The cells are capable of high linearity and wide temperature survival. Figure 55 shows their load sensitivity.

When the biaxial strain tester is mounted in an Instron universal test system the strain rates are controlled by the Instron. The load cell, mounted in the Instron, serves both as a calibrated source and, during an experiment, as a backup for the biaxial tester load cells.

Identical load cells are used in order to guarantee identical deformation contributions to each test direction. When used as a stand-alone device, the load cells are dead weight calibrated and then the sample is loaded to failure while the sample strain is measured by an incremental extensometer. The data taken include strain, stress in the x-direction and the stress in the y-direction all as functions of time. For creep studies the unit is subjected to a constant load while the above parameters are recorded.

A polariscope, with which photoelastic patterns can be observed in loaded polyethylene along with photographs of a grid mesh under varying loads has been used to evolve the grip design as well as to define the region of uniform loading of a test sample.

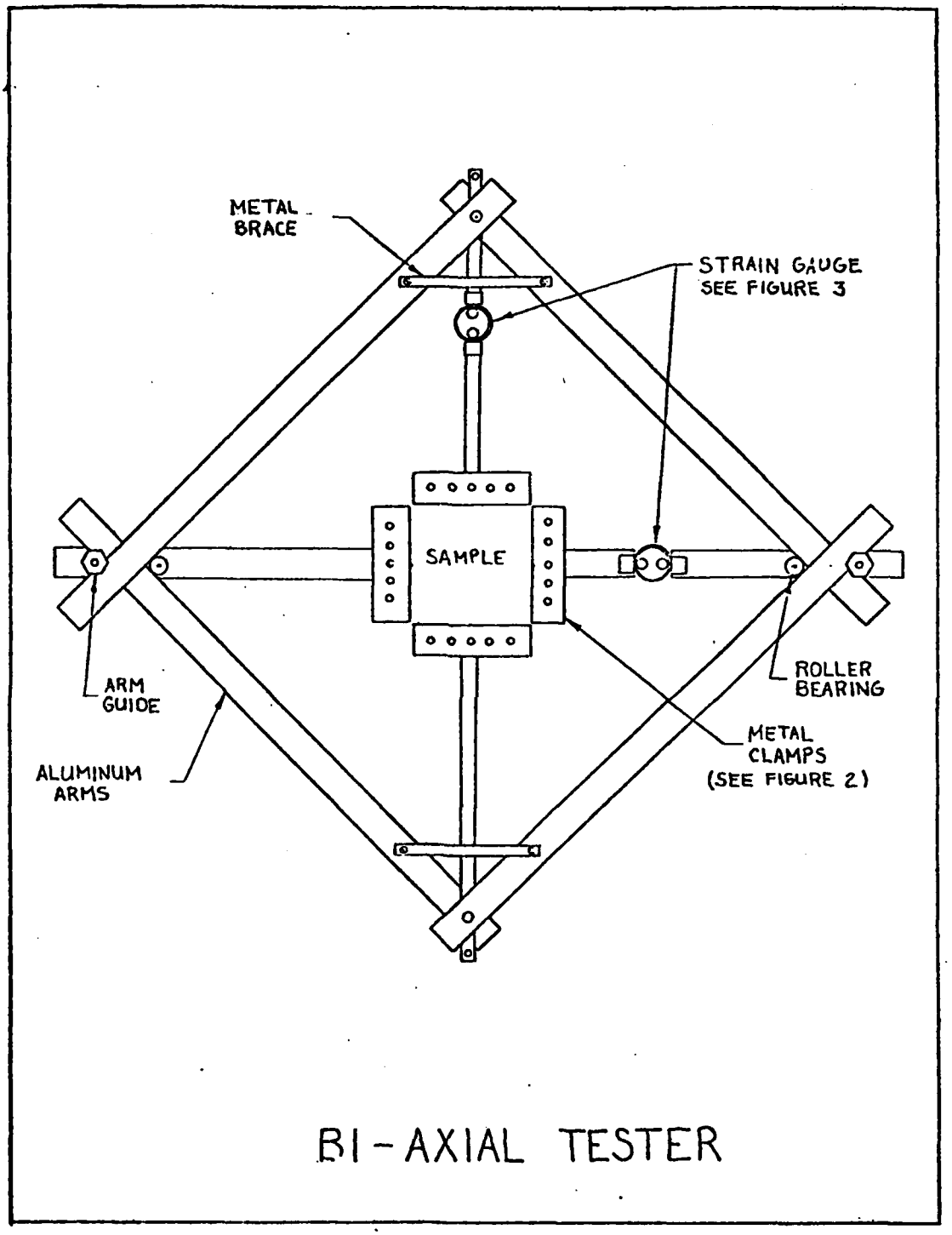

Figure 51. Diagram of the Biaxial Strain Tester.

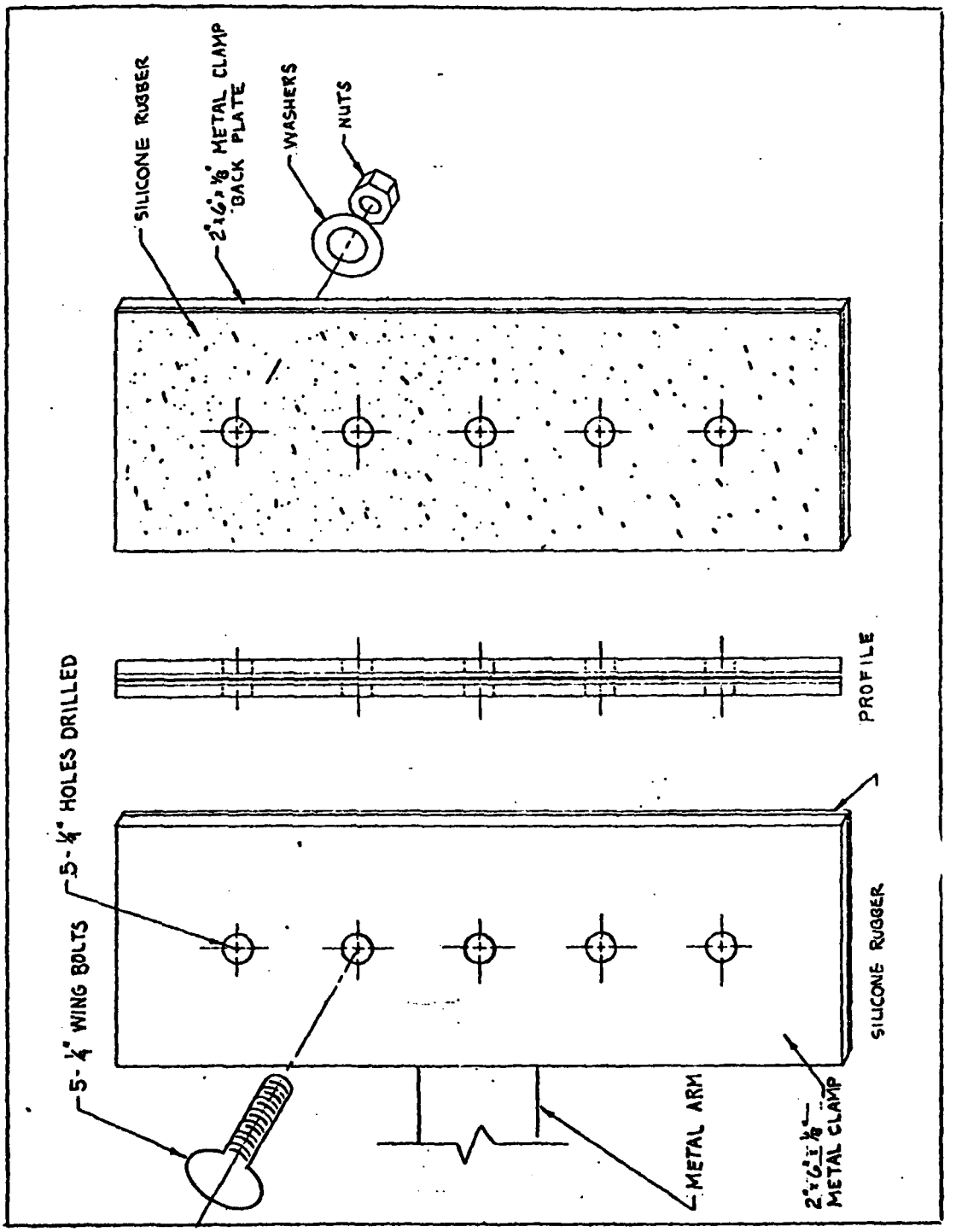

Figure 52. Diagram of a Specimen Clamp from the Biaxial Strain Tester.

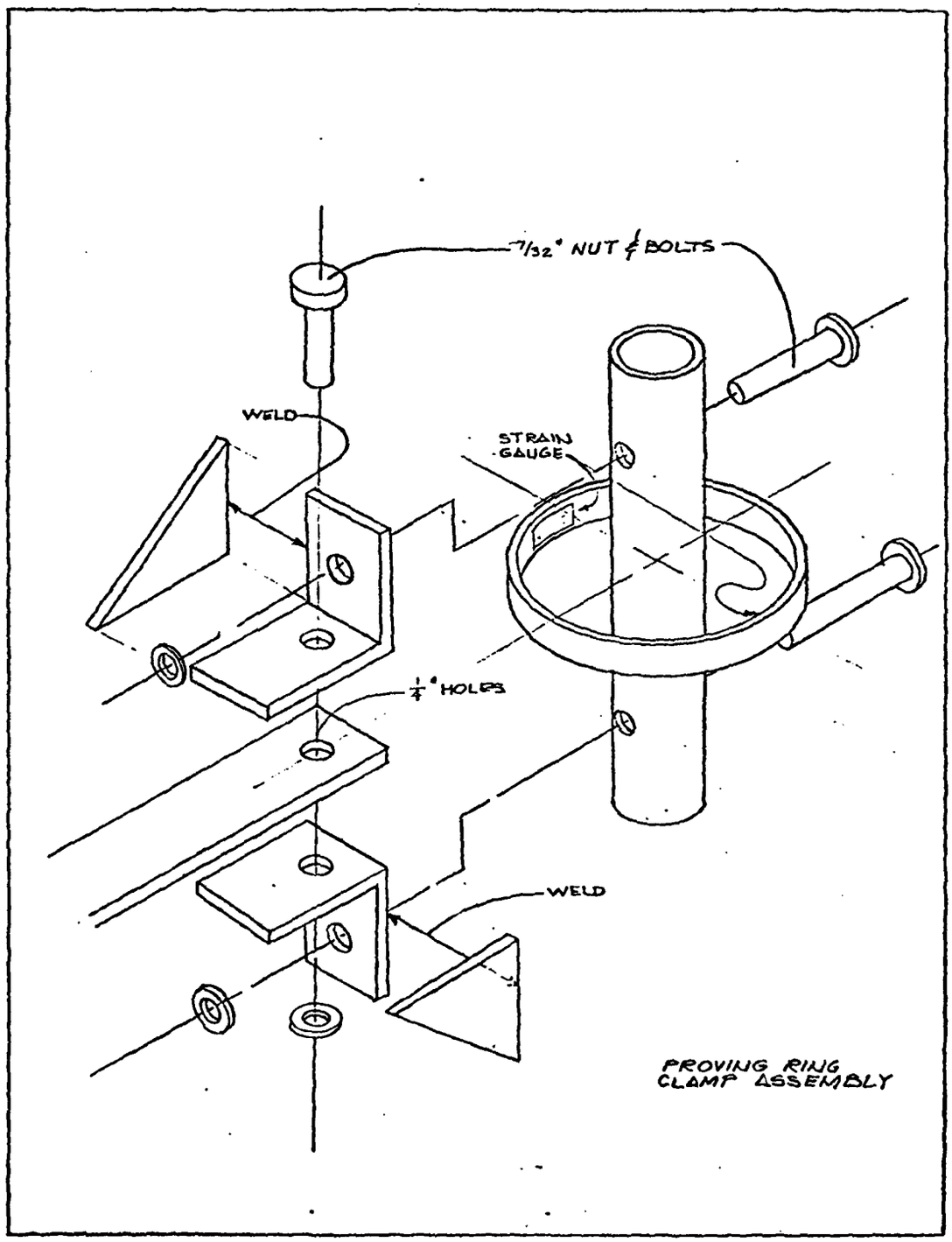

Figure 53. Diagram of a Proving Ring Load Cell From the Biaxial Strain Tester.

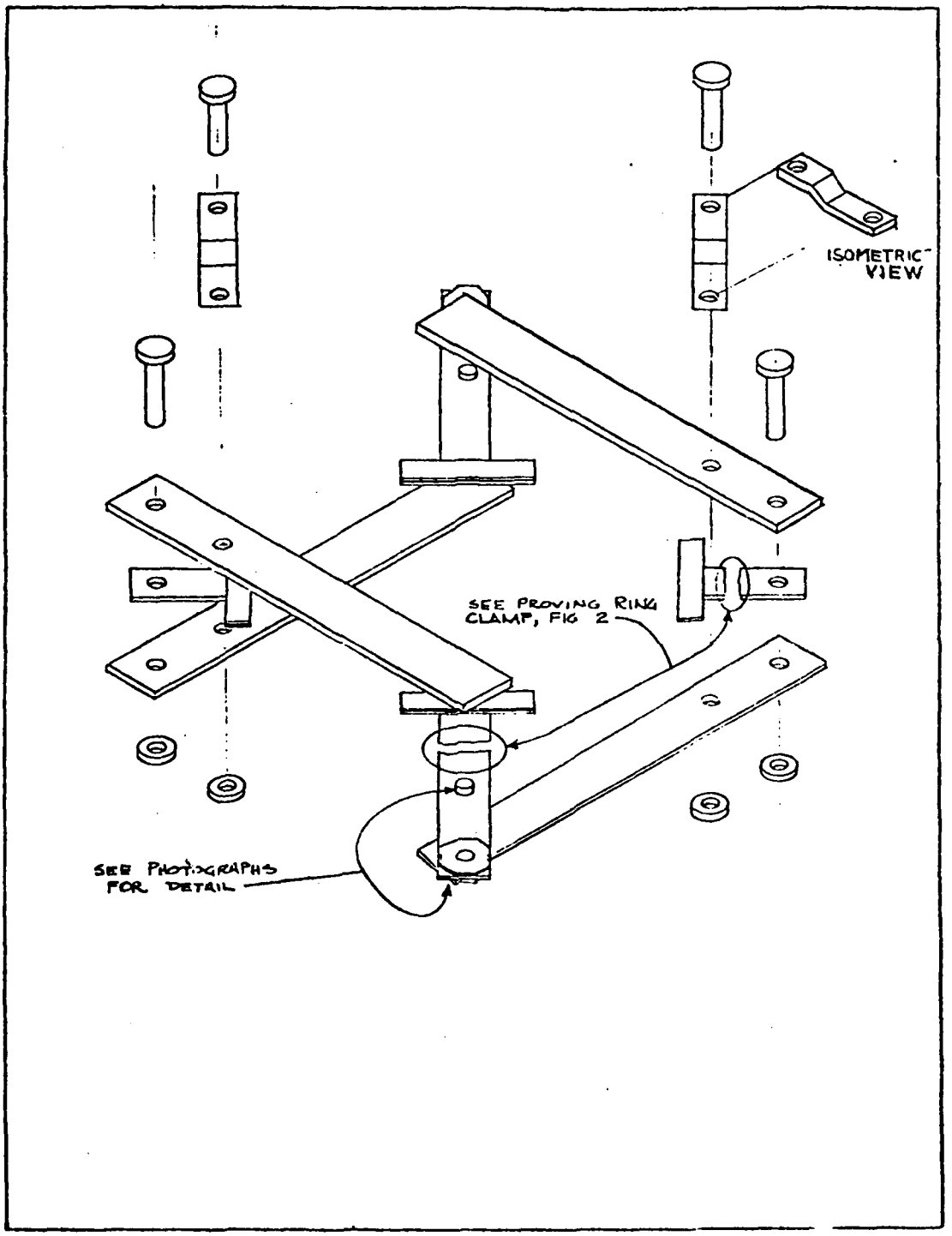

Figure 54. Diagram of the load frame of the Biaxial Strain Tester.

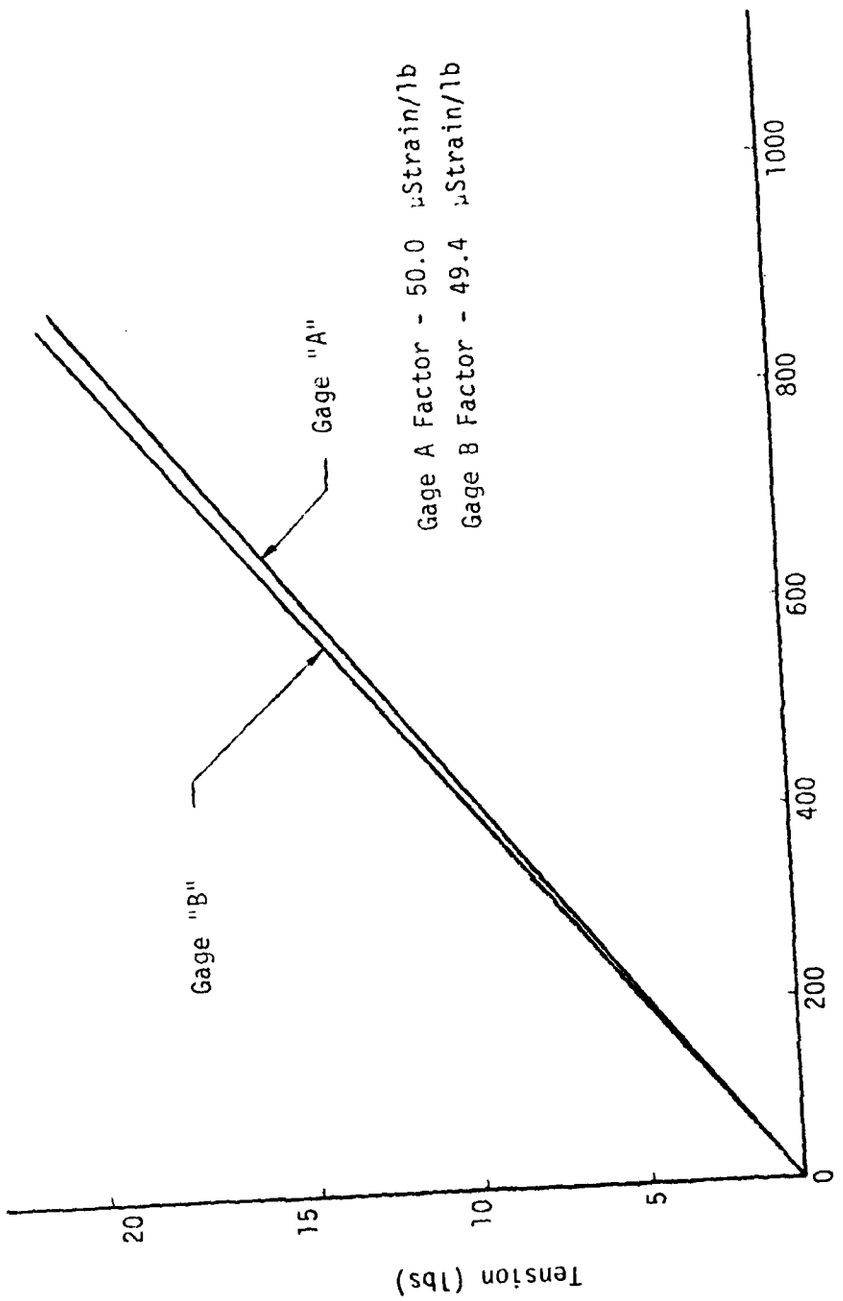

Figure 55. Proving Ring Calibration Flexibility Factors (μ strain/lb).

AD-A098 937 TEXAS A AND M RESEARCH FOUNDATION COLLEGE STATION F/G 1/3
MECHANICAL BEHAVIOR OF BALLOON FILMS.(U)
NOV 78 L D WEBB F19628-76-C-0082
UNCLASSIFIED TAMRF-3332-2 AFGL-TR-79-0026 NL

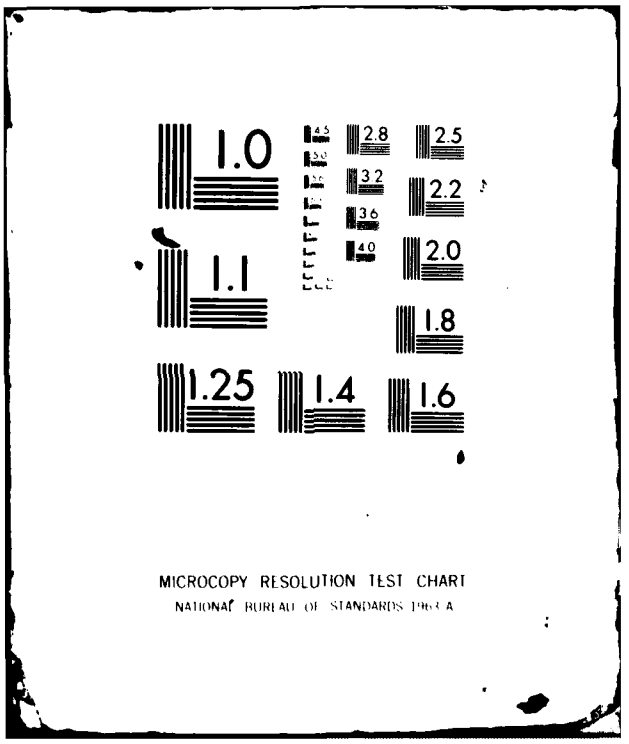
1.0
1.1
1.25
1.4
1.6
1.8
2.0
2.2
2.5
2.8
3.2
3.6
4.0
MICROCOPY RESOLUTION TEST CHART
NATIONAL BUREAU OF STANDARDS 1963 A

Conclusions

Polyethylene film exhibits a mechanical behavior which is load-rate sensitive and temperature dependent as are most polymers.

In addition, perhaps due to its crystallinity, it appears to have a strong dependency on stress history.

All aspects of handling, production, storage, deployment launch conditions and flight influence the film's behavior.

A simple uniaxial strip tensile test is so far removed from service conditions in a balloon that such testing should, if done at all, be only used for quality control purposes.

Biaxial testing where the ratios of stress can be varied from 1-to-1 to 2-to-1 should be adequate for characterizing the as-supplied film. The films strength must be measured in both the machine (extrusion) direction and transverse directions while held under a biaxial stress state as it would be while deployed in a balloon.

Any modification of the film from the state supplied by the manfacturers requires that additional conditions be placed on the mechanical property testing. Sharp creases due to folding and packing must be investigated in biaxial tests where the crease is subject to various stress ratios to determine both the reduction in strength and the importance of orientation of the creases with respect to each gore. When film is heat sealed, a geometrical discontinuity is formed which from geometry alone can reduce the strength of the gore. This is especially evident in tear progagation. Quality control of heat seals is normally accomplished by performing uniaxial pull test orthogonal to the seal. This test does not produce data of value to the designer. Biaxial

testing of a segment of balloon film containing a heat seal is desired but the stress analysis of the variable thickness sample is complex. Testing of segments with and without heat seals will provide a relative strength value of use in design.

Statistically significant testing of balloon films requires extensive testing over temperatures ranging from $-80^{o}C$ to $+ 80^{o}C$ and rates of loading from static (creep) to dynamic, perhaps as high as thousands of pounds per second. As strength can depend upon temperature, rate and immediate stress history, virtually an infinite variety of combinations can exist.

The designer must, therefore, seek out the most severe combinations of loadings which may actually exist during launch, ascent and float. Monitoring instrumentation must be devised to provide these loading conditions. Once actual loads are known, it appears that a Rheological model of polyethylene could be devised which would offer a means of predicting at least the interaction of rate and temperature. The exploratory development in this report of a means of predicting the dynamic mechanical behavior from essentially static creep tests shows the promise of such formulation in minimizing testing. The creep study of polyethylene, initially considered extensive in sample numbers and test conditions proved to be statistically inadequate. A major problem in conducting creep tests is in maintaining a tightly controlled environment. Polyethylene is very temperature sensitive and the very small volume of each creep sample enabled the specimen to respond by changes in length almost instantaneously to variations in environmental temperature. The physical presence of an observer in a cold chamber radiating heat to the samples was found to significantly perturb creep

readings. When this type of creep characterization is to be done, automatic methods of measuring length changes should be employed. Further, creep samples, due to material anisotropy, should be several centimeters wide to get a uniformity of behavior and as long as practical to enhance the changes in length with time. Samples should be approximately 5 cm wide with an active stretch length of at least 25 cm.

If time-temperature super-position relations are to be developed, the experimental program must be carefully planned to accommodate the various steps required in performing superposition. Data are normally generated where the abscissa is strain (or load) rate and the ordinate is a desired mechanical parameter such as creep compliance with temperature as the parameter. The range of rates available in most laboratories is very restricted but not so with respect to temperatures. The temperatures should be chosen close enough together that when data shifting along the logarithmic rate axis ($\log \varepsilon$) is required the data traces, which normally have nonzero slopes, will nearly overlap (Figure 15, Page 38). The lowest rate data point for a warmer temperature should be lower in ordinate value than the highest rate data point for a cooler temperature. Shifting then becomes a relatively straight forward action. Where large gaps exist between temperature data sets, shifting logarithmic scales can lead to vast uncertainties in the computed $\log A_T$ shift factors.


DA
FIL